Chemistry of Angular and Linear [N]Phenylenes

by

Peter Ian Dosa

A. B. (Princeton University) 1995

M. S. (Massachusetts Institute of Technology) 1998

A dissertation submitted in partial satisfaction of the

requirements for the degree of

Doctor of Philosophy

in

Chemistry

in the

GRADUATE DIVISION

of the

UNIVERSITY of CALIFORNIA, BERKELEY

Committee in charge:

Professor K. Peter C. Vollhardt, Chair

Professor Robert G. Bergman

Professor Jeffrey A. Reimer

Fall 2002

Abstract

Chemistry of Angular and Linear [N]Phenylenes

by

Peter Ian Dosa

Doctor of Philosophy in Chemistry

University of California, Berkeley

Professor K. Peter C. Vollhardt

This dissertation discusses several topics relating to the [N]phenylenes, including their behavior under flash vacuum pyrolysis conditions, and the structural characterizations of angular [4]phenylene and a metallacyclopentadiene(alkyne) complex. A novel CpCo-shift that takes place along the linear [5]phenylene frame is also described.

Chapter One. This chapter will review synthetic routes to the [N]phenylenes. In addition, the structural, spectroscopic, and chemical properties of the phenylenes are detailed.

Chapter Two. The development of methodology used to improve access angular [N]phenylenes and to synthesize the previously inaccessible unsubstituted "*anti-doublebent*" [5]phenylene is discussed. Several new X-ray crystal structures are presented in this chapter, including one of angular [4]phenylene and the first structurally characterized metallacyclopentadiene(alkyne) complex, a key intermediate in cobalt-mediated [2+2+2]cycloadditions.

Chapter Three. The flash vacuum pyrolyses of angular [3]-, angular [4]-, and linear [3]phenylenes are described. A ^{13}C-labeling investigation, undertaken to furthering understanding of the mechanisms that form the common (and dangerous) environmental pollutants obtained during these pyrolyses, is presented.

Chapter Four. Approaches to an alkyl-solubilized linear [5]phenylene derivative and the kinetics of a novel CpCo-shift that takes place along the linear [5]phenylene frame are discussed.

Chapter One

An Introduction to the [N]Phenylenes

1.1 Questions

The amazing scientific progress of the last few centuries has been driven to a large extent by attempts to answer fundamental questions like "Where do species come from?" or "What is the nature of matter?" This is true even in the field of chemistry, which has historically been primarily an experimental, rather than theoretical, science. One of the most central questions in chemistry is "What is aromaticity?" To this day, almost a century and a half after August Kekulé proposed his famous structure for benzene,[1] there is still no universally accepted answer to this query.[2] Fittingly, what first caused this question to be raised were experimental results, especially the observation that benzene reacts substantially differently than normal alkenes. Another perplexing fact that needed to be explained was how difficult some seemingly simple molecules like cyclobutadiene were to synthesize.

In 1931, Erich Hückel noticed that cyclic, planar arrangements of p orbitals with $(4n + 2)$ π-electrons (where n is an integer) are unusually stable. Molecules, such as benzene, which fulfill "Hückel's Rule" have come to be called aromatic. Arrangements that instead contain $4n$ π-electrons are unusually unstable. These compounds, like cyclobutadiene, are termed antiaromatic and have in general proven exceptionally difficult to synthesize. According to simple Hückel molecular orbital theory, benzene is

stable because all of its bonding molecular orbitals are filled with π-electrons (Figure 1.1). In contrast, antiaromatic compounds such as (planar) cyclooctatetraene (Figure 1.2) or cyclobutadiene are unstable because some of their π-electrons occupy nonbonding or antibonding molecular orbitals.[3] This theory has been used to successfully predict the (anti)aromaticity of much larger molecules like [16]- or [18]annulene.[2a]
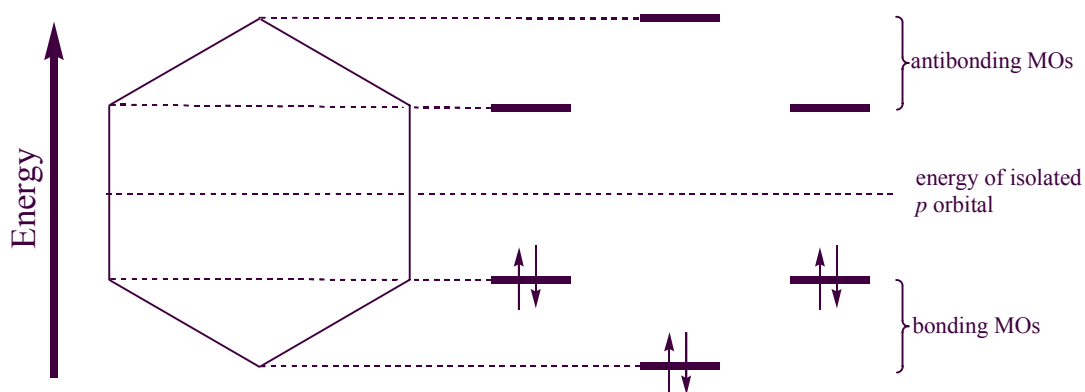

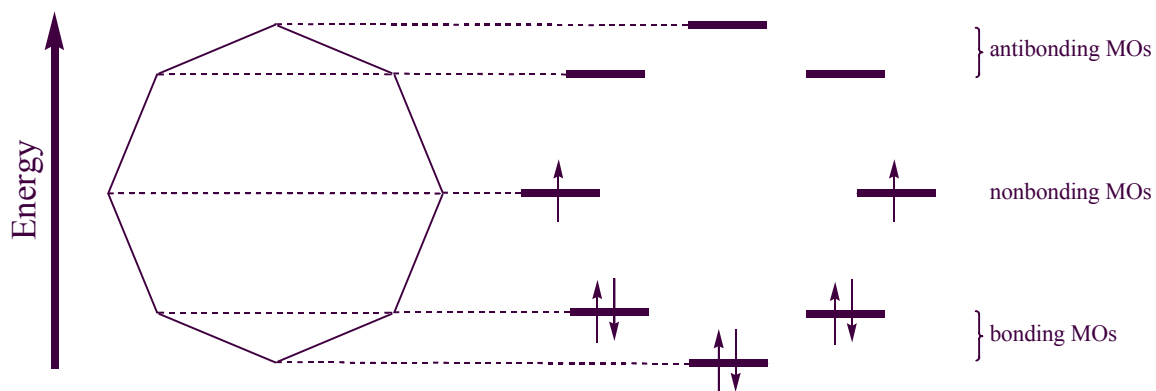**Figure 1.1** Energy level diagram for the π-molecular orbitals of benzene.

Figure 1.2 Energy level diagram for the π-molecular orbitals of cyclooctatetraene.

The primary purpose of research into the [N]phenylenes can be summarized readily with a single question, "What happens when you mix aromatic and antiaromatic circuits?" Biphenylene (**1**), first synthesized in 1941 by Lothrop,[4] is the embodiment of such a juxtaposition. The four distinct resonance structures of biphenylene are shown in Figure 1.3. Structures **1b-d** contain highly destabilizing 4 or 8 electron antiaromatic circuits, while **1a** contains only a 12 electron circuit. Because the energetic costs of these circuits are known to decrease with size,[2a] it is therefore not surprising that the X-ray crystal structure of biphenylene (Figure 1.4) shows bonding that is best described by this resonance structure.[5]
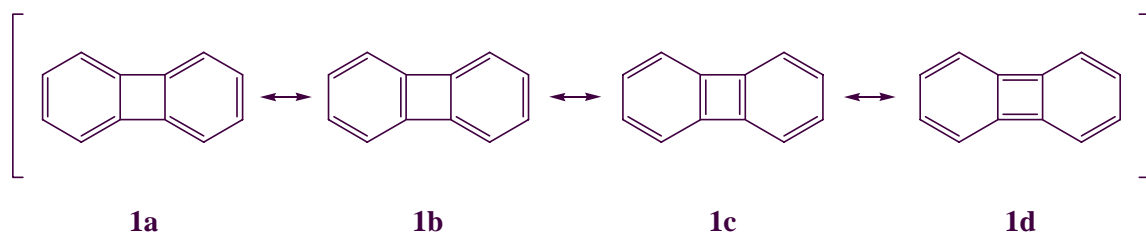

| 1a | 1b | 1c | 1d |

Figure 1.3 The types of resonance structures of biphenylene.

The [N]phenylenes, the main focus of this dissertation, are composed of N benzene rings fused by four-membered rings. While the many different possible topologies each have their own distinctive physical properties and reactivity, at their most basic level, the behavior of the phenylenes serves to answer the question that was posed. When aromatic and antiaromatic circuits are juxtaposed, the molecule will distort in such a way as to maximize its aromaticity while minimizing its antiaromaticity.
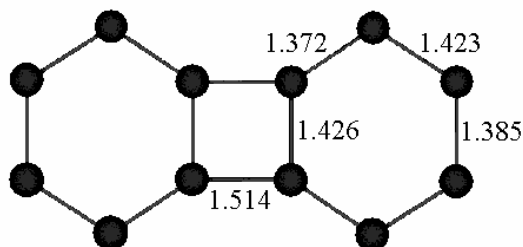
**Figure 1.4** Bond lengths in biphenylene (**1**, Å).

This thesis will deal with several topics relating to the [N]phenylenes. Chapter 2 will discuss the development of methodology used to improve access angular [N]phenylenes and to synthesize the previously inaccessible unsubstituted *"anti-doublebent"* [5]phenylene. Several new X-ray crystal structures will be presented in this chapter, including one of angular [4]phenylene and the first structurally characterized metallacyclopentadiene(alkyne) complex, a key intermediate in cobalt-mediated [2+2+2]cycloadditions. The phenylenes are high-energy potential precursors to polycyclic aromatic hydrocarbons (PAHs) including fullerene substructures, and their behavior under flash vacuum pyrolysis conditions will be investigated in Chapter 3. A ^{13}C-labeling investigation, undertaken to further understanding of the mechanisms that form the common (and dangerous) environmental pollutants obtained during these pyrolyses, will be presented in this chapter. Chapter 4 will discuss approaches to an alkyl-solubilized linear [5]phenylene derivative and the kinetics of a novel CpCo-shift that takes place along the linear [5]phenylene frame. The final chapter will present the experimental details of the preceding studies.

1.2 Synthetic Routes to Biphenylene and Beyond

One of the biggest challenges to studying the properties of the phenylenes is that their syntheses can be quite laborious, particularly for the higher members of the family. A wide variety of methods have been developed to make the simplest phenylene, biphenylene (**1**), since it was first isolated in 1941 by Lothrop.[4,6] These include copper-mediated Ullmann cyclizations of 2,2'-dihalobiphenyls,[4,7] dimerization of benzyne in solution (Scheme 1.1),[8] and pyrolytic extrusions that proceed via benzyne (Scheme 1.2)[9,10] or 2,2'-biphenyl diradicals (Scheme 1.3).[11] Perhaps the most practical synthesis that has been developed is shown in Scheme 1.4. Lithiation of commercially available 2,2'-dibromobiphenyl, followed by transmetallation to zinc and treatment with $CuCl_2$ leads to formation of biphenylene in 80% yield.[12] Unfortunately these methods, with the exception of pyrolytic extrusion, are unsuitable for the synthesis of phenylenes other than **1**.
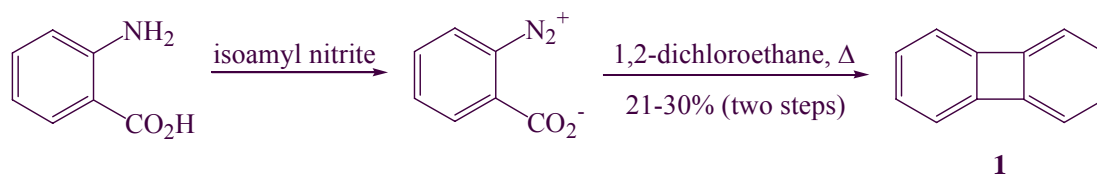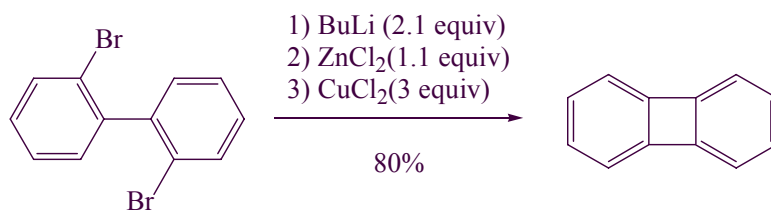

Scheme 1.1 Synthesis of biphenylene (**1**) from benzyne.
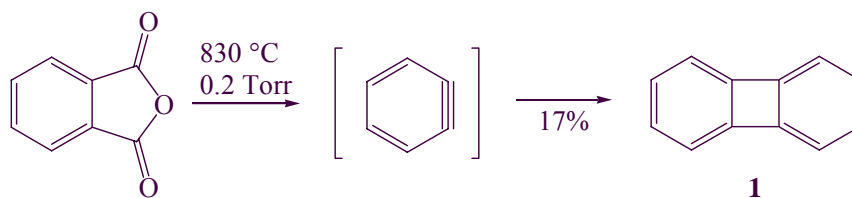
**Scheme 1.2** A flash vacuum pyrolytic synthesis of biphenylene (**1**) that proceeds via benzyne.

Scheme 1.3 A flash vacuum pyrolytic synthesis of biphenylene (**1**) that proceeds via a 2-2'-biphenyl diradical.


**Scheme 1.4** A copper-mediated synthesis of biphenylene (**1**).

Pyrolytic extrusion of nitrogen from benzodicinnolines was used by Barton to synthesize linear [3]phenylene (**2**)[13] and angular [3]phenylene (**3**)[14] (Schemes 1.5 and 1.6). This methodology suffers from severe drawbacks that has prevented its successful application to phenylenes with more than three benzene rings. These problems include the difficulty of synthesizing the necessary starting materials, the requirement that the precursors be volatile, and the possibility of side reactions induced by the high temperatures applied during pyrolysis. A graphic example of this last problem was seen by Barton when he attempted to synthesize triangular [4]phenylene (**4**). Pyrolysis of benzotricinnoline **5** leads not to **4** but rather to the formation of tribenzocyclyne **6**, presumably by retrocyclization of **4** (Scheme 1.7).[15] When triangular [4]phenylene was finally synthesized in 1986, experiment confirmed that it does indeed rearrange to **6** under flash vacuum pyrolysis conditions (700 °C, 10^{-2} mm).[16]
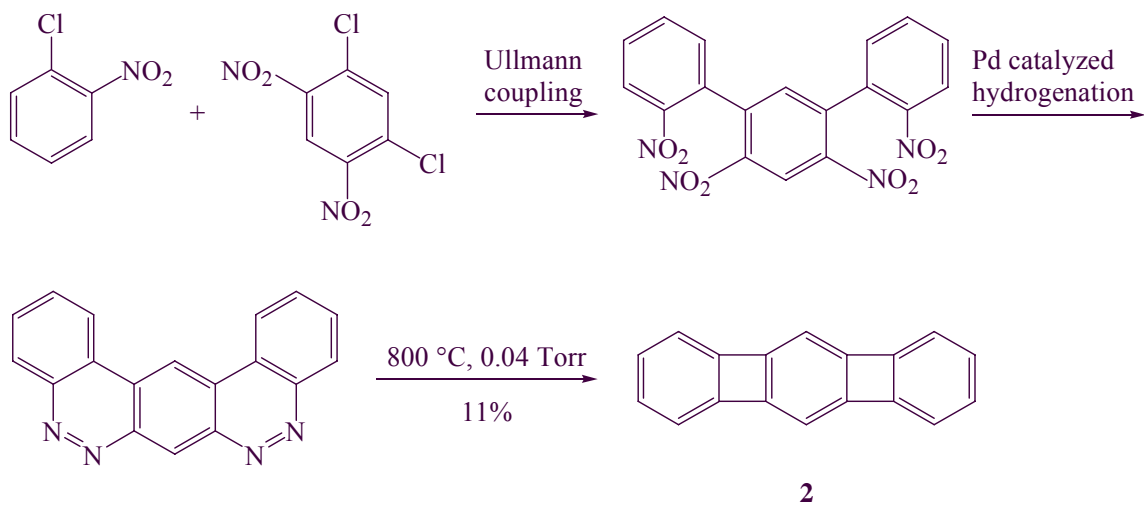
Scheme 1.5 Pyrolytic synthesis of linear [3]phenylene (**2**).
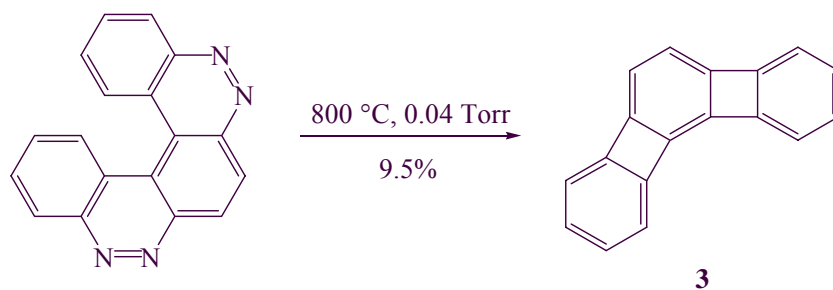

**Scheme 1.6** Pyrolytic synthesis of angular [3]phenylene (**3**).
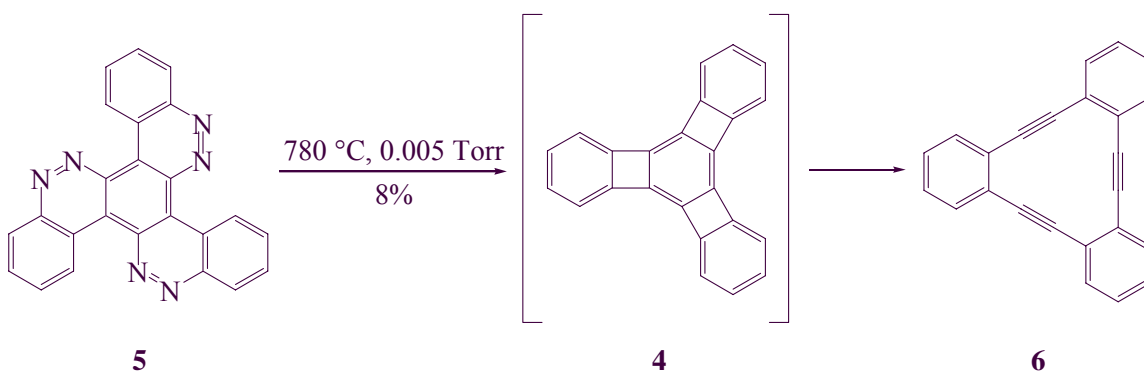
Scheme 1.7 Barton's failed pyrolytic synthesis of triangular [4]phenylene (**4**).

The most general and, for the higher members, only route to the phenylenes is the cobalt-mediated [2+2+2]cycloaddition of *o*-diethynylarenes to alkynes. First used by Rausch in 1981 to synthesize 1,2,4-triphenyl-3-(*o*-phenylethynylphenyl)biphenylene (**7**) from 1,2-bis(phenylethynyl)benzene (**8**) (Scheme 1.8),[17] this method takes advantage of the large amount of energy released when three alkynes are cyclotrimerized to an arene to overcome the strain associated with the generation of the four-membered ring. Subsequently, Gesing reported a very similar reaction, namely the dimerization of 1,2-bis[(trimethylsilyl)ethynyl]benzene (**9**) to 1,2,4-tris(trimethylsilyl)-3-[*o*-(timethylsilyl)-ethynylphenyl]]biphenylene (**10**) in 72% yield (Scheme 1.9).[18] Use of a stochiometric amount of CpCo(CO)$_2$ led to a drastic decrease in the yield of desired product (to 8%) and to the formation of multiple cobalt complexes.
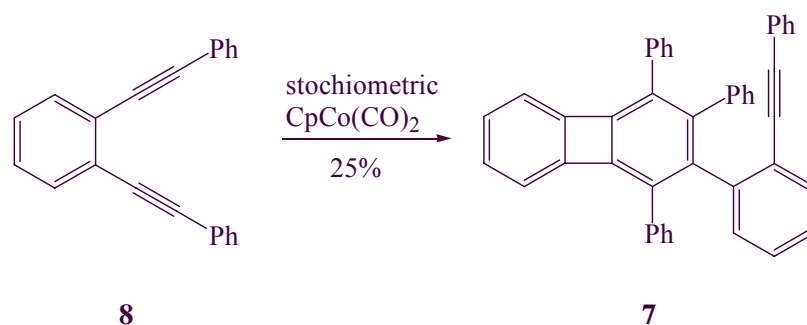

Scheme 1.8 The first reported CpCo(CO)$_2$-mediated cyclotrimerization of alkynes.
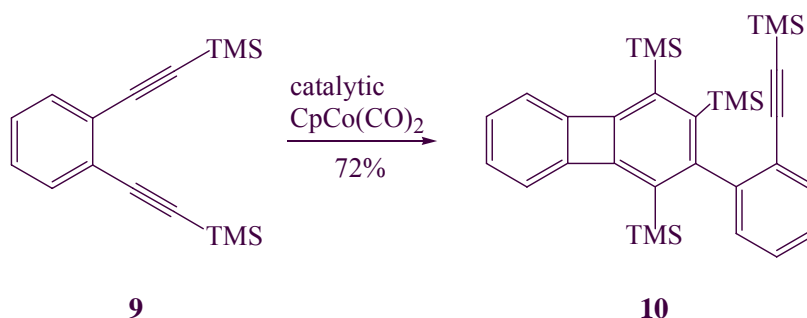
Scheme 1.9 Gesing's CpCo(CO)$_2$-mediated cyclization of **10**.

Shortly after Gesing's publication, Vollhardt et al. demonstrated that this methodology could be generalized. An array of substituted alkynes were co-cyclized with *o*-diethynylbenzene (**11**) to produce 2,3-substituted biphenylenes in yields ranging from 25 to 96% (Table 1.1).[19] The best results were obtained when bis(trimethylsilyl)acetylene (BTMSA) was both solvent and reactant. The purpose of irradiation (employing a white light source during the reaction) was thought to be solely decarbonylative catalyst activation. However, as Chapter 2 will show, light may also affect product distribution.

Table 1.1 Co-cyclization of *o*-diethynylbenzene with substituted alkynes.
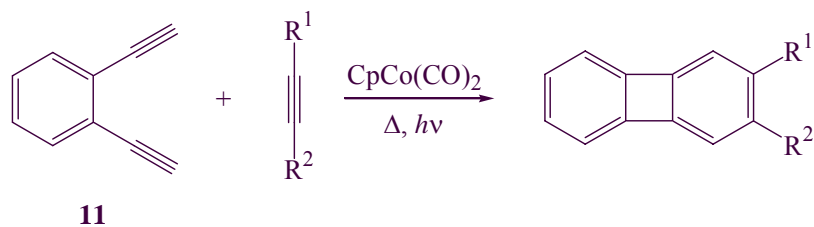
R^1	R^2	Yield(%)
TMS	TMS	96 (run in BTMSA)
TMS	C_5H_{11}	58
H	C_5H_{11}	41
Bu	Bu	44
H	Ph	25
Ph	Ph	35
CO_2Me	CO_2Me	30

Two related cobalt reagents, $CpCo(CO)_2$ and $CpCo(C_2H_4)_2$,[20] have commonly

been used by Vollhardt et al. to perform these cyclizations. Of the two, $CpCo(CO)_2$ has

been used more extensively (and almost exclusively to synthesize phenylenes), primarily

because it is commercially available and less sensitive to air and heat than $CpCo(C_2H_4)_2$.

The synthesis of $CpCo(C_2H_4)_2$ (Scheme 1.10) suffers from highly variable yields and the

product can be very difficult to purify if it is not initially produced cleanly.
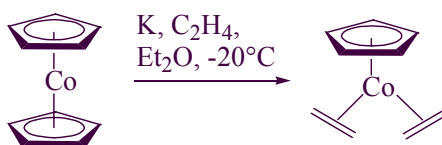
Scheme 1.10 Synthesis of $CpCo(C_2H_4)_2$.

Investigations into the mechanism of the cobalt-mediated [2+2+2]cycloaddition

of alkynes will be one of the main topics of Chapter 2 of this thesis. The proposed

mechanism for this process is shown in Figure 1.5.[21] With either of the $CpCoL_2$ reagents,

the two ligands must be displaced by alkynes before the cyclization can take place.

When L = CO, light or heat are required for the exchange, while simply ambient thermal

conditions may be used when L = C_2H_4. In both cases, after the formation of

$CpCo(C_2H_2)_2$, oxidative coupling can take place to form metallacycle **12**. This 16-

electron species can coordinate another alkyne to generate the saturated

metallacyclopentadiene(alkyne) complex **13**. From this intermediate, two pathways are

typically formulated. One is insertion to give metallacycloheptatriene **14**, which can then

undergo reductive-elimination to generate the $CpCo(\eta^4\text{-arene})$ complex **16**.

Alternatively, **16** may be formed directly (or via intermediate **15**) by a double vinyl shift

(topologically equivalent to an intramolecular Diels-Alder cycloaddition). Decomposition of **16** frees the arene and allows the CpCo-unit to reenter the catalytic cycle. In Chapter 2 of this thesis, the isolation and structural characterization of a metallacyclopentadiene(alkyne) complex analogous to **13** will be reported, providing a key piece of evidence in support of the proposed mechanism.
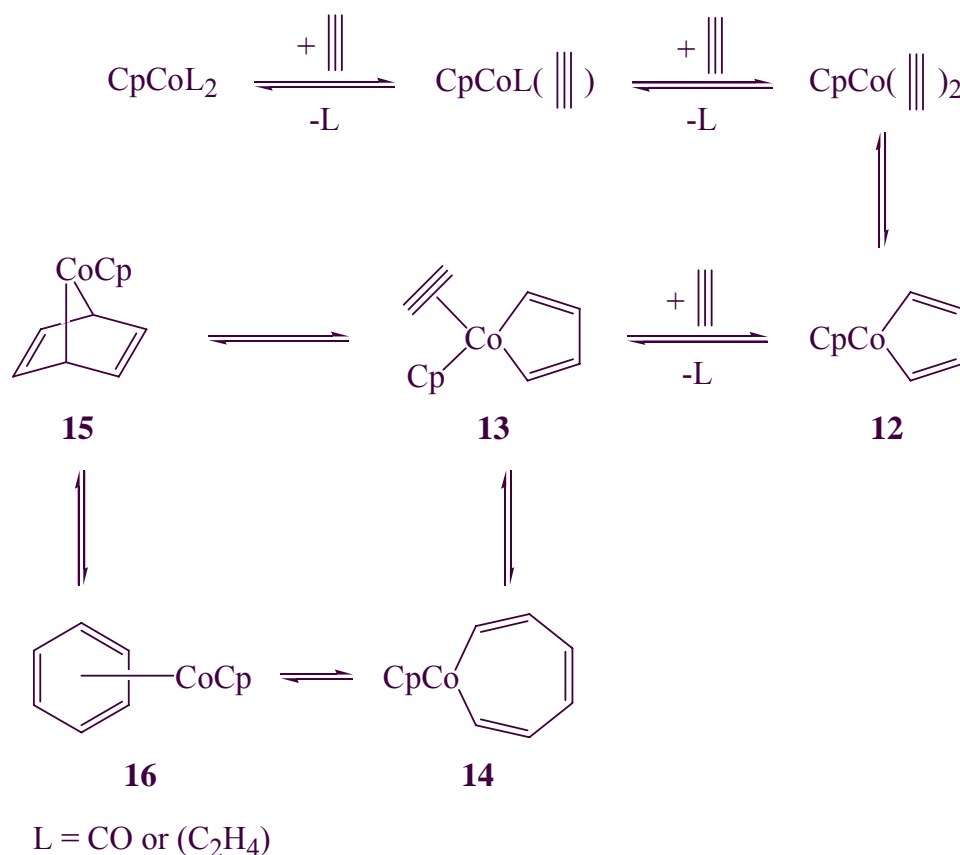

Figure 1.5 The mechanism of CpCo(L)$_2$-mediated [2+2+2]cyclotrimerization of alkynes.

Over the past two decades, cobalt-mediated [2+2+2]cycloaddition methodology has been used to synthesize phenylenes with a wide array of topologies, some examples of which are shown in Figure 1.6.[22] The following section will discuss the synthetic

11

routes used to produce the linear and triangular topologies. In Section 1.4 approaches to angular and zigzag phenylenes will be detailed. Efforts to improve the methodology used to synthesize these types of molecules will be a major topic of discussion in Chapters 2 and 4 of this thesis.

Linear [3]Phenylene (**2**)   Angular [3]Phenylene (**3**)   Triangular [4]Phenylene (**4**)

Zigzag [4]Phenylene (**17**)   Bent [5]Phenylene (**18**)   Helical [7]Phenylene (**19**)
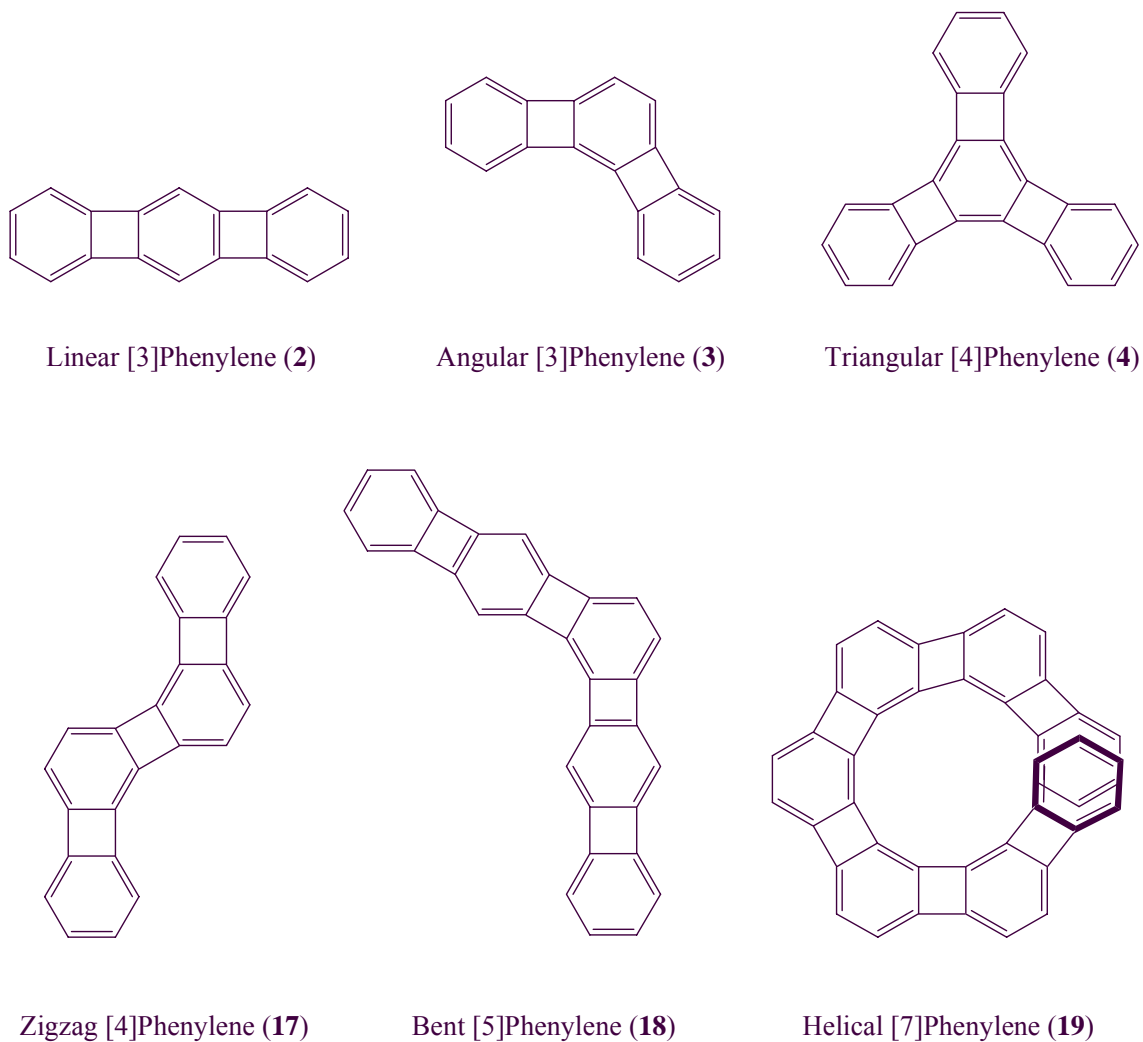
**Figure 1.6** Some phenylene topologies that have been synthesized.

1.3 Synthesis of Linear and Triangular [N]Phenylenes via Intermolecular Cobalt-Mediated [2+2+2]Cycloadditions

The cobalt-mediated [2+2+2]cycloaddition methodology opened new avenues to larger phenylenes.[22a] In a first extension of the strategy to 2,3-bis(trimethylsilyl)biphenylene from **11** (Table 1.1), 2,3-diethynylbiphenylene (**21**) was cyclized with BTMSA to generate substituted linear [3]phenylene (**22**). The starting material necessary for this reaction was produced from **20** in three steps. First, silyl-iodine exchange with ICl led to **23** in 63% yield. Then, a palladium-catalyzed Sonogashira coupling with trimethylsilylacetylene (TMSA), followed by desilylation with KOH, generated **21** in 75% yield (Scheme 1.11).[23] Subjecting **21** and BTMSA to cobalt-mediated [2+2+2]cycloaddition conditions provided silyl-protected linear [3]phenylene **22** in 36% yield, demonstrating the feasibility of an iterative chain extension on route to linear phenylene fragments.
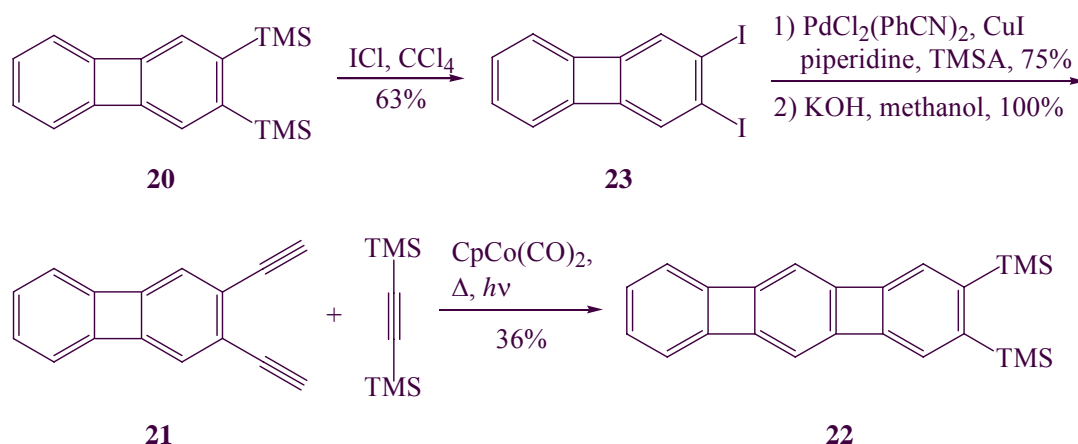
Scheme 1.11 An iterative approach to the linear [3]phenylene frame.

Soon after this iterative approach had been developed, a much shorter route to linear [3]phenylene was found that took advantage of the ability of 1,2,4,5-tetraethynylbenzene (**26**) to cyclize with BTMSA twice (Scheme 1.12). The resulting tetrasubstituted linear [3]phenylene **27** was desilylated under basic conditions to generate the parent system **2**.
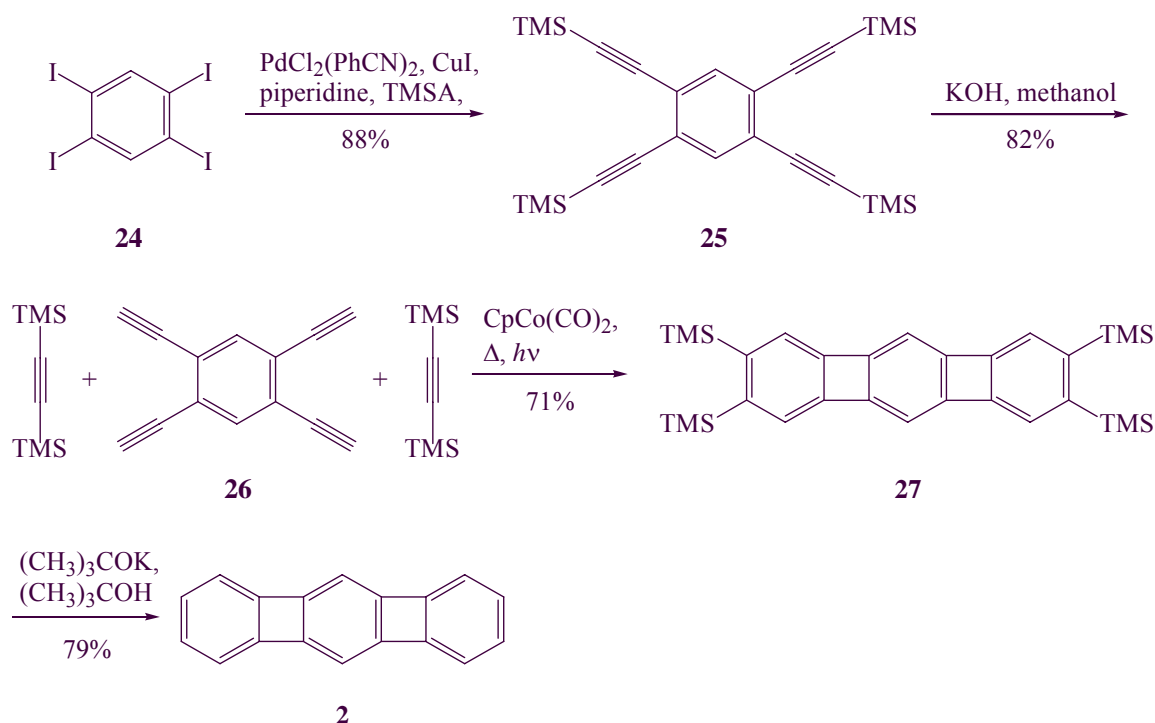
Scheme 1.12 A faster approach to linear [3]phenylene.

Linear [4]phenylene derivative **28** could also be synthesized using the double cobalt-mediated cyclization protocol. Starting with tetrabromobiphenylene **29**, palladium-catalyzed Sonogashira coupling with TMSA, followed by deprotection to **30** and double cycloaddition with BTMSA led to the isolation of a cobalt complex **31** of tetrasilylated linear [4]phenylene (Scheme 1.13).[24] The CpCo-unit could be removed

from **31** by treatment with CO at 120 °C to generate the desired tetrasubstituted linear [4]phenylene **28**.
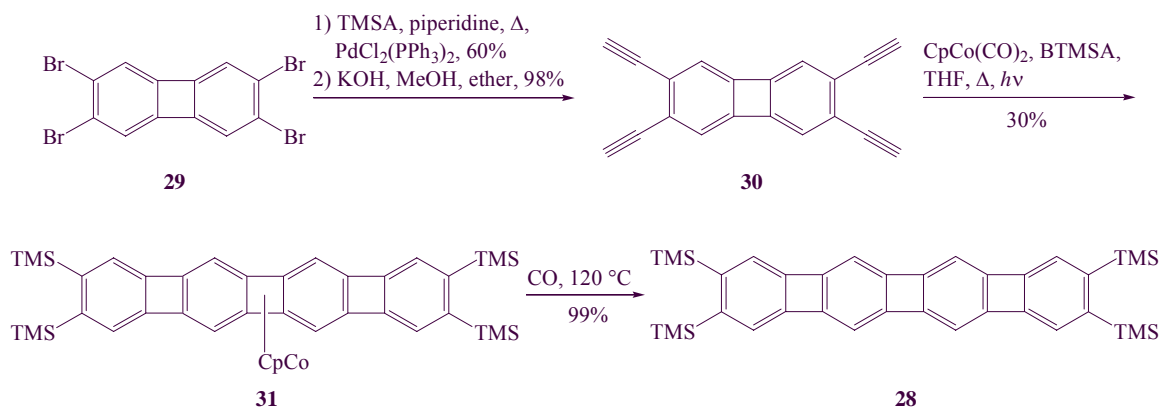
Scheme 1.13 A double cyclization approach to the linear [4]phenylene frame.

The double cyclization schemes employed in the construction of linear [N]phenylenes were extended to triple cyclizations as a means to access C_3-symmetric phenylenes. The key precursor, hexaethynylbenzene (**32**), could be synthesized by Sonogashira coupling of hexabromobenzene with TMSA, followed by deprotection with KF and 18-crown-6 ether.[16,25] Polyethynylbenzenes like **26** and **32** are extremely unstable as solids and **26** has even been known to explode. This problem can be avoided by cyclizing the deprotected alkynes without ever isolating them. Thus, treatment of a solution of **32** generated in situ with BTMSA and CpCo(CO)$_2$ led to the formation of triangular [4]phenylene (**4**) after desilylation with trifluoroacetic acid (Scheme 1.14).
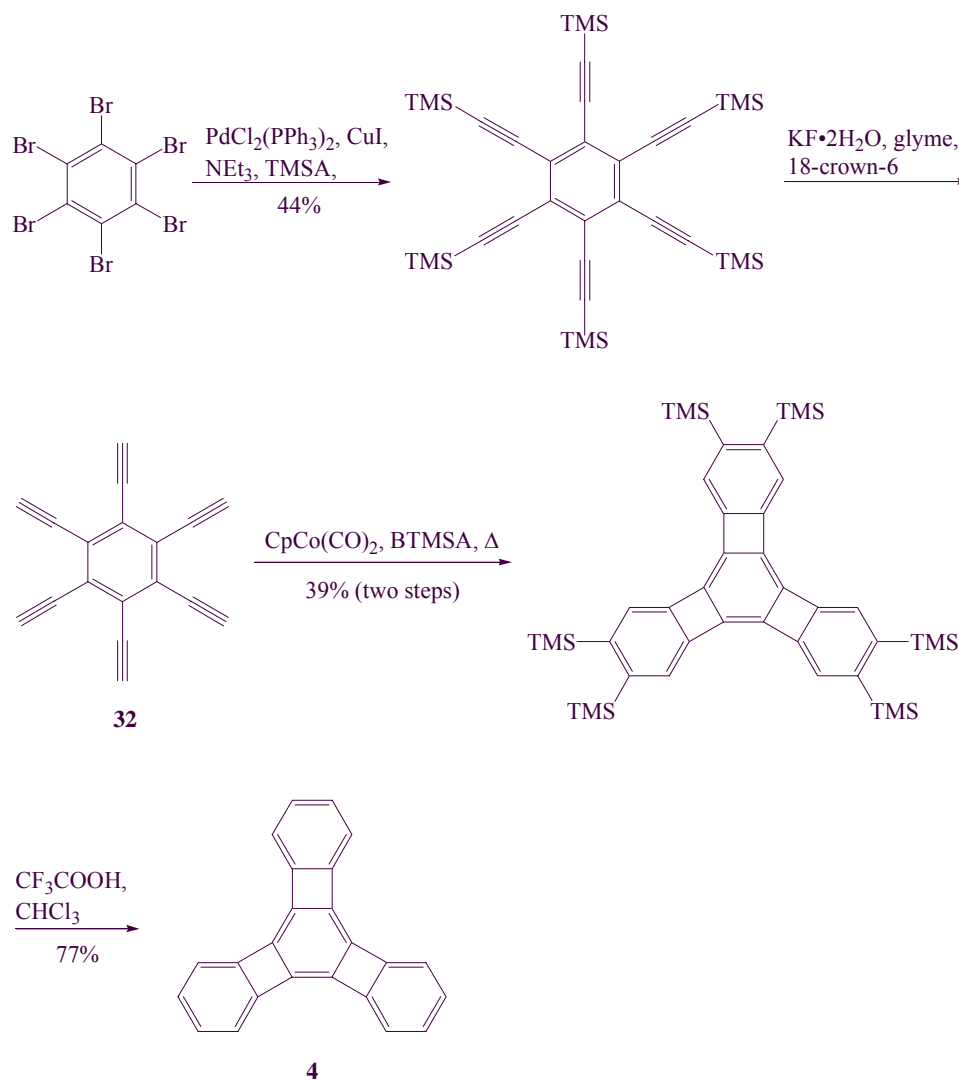
Scheme 1.14 A triple cyclization leads to triangular [4]phenylene.

The preparation of the higher phenylenes was greatly simplified by the discovery

that 1,6-bis[(triisopropylsilyl)ethynyl]-1,3,5-hexatriyne (**33**) could be used as a

cycloaddition partner in the key steps of the syntheses. The large triisopropylsilyl (TIPS)

protecting groups serve to block the terminal triple bonds of **33** to ensure a regioselective

outcome of the cyclization. This selectivity was key to the successful synthesis of the

triangular [7]phenylene frame.[26] Hexaethynylbenzene was cyclized with **33** to generate

the hexaethynylsubstituted triangular [4]phenylene **34**. Desilylation, followed by a second cobalt-mediated cyclization with BTMSA led to the formation of triangular [7]phenylene **35** (Scheme 1.15). The application of an analogous protocol to synthesize linear [5]phenylene from 1,2,4,5-tetraethynylbenzene (**26**) will be discussed in Chapter 4.
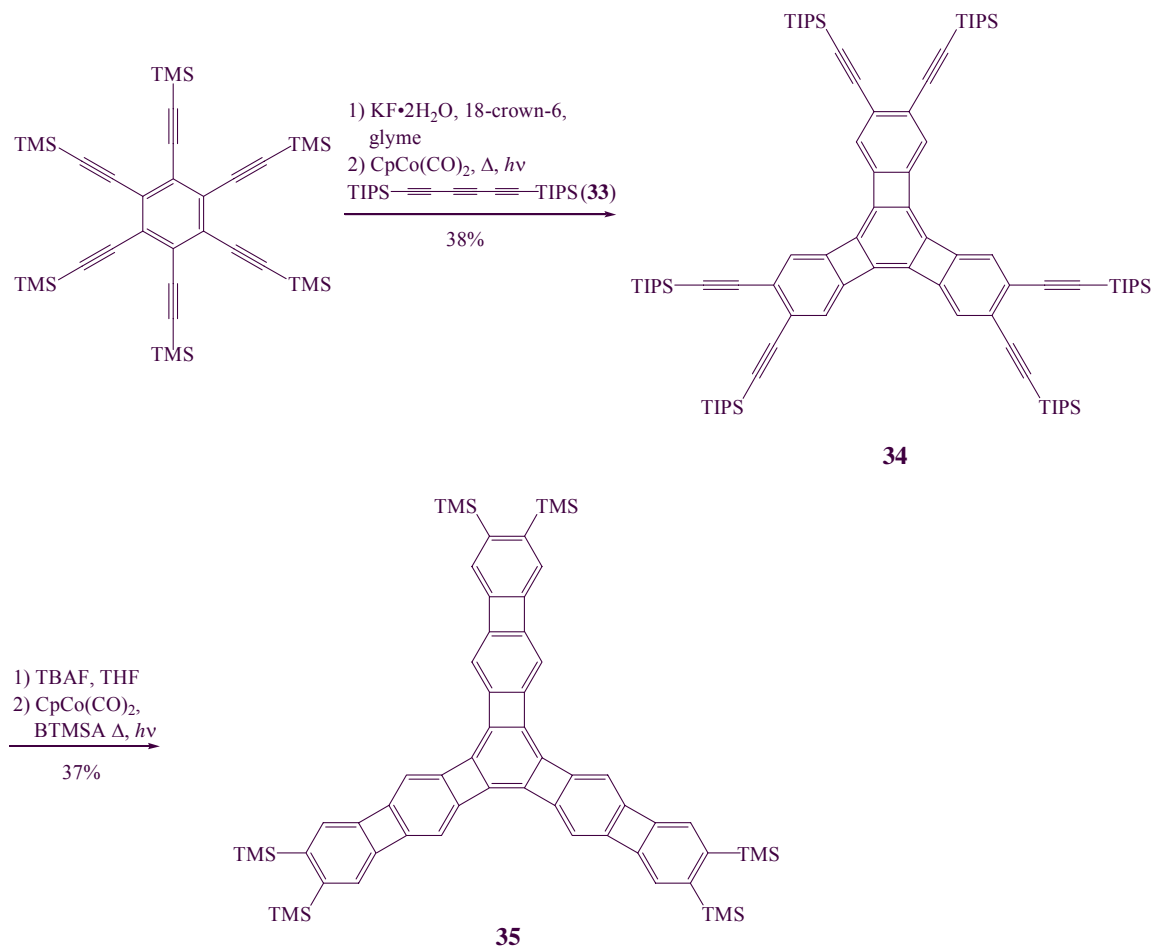
Scheme 1.15 Two triple cyclizations lead to triangular [7]phenylene **35**.

17

1.4 Synthesis of Angular and Zigzag [N]Phenylenes via Intramolecular Cobalt-Mediated [2+2+2]Cycloadditions

Mechanistic investigations relating to the synthesis and thermal behavior of angular phenylenes will be the primary topics of the next two chapters of this dissertation. While linear and triangular phenylenes have been made by intermolecular cobalt-mediated [2+2+2]cycloadditions, their angular counterparts have relied on intramolecular variants. In this way, angular [3]phenylene (**3**) was first made in 1986 from triyne **40** (Scheme 1.16).[27] The later was originally produced in five steps from 1-bromo-2-iodobenzene (**36**). First, a palladium-catalyzed Sonogashira coupling with TMSA followed by desilylation under basic conditions generated 1-bromo-2-ethynylbenzene (**37**). Then, a second Sonogashira coupling with 1-bromo-2-iodobenzene furnished bis(2-bromophenyl)ethyne (**38**). A third palladium coupling, again with TMSA, was followed by desilylation to yield **40**. Its cycloisomerization was effected by slow addition in the presence of $CpCo(CO)_2$ to an irradiated, refluxing solution of xylenes. A substantial improvement of this synthesis was achieved through faster assembly of **38** by coupling acetylene directly with two equivalents of 1-bromo-2-iodobenzene, eliminating two steps (Scheme 1.17).[28]
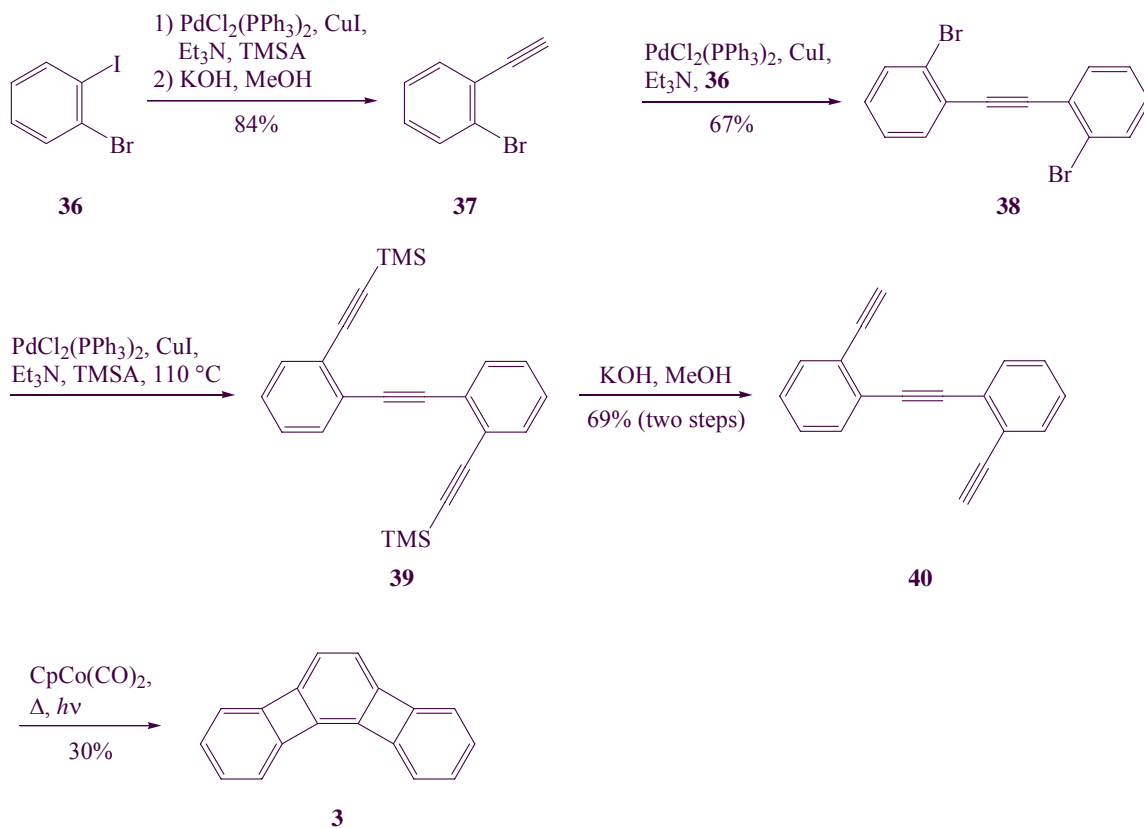
Scheme 1.16 Synthesis of angular [3]phenylene (**3**).
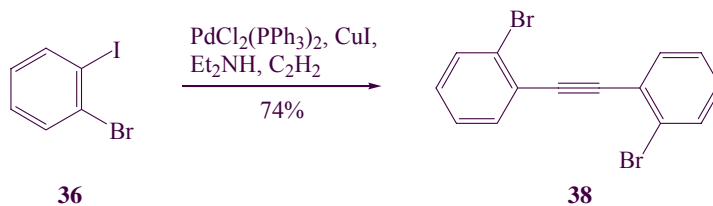
Scheme 1.17 An improved synthesis of **38**.

Larger angular [N]phenylenes can be made by cyclizations of more complicated starting materials. The required precursor for angular [4]phenylene (**47**), triyne **46**, was synthesized in eight steps from **36** (Scheme 1.18).[29] A pair of Sonogashira couplings, first with TMSA, then with (dimethyl)thexylsilylacetylene (DMTSA), led to **41**. The

difference in the sensitivity to basic conditions of the silyl-protecting groups of **41** was exploited to selectively remove only the TMS group. A cobalt-mediated [2+2+2]cycloaddition of **42** formed biphenylene **43**. Next, treatment with ICl generated 1,2-diiodobiphenylene (**44**). This compound is a key intermediate in the synthesis of many of the larger angular phenylenes. Under Sonogashira conditions, it will alkynylate selectively first at the 2- and then at the 1-position. Coupling with TMSA, followed by that with alkyne **42** and desilylation gave **46**, whose cyclization furnished angular [4]phenylene (**47**).
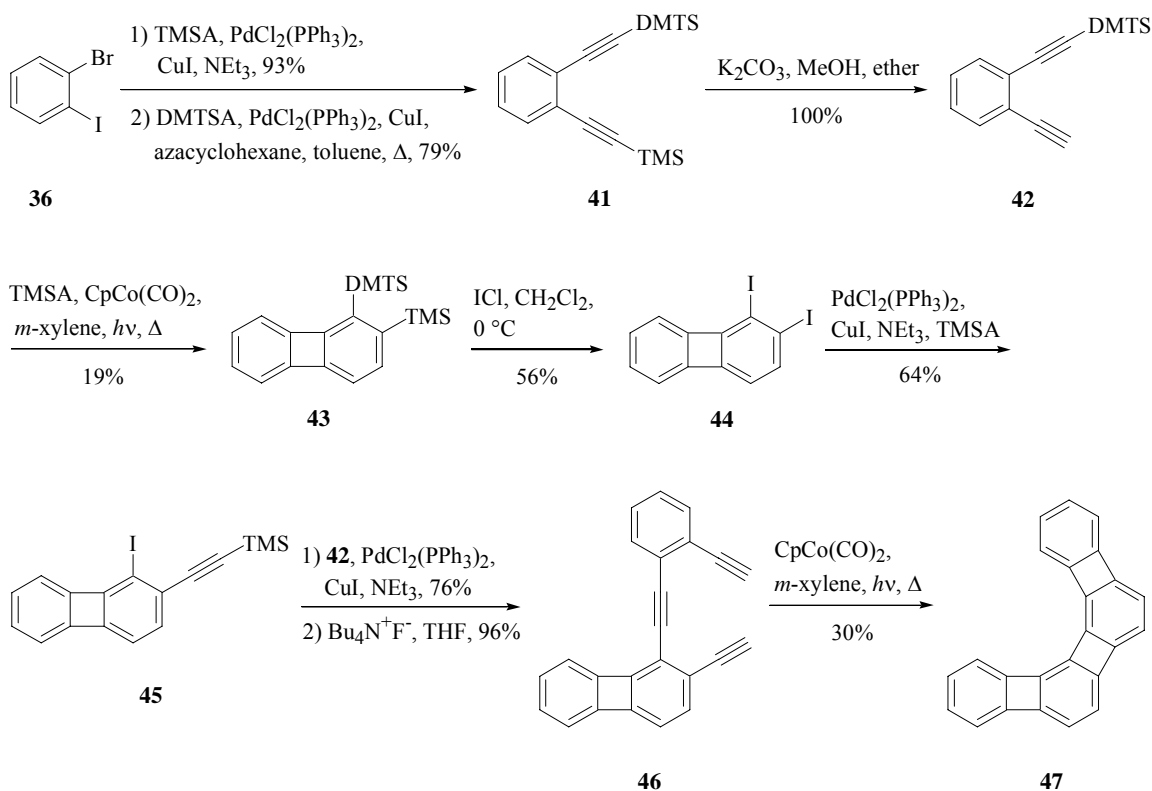
DMTS = (dimethyl)thexylsilyl

Scheme 1.18 Synthesis of angular [4]phenylene (**47**).

A strategic modification to the synthetic route used to synthesize **47** allowed the construction of the zigzag phenylene topology. Starting with **44**, but reversing the order of Sonogashira couplings (first adding **42**, then TMSA), furnished triyne **49** (Scheme 1.19).[22b] Desilylation, followed by cobalt-mediated [2+2+2]cycloaddition, provided zigzag [4]phenylene (**12**).
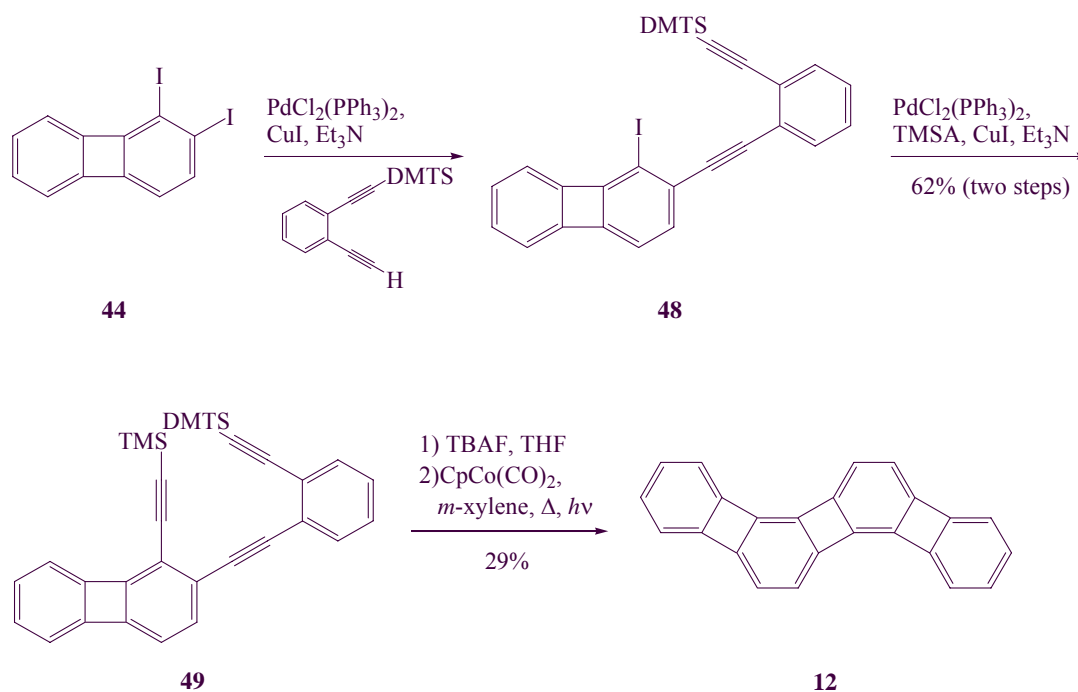
Scheme 1.19 Synthesis of zigzag [4]phenylene.

Extension of this methodology to the double and triple cycloisomerization of appropriate hexa- and nonaynes has allowed the synthesis of zigzag [5]phenylene,[22b] as well as a series of angular phenylenes, culminating in the helical angular [9]phenylene (**51**) made by isomerization of **50** (Scheme 1.20).[22d]

21
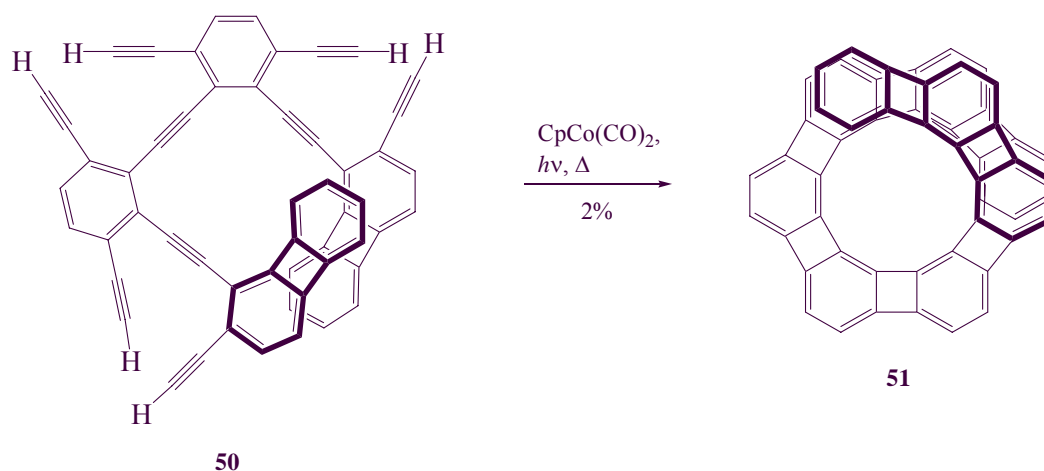
Scheme 1.20 A triple cyclization leads to helical [9]phenylene.

These types of synthetic pathways have been used to produce a large number of phenylenes. Two of the tools employed in the study the properties of these products, X-ray crystallography and NMR spectroscopy, will be the focus of the next sections, to prepare the reader with the necessary background for the further advances made in this thesis.

1.5 X-Ray Crystal Structures of Phenylenes

Among the criteria that have been used to evaluate the aromaticity of a molecule are resonance stabilization energy, planarity, reactivity, bond non-alternation, and magnetic effects. This thesis will discuss the tools used to investigate the last two criteria: X-ray crystallography (this section) and Nuclear Magnetic Resonance (next section).

The X-ray crystal structure of biphenylene (**1**) reveals an average difference in length between the long and short bonds in the benzene rings (ΔD) of 0.048 Å (Figure 1.4). This number is roughly half that calculated for an idealized cyclohexatriene (0.111 Å).[30] Historically, this bond alternation was initially believed to be caused solely by the molecule's desire to minimize cyclobutadienoid/ benzocyclobutadienoid circuits. More recently, in addition to this π effect, strain induced bond localization (SIBL) was recognized to play an important role. Here, the σ distortions generated by fusing a four-membered ring to benzene will have a similar effect.[31] A hybridization change occurs to accommodate the required 90° angles, resulting in increased *p*-character in the C1-C6, C1-C12, C6-C7, and C7-C12 bonds (see Figure 1.7 for labeling) and more *s*-character in the C1-C2, C5-C6, C7-C8, and C11-C12 bonds. This difference in hybridization will cause the C1-C6 bond to be shorter than the C1-C2 bond. Stanger has argued that the bond alternation observed in phenylenes is entirely due to SIBL,[32] but it seems more reasonable that the truth lies closer to the roughly equal contribution of σ and π effects calculated by Streitwieser et al.
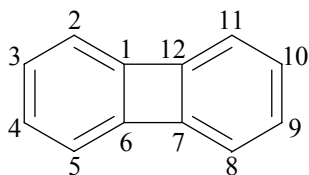
Figure 1.7 Numbering scheme used in discussion of biphenylene.

Angular benzocyclobutadienofusion reinforces the bond localization observed for

1. An X-ray crystal structure (Figure 1.8) shows the central benzene ring of **3** even more

highly bond fixed than that of **1** ($\Delta D = 0.099$ Å), while little bond alternation is observed

at the termini ($\Delta D = 0.035$ Å).
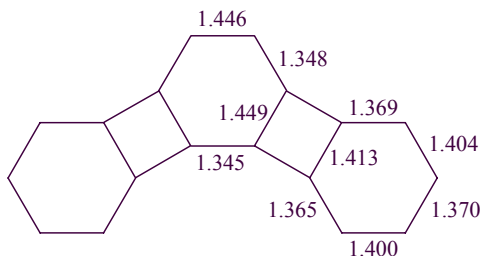
Figure 1.8 Bond lengths for **3** (Å).

Perhaps the most dramatic example of the tradeoff between aromaticity and

antiaromaticity is seen in triangular [4]phenylene (**4**, Figure 1.9).[33] By completely

sacrificing aromaticity in the center ($\Delta D = 0.154$ Å), the three terminal rings in **4** are

maximally aromatic ($\Delta D = 0.034$ Å).

24
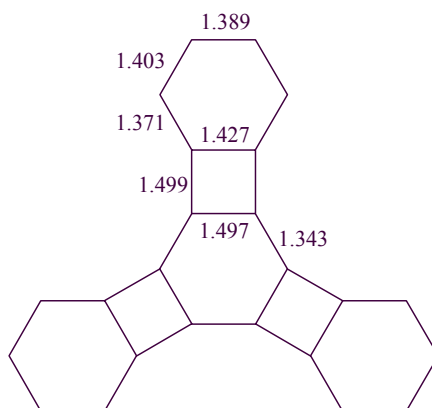
Figure 1.9 Averaged bond lengths for **4** (Å).

The X-ray crystal structure of linear [3]phenylene (**2**, Figure 1.10)[34] reveals relatively little bond alternation in the central ring as a result of the counteracting effects of linear fusion. With a linear phenylene, it is much harder for the molecule to reduce antiaromaticity by distorting (there is no resonance structure that can be drawn that does not contain a cyclobutadienoid circuit). This results in the benzene rings retaining much of their aromaticity, but this comes with the cost of significant antiaromaticity in the four-membered rings, a conclusion supported by NICS data (Section 1.7). Structurally, the compromise of linear fusion is (logically) a bisallyl system, linked by long bonds.
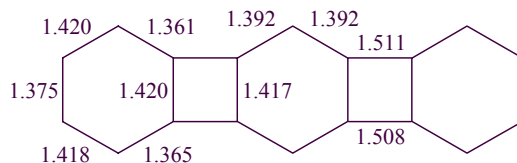
Figure 1.10 Averaged bond lengths for **2** (Å).

Recent results by Vollhardt et al. have greatly increased the number of angular [N]phenylenes for which crystal structures have been obtained. In Section 2.3 of this

thesis, the X-ray crystal structure of angular [4]phenylene (**47**) will be presented, which will allow a discussion of bond alternation in angular [3-8]phenylenes.

1.6 NMR Spectroscopy of Phenylenes

Magnetic effects, measured mostly by ^{1}H NMR spectroscopy, are a more general, and by far more invoked criterion of aromaticity than bond localization. The location of an ^{1}H NMR signal is highly sensitive to the magnetic environment of the observed proton. An aromatic circuit produces a diamagnetic ring current, deshielding protons located on the outside of the ring.[2,35,36] Decreasing the aromaticity of a circuit leads to increased shielding of its external protons. The protons on benzene, the archetypal aromatic molecule, resonate at δ 7.36 in $CDCl_3$,[37] while the protons on biphenylene (**1**), which are in a less aromatic environment, resonate significantly upfield of this value at δ 6.60 and 6.70 (Figure 1.11). Significantly, H2 (see Figure 1.7 for labeling) is at a higher field than H3, a shift caused by the paratropism of the neighboring four-membered ring. Nucleus-independent chemical shifts (NICS) calculations, a theoretical method of quantifying magnetic information, confirm the strong paratropism of this ring (Figure 1.11).[38]

Angular benzocyclobutadienofusion to **1**, which generates **3**, decreases the aromaticity of the central benzene ring, resulting in a greater NICS value for this ring and increased shielding of its protons (Figure 1.11). This decrease allows greater aromaticity to be present in the neighboring terminal benzene rings, consistent with the lower NICS values and proton deshielding observed. The angular [N]phenylenes show a strong correlation between degree of bond fixation and proton shielding. In Figure 1.12, the average proton chemical shifts of angular [3-6]phenylenes are plotted versus bond fixation. While there is scatter, the trend is unmistakable.
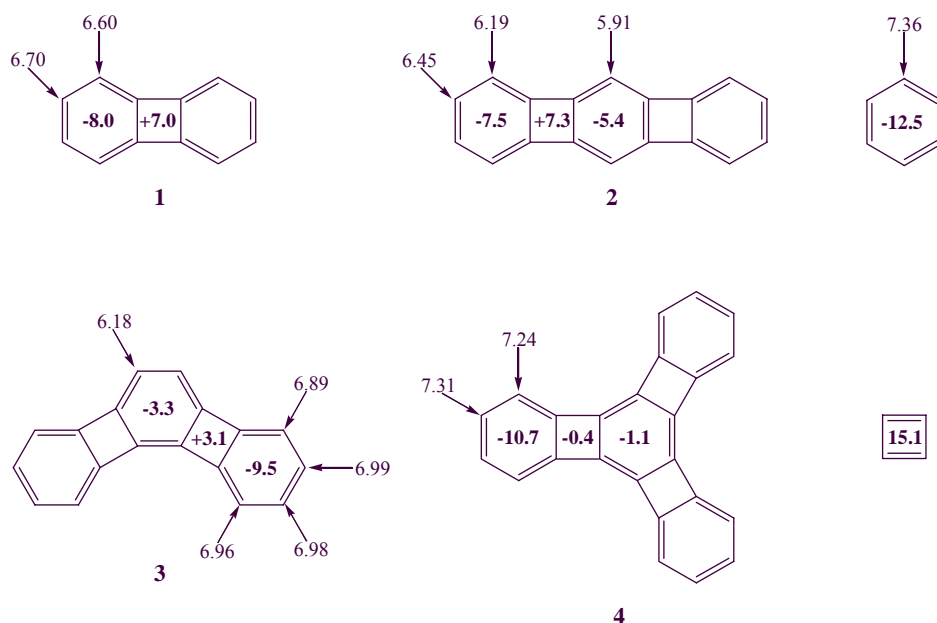
Figure 1.11 ^{1}H NMR chemical shifts in ppm and NICS(1) values of **1-4**, benzene, and cyclobutadiene. The NICS(X) value for a ring provides information about the magnetic shielding at a point X Å above the ring centroid. A negative NICS value indicates aromaticity, while a positive NICS value denotes antiaromaticity.
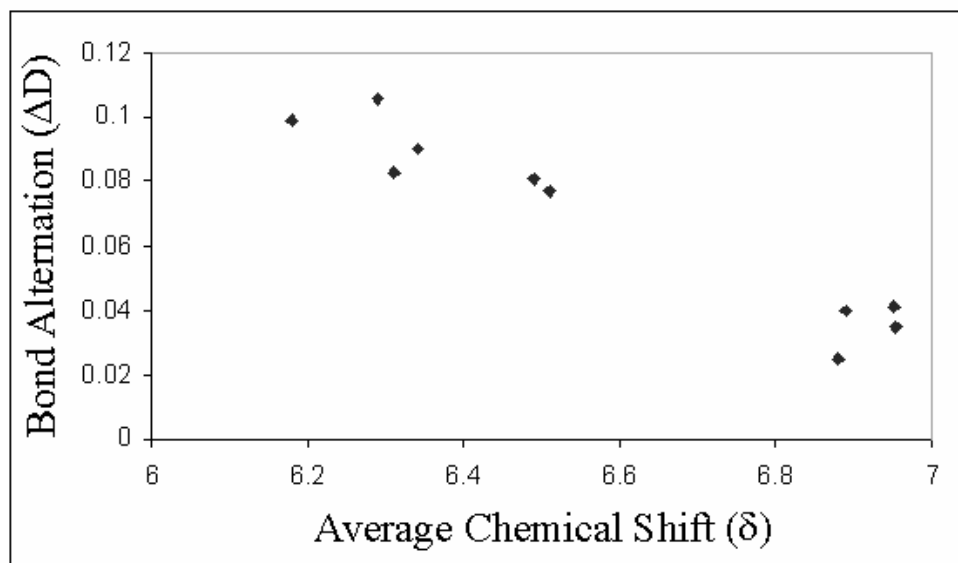
Figure 1.12 A plot of bond alternation (in Å) vs. average ^{1}H NMR chemical shifts (δ, in CD_2Cl_2) in the benzene rings of angular [3-6]phenylenes.

As was discussed in the previous section, the inner benzene ring of triangular [4]phenylene (**4**) is almost completely bond fixed, allowing the terminal rings to be highly aromatic. The lack of a proton on the central ring of **4** prevents ^{1}H NMR information from being obtained, but the large downfield shift relative to **1** of the protons on the terminal rings (Figure 1.11) is consistent with the highly aromatic environment suggested by the X-ray crystal structure and NICS calculations.

With linear [3]phenylene (**2**), the protons on the central ring are shielded relative to those on the terminal rings. According to NICS calculations, this central ring is still highly aromatic. The source of the shielding of the central ring's protons are the two adjacent highly paratropic cyclobutadiene rings. The cyclobutadiene rings also shield the α-protons on the terminal rings of **2** by δ 0.26 relative to the β-protons. The protons on the central rings of the larger linear [N]phenylenes are even more shielded (δ 5.89 for N = 4, δ 5.56 for N = 5), consistent with NICS calculations which find decreased aromaticity in these rings and increased paratropism of the neighboring cyclobutadiene rings.

^{13}C NMR spectroscopy is not useful in evaluating the aromaticity because of the position of the carbon frame relative to the locally induced magnetic field and the large chemical shift range. The δ values for biphenylene (**1**)[22a] and angular [3]phenylene (**3**)[39] are presented in Figure 1.13. Most diagnostic are the quaternary carbon resonances near δ 150, which are deshielded relative to normal aromatic rings, and the shielding effect of bond alternation (rehybridization) on these carbons.
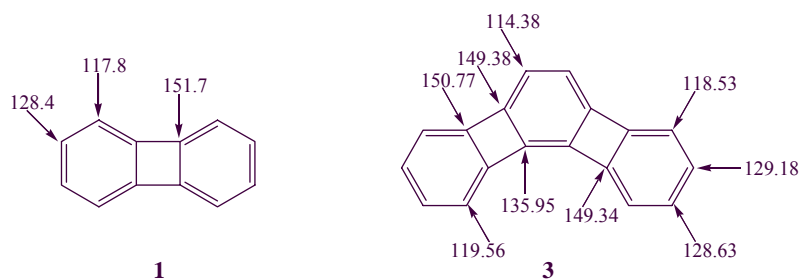
Figure 1.13 ^{13}C NMR data of **1** (δ, in CDCl$_3$) and **3** (δ, in CD$_2$Cl$_2$).

The information presented in this section, especially the very different explanations for the similar chemical shifts of the central ring protons on **2** and **3**, makes it clear that a wide range of theoretical and experimental techniques must be applied in order to fully understand the phenylenes. To this end, a number of reactivity studies have been conducted with the phenylenes, and these experiments will be the topic of discussion in the next section of this thesis.

1.7 Reactivity of Phenylenes

While the reactivity of phenylenes in solution is not a primary focus of this thesis, to provide context for some of the chemistry to be described, a brief overview of this subject will be presented in this section. This topic is relatively unexplored, and relatively extensive studies have been executed for only **1-4**. The parent molecule, biphenylene (**1**), undergoes a range of electrophilic aromatic substitution reactions regioselectively at the β-position. Two of these reactions, bromination and Friedel-Crafts acylation, are shown in Scheme 1.21.[40]
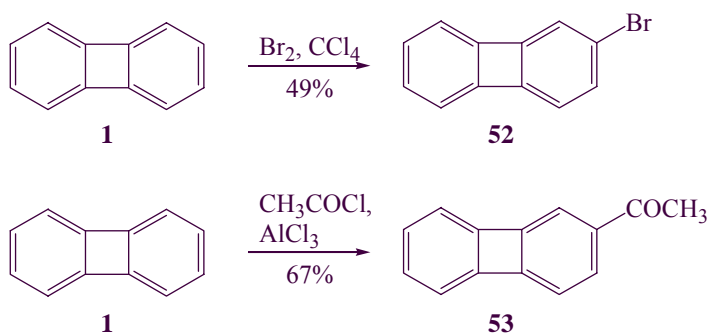
Scheme 1.21 Bromination and Friedel-Crafts acylation of biphenylene (**1**) occur regioselectively.

With larger phenylenes, which all have at least one benzene ring that is less aromatic than those of **1**, electrophilic aromatic substitution is replaced by addition. Hydrogenation, which is typically very slow in fully benzenoid systems, is facile for **2** and **4**,[41] occurring stereo- and regioselectively at the most activated benzene ring (Scheme 1.22). The ease of hydrogenation of **3** is somewhat attenuated and requires more forcing conditions (Scheme 1.23). The highly bond fixed central ring of **4** reacts like a cyclohexatriene. In addition to hydrogenation, epoxidation and cyclopropanation

occur under mild conditions (Scheme 1.24).[42] In both cases, the resulting products are all

cis-substituted.
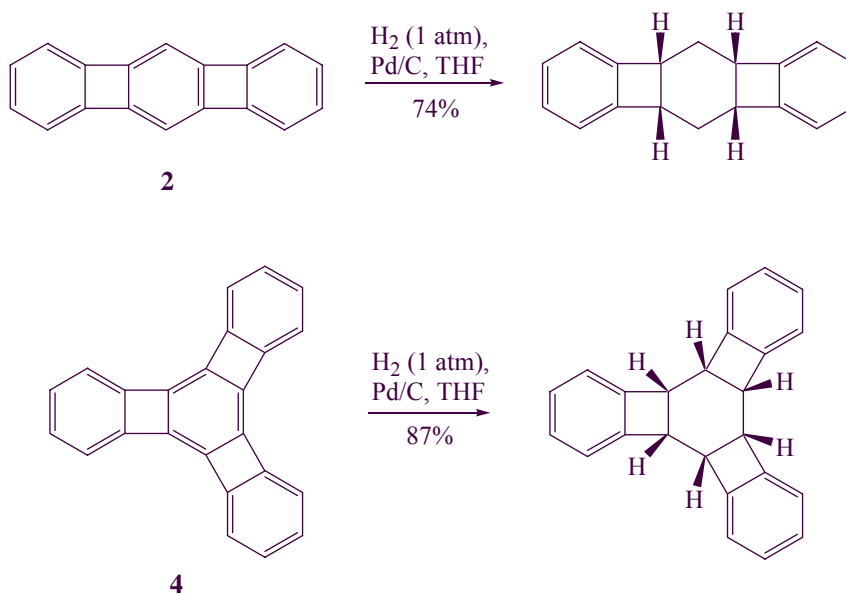
Scheme 1.22 Hydrogenation of **2** and **4** occurs under mild conditions.
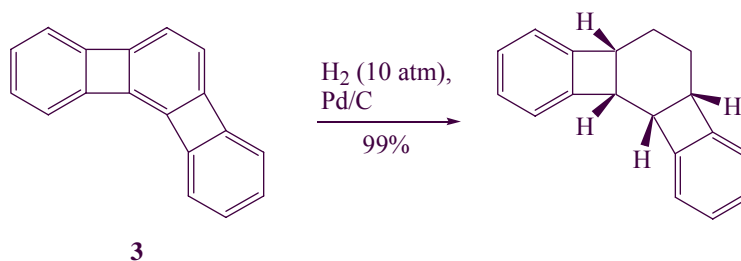
Scheme 1.23 Hydrogenation of **3** requires harsher conditions.

Reactions that disrupt the σ-frame of a phenylene have also been found to take place. Two examples of this can be observed with **27**, which undergoes oxidation when left standing in the presence of O_2 (Scheme 1.25)[43] and metal insertion when heated with

Fe$_2$(CO)$_9$ (Scheme 1.26). Further examples of the reactivity of the phenylenes will be discussed within the context of the investigations presented in the following chapters.
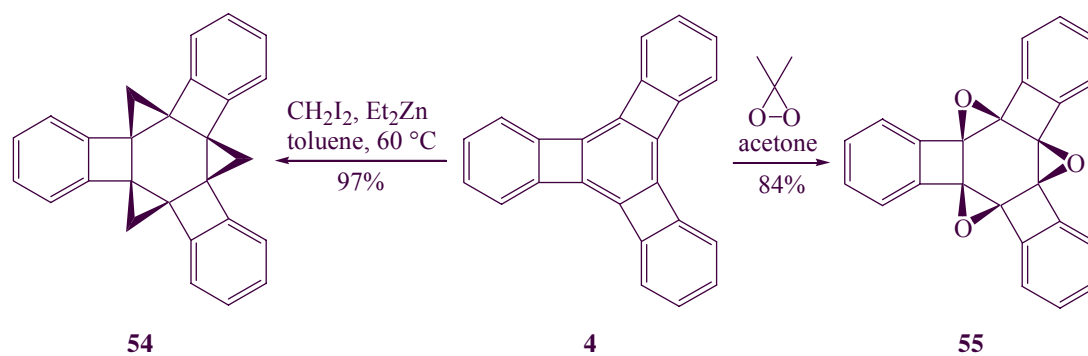
Scheme 1.24 The central ring of **4** reacts like a cyclohexatriene in (oxa)cyclopropanations.
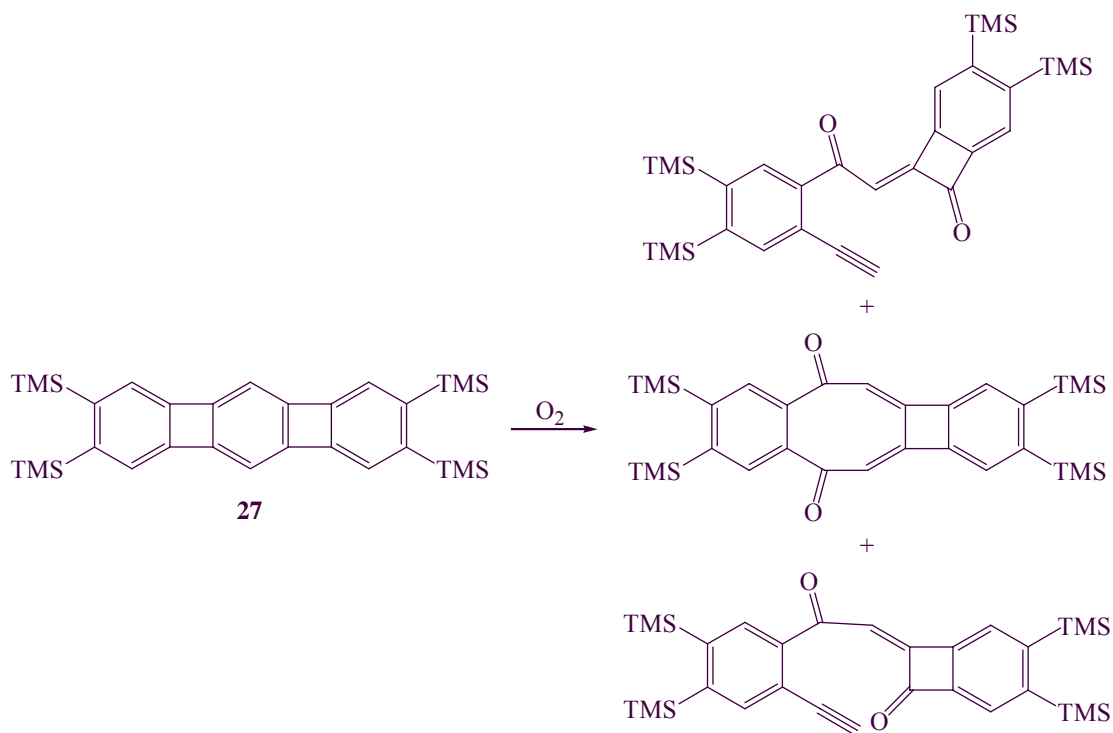
Scheme 1.25 Oxidation of **27** with O$_2$ forms a mix of products.
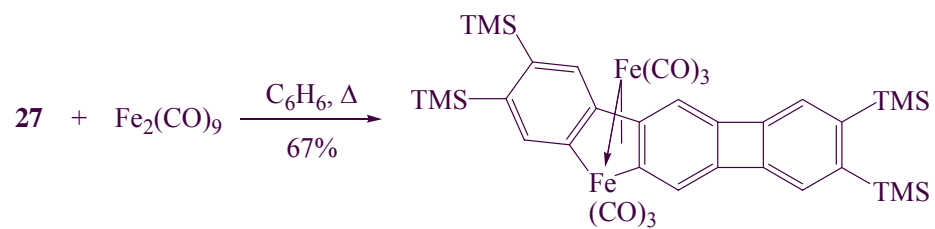
Scheme 1.26 Insertion occurs when **27** is heated with $Fe_2(CO)_9$.

Chapter Two

Cobalt-Mediated Synthesis of Phenylenes: Improved Methodology and Structural Characterization of a Metallacyclopentadiene(Alkyne) Intermediate on the Way to Angular [4]Phenylene

2.1 Introduction

Until recently, nearly all the published cobalt-mediated syntheses of phenylenes have used $CpCo(CO)_2$ as a catalyst. While $CpCo(CO)_2$ has the practical advantage of being commercially available, it suffers from a serious drawback: light and/or high heat are required to facilitate dissociation of the carbonyl ligands (Figure 1.4). Such ligand dissociations are much more facile for $CpCo(C_2H_4)_2$, a property that can lead to increased yields and selectivity of the [2+2+2]cycloaddition.[44] In some cases, $CpCo(C_2H_4)_2$ has been found to be superior to $CpCo(CO)_2$, even under the same conditions. For example, substitution of $CpCo(C_2H_4)_2$ for $CpCo(CO)_2$ increased the yield of the products of the cycloaddition of BTMSA to pyrrole **56** from 64% to 92% (Scheme 2.1).[45]

The first application of $CpCo(C_2H_4)_2$ in the construction of phenylenes was made in 1986, as part of a study of the synthesis and properties of angular [3]phenylene (**3**). Diercks and Vollhardt reported that **3** could be synthesized in 70% yield from **40a** in two steps. Triyne **40a** was first treated with $CpCo(C_2H_4)_2$ at −30 °C and then heated to 100 °C under a CO atmosphere. A more detailed study came years later during a mechanistic

investigation of the cobalt-mediated [2+2+2]cycloaddition of alkynes.[46] Treatment of

triyne **40a** with CpCo(C$_2$H$_4$)$_2$ at low temperatures (-20 to -23 °C) led to the generation of

57a (Scheme 2.2). Metallacyclopentadienes coordinated to alkynes, such as **57a**, had

long been postulated as key intermediates in metal-catalyzed cyclotrimerizations of

alkynes, but **57a** was the first such mononuclear complex isolated. The proposed

structure for **57a** was based on spectroscopic and reactivity data, but no crystal structure

could be obtained to confirm it. Several related compounds (**57b-e**) were synthesized in

an attempt to find a more crystalline derivative, but these efforts proved futile.[46]

L	yield (%)	
CO	51	13
C$_2$H$_4$	74	18
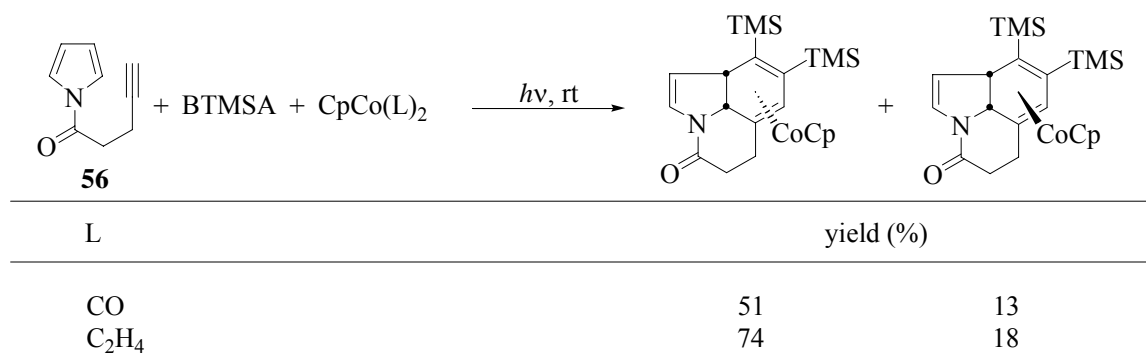
Scheme 2.1 Cobalt-mediated cocyclization of **56** with BTMSA.

40a (R = H)
40b (R = *i*-Pr)

57a (R = H, Cp' = C$_5$H$_5$)
57b (R = H, Cp' = C$_5$Me$_5$)
57c (R = H, Cp' = C$_5$H$_4$Me)
57d (R = H, Cp' = indenyl)
57e (R = *i*-Pr, Cp' = C$_5$H$_5$)
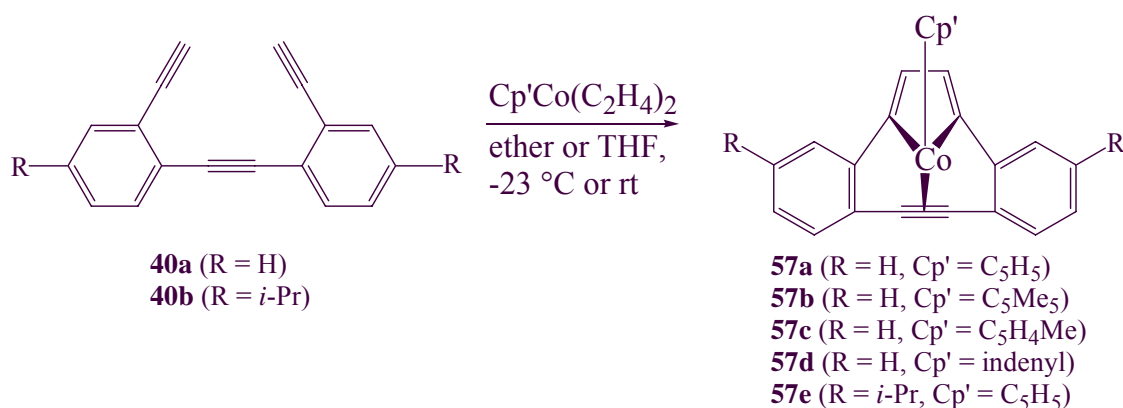
Scheme 2.2 Synthesis of metallacyclopentadiene(alkyne) complexes **57a-e**.

The metallacyclopentadiene(alkyne) complex **57a** furnished angular [3]phenylene (**3**) upon thermolysis (Scheme 2.3). This process was believed to occur via the CpCo-angular [3]phenylene complex **58a**, from which **3** was displaced by added external ligands or solvent. Under the conditions used for the thermolysis (100-130 °C), the presence of an active CpCo species appears to be hazardous to the desired product. Jones et al. found that Cp*Co(C$_2$H$_4$)$_2$ inserted into biphenylene (**1**) when heated to 83 °C (Scheme 2.4).[47] Similarly, Jalisatgi observed that **3** and CpCo(C$_2$H$_4$)$_2$ at 80 °C formed the unusual complex **59**, whose structure was confirmed by X-ray crystallography (Scheme 2.5).[48] These undesired side reactions can be minimized by the addition of an external ligand, such as CO or hexamethylbenzene, which can trap reactive CpCo species, allowing the conversion of **57a** to **3** to proceed more cleanly.
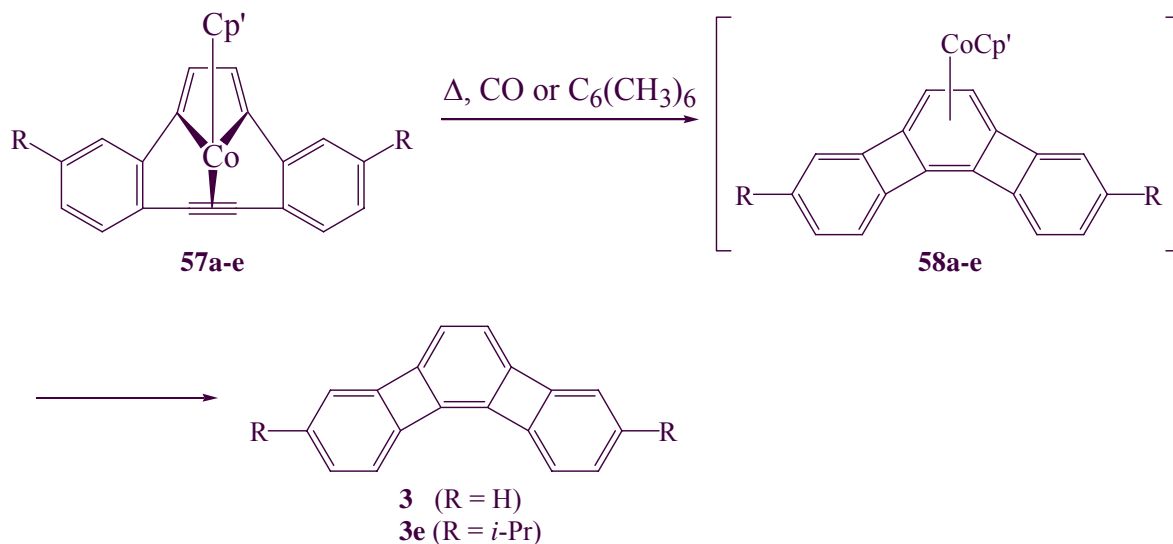
Scheme 2.3 Thermal conversion of complexes **57a-e** to angular [3]phenylenes.
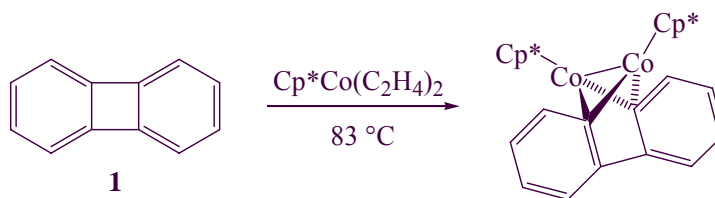
Scheme 2.4 Cp*Co(C$_2$H$_4$) inserts into biphenylene (**1**) at elevated temperatures.
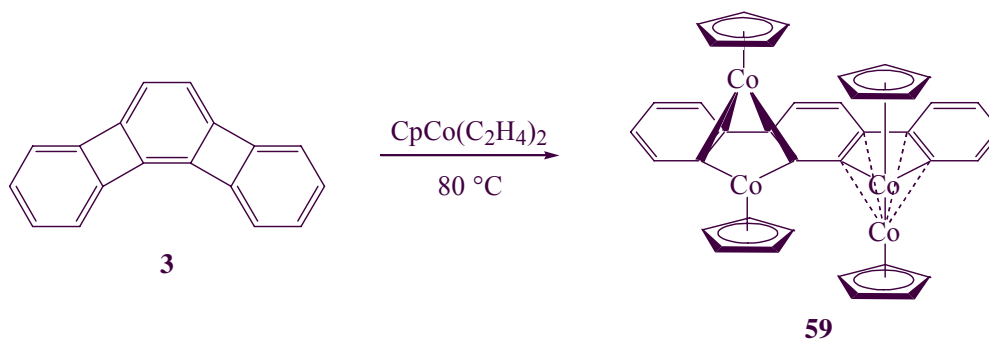
Scheme 2.5 CpCo(C$_2$H$_4$) reacts with angular [3]phenylene (**3**) at elevated temperatures.

While the hypothesized intermediate **58a** could not be isolated during the conversion of **57a** to **3**, the analogous Cp* complex **58b** was obtained upon heating **57b** to 85 °C. This molecule was successfully characterized by X-ray crystallography (Figure 2.1). In this 18-electron complex, the cobalt is bound in an η^4-fashion to the central benzene ring of the angular [3]phenylene. This stands in contrast to the CpCo-linear [N]phenylene complexes that have been isolated, which have all involved CpCo's ligated to the cyclobutadiene rings (see Chapter 4).
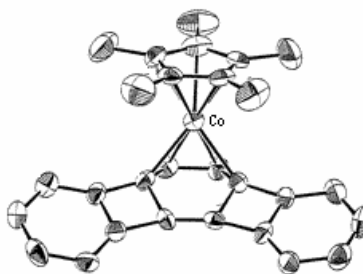
Figure 2.1 X-ray crystal structure of **58b**.

This chapter will describe methodology using CpCo(C$_2$H$_4$)$_2$ developed to improve access to angular phenylenes (Section 2.2), as well as to synthesize the previously unknown *anti*-doublebent [5]phenylene (Section 2.5). An X-ray crystal structure of angular [4]phenylene (**47**) will be presented in Section 2.3, which will allow a discussion of the structural details of a series of angular phenylenes. In Section 2.4, the synthesis and structural characterization of an angular [4]phenylene analog of **57** will be described.
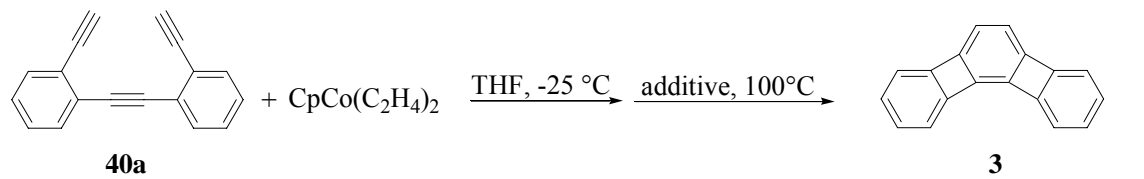
2.2 Synthesis of Angular [3]- and [4]Phenylenes Using CpCo(C₂H₄)₂

While conducting a labeling study into the behavior of phenylenes under flash vacuum pyrolysis conditions (Chapter 3), it became necessary to synthesize $^{13}C_2$-labeled angular [3]phenylene (**3f**) from $^{13}C_2$-labeled triyne **40f** (Scheme 2.6). The reported method, slow addition of **40** and CpCo(CO)₂ to irradiated, refluxing *m*-xylene, proceeded in 30% yield (Scheme 1.16). Unfortunately, these yields were difficult to reproduce, varying from 15 to 25%. In the hope of developing a higher yielding, more reproducible synthetic method, CpCo(C₂H₄)₂ was investigated as a mediator for this reaction. The previous syntheses of **3** using CpCo(C₂H₄)₂ were reported to proceed cleanly,[27,46] but had seemingly been restricted to NMR-scale experiments. Attempts to repeat such an experiment [e.g., treatment of **40a** with CpCo(C₂H₄)₂ at –25 °C, followed by thermolysis at 100 °C in the presence of the CpCo trap hexamethylbenzene] on a synthetic scale (0.16 mmol), resulted in only 26% isolated yield of **3** (Table 2.1). Several other additives were tried, the most effective of which, 1,3-cyclohexadiene, allowed **3** to be synthesized in 32% yield. When this reaction was repeated using $^{13}C_2$-labeled triyne **40f**, $^{13}C_2$-labeled angular [3]phenylene **3f** was obtained in 30% yield.

3f   40f
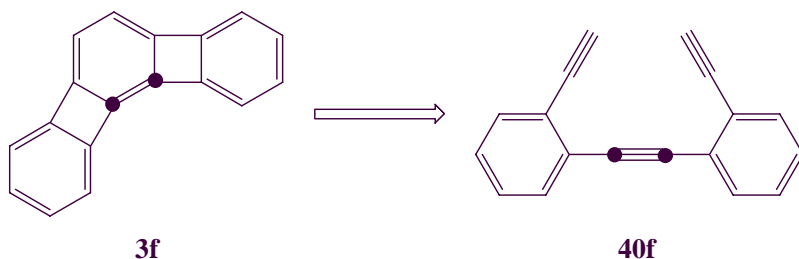
Scheme 2.6 A reliable method of synthesizing **3f** from **40f** needed to be developed.

Table 2.1 The application of additives during the CpCo(C$_2$H$_4$)$_2$-mediated cyclization of **40a**.

Additive	yield (%)
Hexamethylbenzene	26
TMEDA	26
TMEDA (DME used as solvent)	23
1,3-Cyclohexadiene	32
1,3-Cyclohexadiene (with **40f**)	30

To further investigate the use of CpCo(C$_2$H$_4$)$_2$ in phenylene synthesis, triyne **46**, the precursor to angular [4]phenylene **47**, was synthesized (Scheme 1.18) and subjected to cyclization conditions. The yield of **47** was 51% (Scheme 2.5), significantly higher than the 30% obtained with CpCo(CO)$_2$.
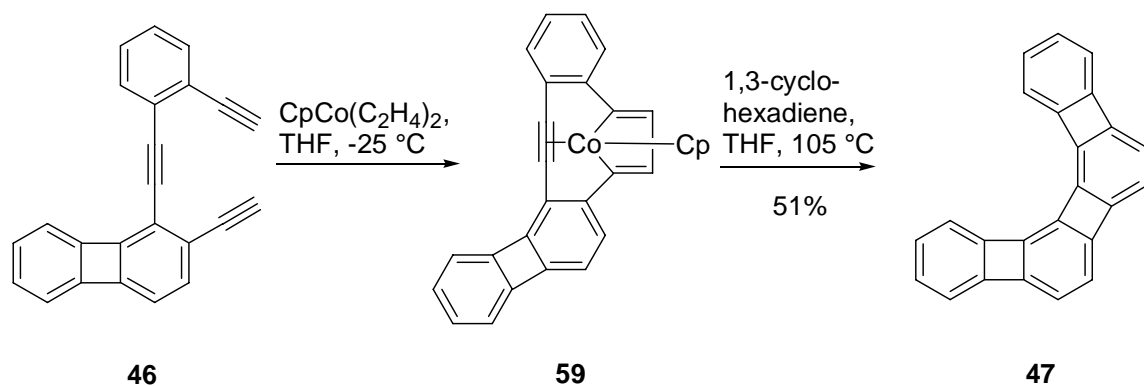
Scheme 2.5 Synthesis of angular [4]phenylene (**47**) with CpCo(C$_2$H$_4$)$_2$.

Importantly, the results obtained through this methodology proved to be quite reproducible, with yields varying only slightly. The products obtained from these experiments were used to conduct much of the research in this thesis, including flash vacuum pyrolysis studies with **3**, **3f**, and **47** (Chapter 3), and to obtain an X-ray crystal structure of **47** (next section).

2.3 Crystal Structure of Angular [4]Phenylene

While a variety of phenylenes have been synthesized, few X-ray crystal structures of these molecules have been reported that are undistorted by substituents.[49] However, recently it became possible to determine the structures of angular [5-8]phenylenes.[22d,50] Nevertheless, missing from this series was such a determination for angular [4]phenylene (**47**). Having achieved access to **47** via Scheme 2.5, attempts were made to grow suitable crystals. Because the molecule forms needlelike crystals too thin to be subjected to conventional X-ray sources, a set of diffraction data was collected using synchrotron radiation. Such radiation had already been necessary to obtain the X-ray crystal structures of linear [3]-, helical [6]-, and helical [8]phenylenes.[22d]

The crystal structure of **47** (Figure 2.2) reveals a significant amount of bond alternation, especially in the internal benzene rings of the molecule. Using the exocyclic diene portion of 3,4-dimethylenecyclobutene (1.497, 1.338 Å) as a 100% standard,[51] the internal benzene rings of **47** are 52% bond fixed. This phenomenon is less pronounced (25%) in the terminal rings, classifying them as more aromatic by this criterion. The structure is in excellent agreement with calculations at the B3LYP/6-31G* level conducted by Professor P. von Ragué Schleyer (Figure 2.3).[52] The maximum deviation of the calculated from the experimental bond lengths is 0.025 Å and the average deviation is 0.012 Å. The difference in aromatic character can also be observed in the ^{1}H NMR spectrum of **47**: the protons on the internal rings (δ = 6.31 ppm, CD_2Cl_2) are shielded relative to those on the terminal rings (δ_{avg} = 6.89 ppm),[22,29] consistent with a more cyclohexatrienic environment for the former.
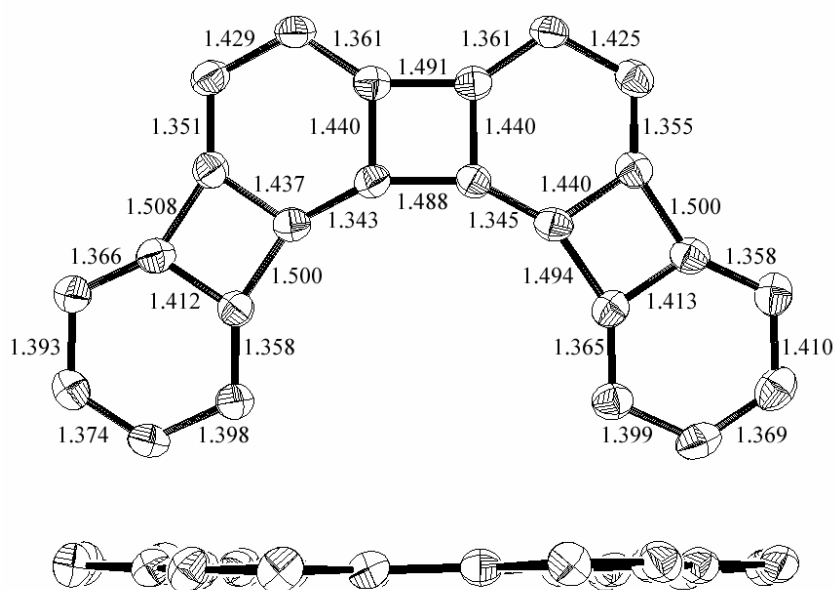
Figure 2.2 Crystal structure of **47**: views from above (top) and the side (bottom). Bond lengths (Å ; ±0.004).

It is instructive to compare **47** with its lower analog, angular [3]phenylene (**3**), in which the respective extent of bond alternation is 62% and 22%, and the central ring protons are shielded ($\delta = 6.18$ ppm) relative to those in **1**, in agreement with nucleus-independent chemical shift (NICS) calculations (Figure 2.3). These trends can be understood if one views **47** as the result of benzocyclobutadienofusion of **3**. In **3**, the terminal rings maximize their aromaticity by acting in concert to induce bond alternation in their central neighbor. Alteration of **3** to **47** induces increased bond alternation in one of the formerly terminal rings, thus relieving the "pressure" to bond fixation in the opposing internal ring. Because of symmetry, the net result is less reduction in the aromatic character of the inside benzenes in **1** relative to that in **7**.
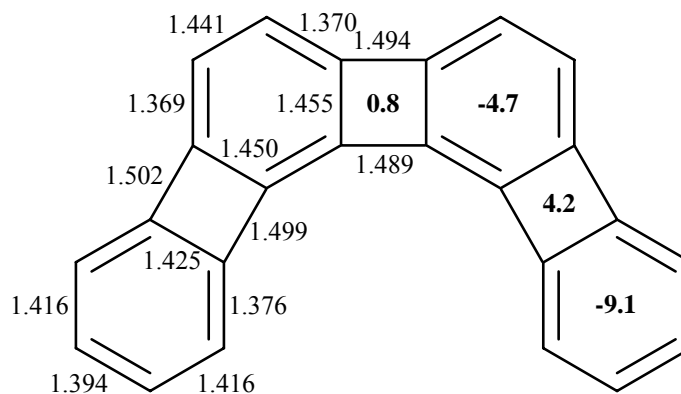
Figure 2.3 NICS (1) values (in bold) and calculated bond distances (Å) in **47**.

The geometry of **47** is unusually flat (Figure 2.2), with a median angle of 0.7° between the least-square planes of each ring, ranging from 0.1° to 1.1°. In contrast, most phenylenes show significantly larger deviations from planarity, a testament to their ready deformability.[49d] For example, in triangular [4]phenylene (**4**), an isomer of **47**, the corresponding median angle between planes is 2.0°, ranging from 0.7° to 3.5°.[49d]

With these data in hand, it is now possible to present a comprehensive tabulation of bond fixation in angular [N]phenylenes (for N ≤ 8). As can be seen in Table 2.2, the terminal rings are consistently the most aromatic, their neighbors the least. For systems with three types of benzene rings (N = 5 or 6), the first internal benzene rings are significantly cyclohexatrienic in character, allowing the central ring(s) to be relatively aromatic. As the phenylenes get larger, the difference in aromaticity between the internal rings decreases until for angular [8]phenylene it is very small (≤ 2%). This convergence suggests that bond fixation in polyheliphenylene may be about 53%.[22d]

Table 2.2 Bond fixation (ΔD) in angular [N]phenylenes in Å and %.[e]

[N]Phenylene	Terminal	2nd	3rd	4rd
2[a]	0.048 (30%)			
3[b]	0.035 (22%)	0.099 (62%)		
4	0.040 (25%)	0.083 (52%)		
5[c]	0.041 (26%)	0.106 (67%)	0.077 (48%)	
6[c]	0.025 (16%)	0.090 (57%)	0.081 (51%)	
7[c]	0.037 (23%)	0.085 (53%)	0.075 (47%)	0.080 (50%)
8[d]	0.046 (29%)	0.086 (54%)	0.083 (52%)	0.086 (54%)

a) Ref. 5, b) Ref. 27, c) Ref. 50 d) Ref. 22d. e) Ref. 51.

The availability of the materials employed to synthesize **47** for this crystallographic study also facilitated renewed investigation of the mechanistic details of the cobalt-mediated [2+2+2]cycloaddition. The results of these efforts will be discussed in the next section.

2.4 Structural Characterization of a Metallacyclopentadiene(Alkyne) Intermediate and Its Thermal and Photochemical Conversion

The ready generation of metallacycle **59** (Scheme 2.5), formed in analogy to its debenzocyclobutadieno relatives on route to **3** (Scheme 2.2), spurred renewed efforts to obtain crystals suitable for an X-ray analysis, a task that had proven impossible with several previous derivatives (Section 2.1). Unfortunately, attempts to obtain X-ray quality crystals from **59** were unsuccessful. Because Cp* compounds are often more crystalline than their Cp analogues, metallacyclopentadiene(alkyne) complex **60** was synthesized. $Cp*Co(C_2H_4)_2$[53] is less reactive than its Cp analogue, which necessitated the use of higher temperatures. Complex **60** was formed in 93% yield by treating triyne **46** with $Cp*Co(C_2H_4)_2$ at rt for 3 days (Scheme 2.6). For the same reasons, a $(CpMe_4Et)Co$ analogue of **60** was also synthesized, as literature precedent suggested similarly improved crystallinity with this ligand.[54] Treatment of triyne **46** with $(CpMe_4Et)Co(C_2H_4)_2$[55] led to the formation of metallacyclopentadiene(alkyne) complex **61** in 80% yield (Scheme 2.7). Unexpectedly, this complex was not very crystalline and an X-ray structure could not be obtained despite extensive efforts.
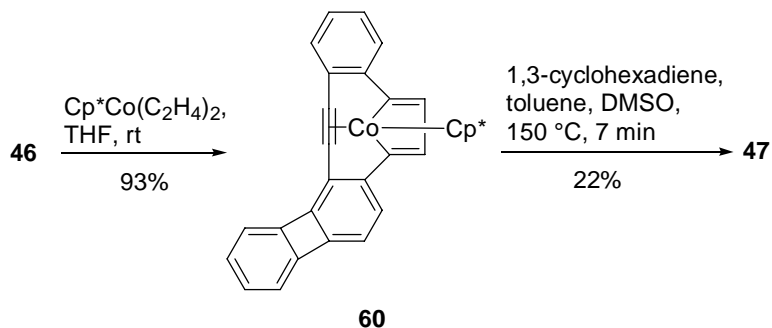
Scheme 2.6 Synthesis of angular [4]phenylene **47** using $Cp*Co(C_2H_4)_2$.
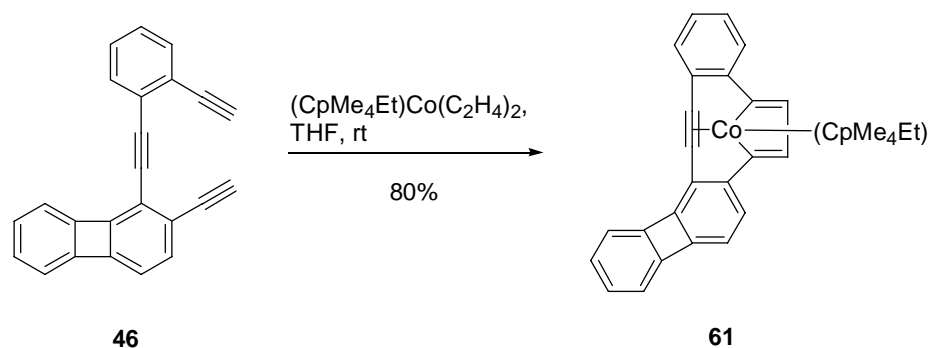
Scheme 2.7 Synthesis of metallacyclopentadiene(alkyne) complex **61**.

Fortunately, high-quality crystals of **60** were eventually obtained by slow evaporation of a toluene solution, resulting in an X-ray structure with adequate resolution (R = 5.32%, Figure 2.4). This is the first X-ray crystal structure of a mononuclear metallacyclopentadiene bearing a π-bound alkyne ligand and provides key support for the cobalt-mediated [2+2+2]cycloaddition mechanism presented in Figure 1.4.

The geometry of the ligating triple bond in **60** closely resembles that calculated for the analogous (CpCo) organometallic precursor to angular [3]phenylene (C≡C 1.242 Å, Co-C≡ 2.097 Å, C≡CC 165.97°),[46,56] as well as the parent CpCo(C_4H_4)(C_2H_2). While a search of the Cambridge Structural Database failed to uncover another example of a structurally characterized Co(III)-alkyne complex, the Co-C_{alkyne} bond distances in **60** are large in comparison with the cobalt(I)-alkyne complexes that have been characterized.[57] This is in agreement with the notion of an intrinsically weak cobalt-alkyne bond in **60**.
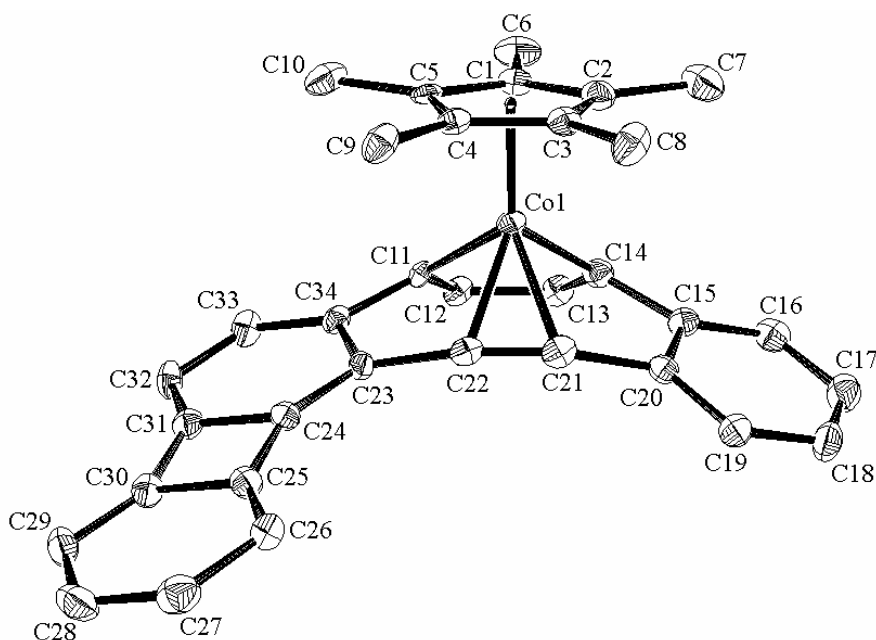
Figure 2.4 Crystal structure of metallacycle **60**. Selected bond lengths (Å; ±0.007): Co1-C11 1.920, Co1-C14 1.923, Co1-C21 2.039, Co1-C22 2.042, C11-C12 1.358, C12-C13 1.455, C13-C14 1.353, C14-C15 1.483, C15-C20 1.417, C20-C21 1.469, C21-C22 1.232, C22-C23 1.451, C23-C34 1.460, C11-C34 1.467, Co1-Ct 1.721. Selected bond angles (°): C20-C21-C22 164.7, C21-C22-C23 165.7.

Thermolysis of **60** in the presence of 1,3-cyclohexadiene generated **47** in 22% yield (Scheme 2.6). During attempts to improve yields of **47**, complex **60** was irradiated with a slide projector lamp. Surprisingly, the product obtained from this reaction was not **47**, but rather the bright orange cyclobutadiene (Cb) complex **62** (Scheme 2.8). While CbCo complexes are common byproducts of cobalt-mediated alkyne oligomerizations, no such species has ever been observed during the synthesis of angular phenylenes. The mechanism commonly proposed to explain the formation of this type of CbCo complex involves reductive-elimination from a coordinatively unsaturated cobaltacyclopentadiene.[21] In the case of **60**, light may cause dissociation of the alkyne ligand as a first step toward the formation of **62**, although a direct photoisomerization is entirely possible.
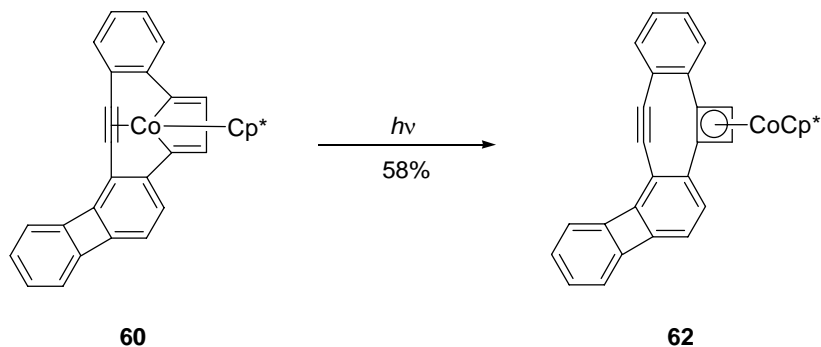
Scheme 2.8 Irradiation of **60** leads to formation of **62**.

The structure of **62** was confirmed by X-ray crystallography (Figure 2.5). Constraining the triple bond into an eight-membered ring leads to bond angles (C21-C22-C23 156.3°, C20-C21-C22 157.6°) that deviate significantly from linearity. Similar distortions are found in related cyclynes,[58] such as 1,2,5,6-dibenzocyclooct-3-en-7-yne **63**, which has acetylenic bond angles of 154°.[59] The strain inherent in the molecule also causes the cyclobutadiene ring to distort into a trapezoidal configuration: the bond of fusion (C11-C14) is significantly longer and C12-C13 shorter than normal (~1.46 Å).[60] This distortion is not present in **64**, a closely related complex lacking a triple bond. In this molecule, the carbon-carbon bond distances in the four-membered rings all fall in a narrow normal range (1.460 to 1.477 Å).
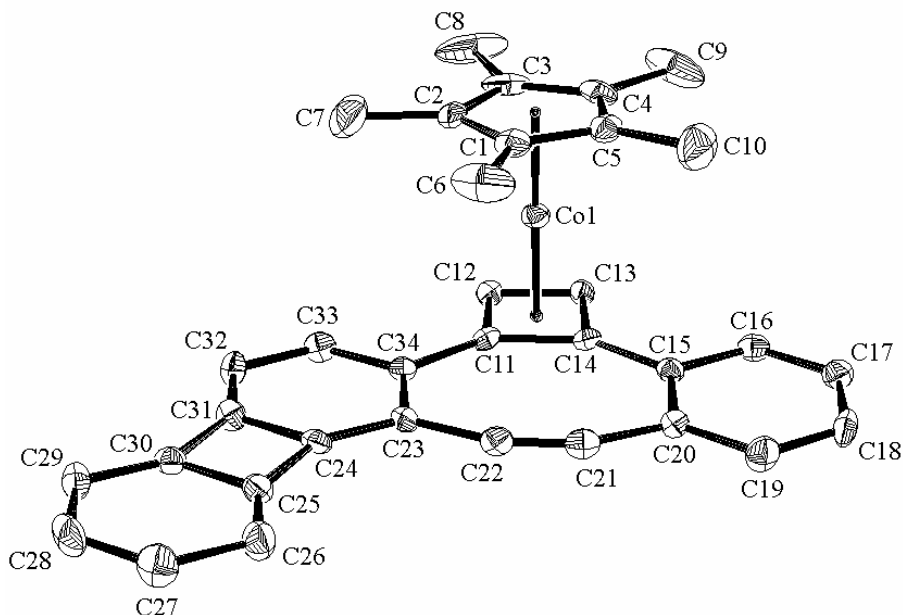
Figure 2.5 Crystal structure of **62**. Selected bond lengths (Å; ±0.005): C11-C12 1.455, C12-C13 1.421, C13-C14 1.461, C11-C14 1.500, C21-C22 1.196. Selected bond angles (°): C20-C21-C22 157.6, C21-C22-C23 156.3, C12-C11-C14 88.9, C11-C14-C13 88.0, C11-C12-C13 91.3, C12-C13-C14 91.8.

63
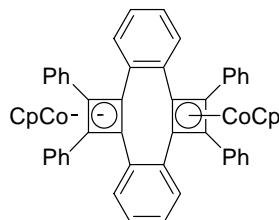
64

The unexpected isolation of **62** led to a closer examination of the side products obtained during the synthesis of **47** (Scheme 2.5). There are many other possible compounds that could conceivably be produced during the reaction of **46** with CpCo(C$_2$H$_4$)$_2$. These include the products of intermolecular alkyne cyclizations and insertion products analogous to those formed by **1** (Scheme 2.4) and **3** (Scheme 2.5). A control experiment showed that angular [4]phenylene also reacts with CpCo(C$_2$H$_4$)$_2$ upon

heating to 75 °C, generating large numbers of what are believed to be insertion products on the basis of ^{1}H NMR evidence, though none of these complexes could be definitively identified. From the numerous minor products formed from the reaction of **46** and CpCo(C$_2$H$_4$)$_2$, Cp complex **65** could be isolated in 16% yield (Scheme 2.9). The yield of **65** remained unchanged even when light was rigorously excluded from the reaction, demonstrating that CoCb complexes can be produced under both thermal and photochemical conditions.
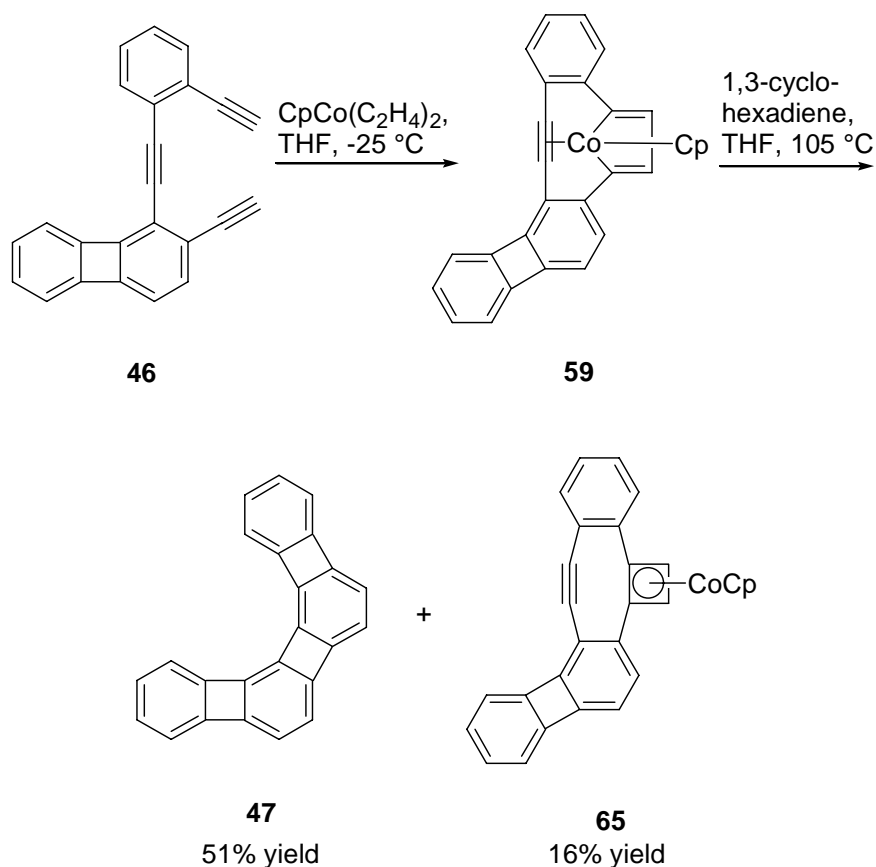
Scheme 2.9 Thermolysis of **59** leads to the formation of two major products.

The results presented in this section provide strong support for the proposed mechanism of the cobalt-mediated [2+2+2]cycloaddition (Figure 1.5). The observation that white light can cause a generally undesired side reaction suggests that care must be taken to avoid overirradiation during cyclization reactions with $CpCo(CO)_2$. The problem of light-induced cyclobutadiene formation can be completely avoided by employing $CpCo(C_2H_4)_2$. The use of this reagent in the synthesis of *anti*-doublebent [5]phenylene (**66**) will be the subject of the next section.

2.5 Synthesis and Structure of *anti*-Doublebent [5]Phenylene Using a CpCo(C$_2$H$_4$)$_2$-Mediated Double Cyclization

Replacing the standard CpCo(CO)$_2$ cyclization conditions with milder ones utilizing CpCo(C$_2$H$_4$)$_2$ improved the yields of both **3** and **47**. In order to determine whether the methodology presented in Section 2.2 could be extended to a double cyclization, the CpCo(C$_2$H$_4$)$_2$-mediated cycloisomerization of hexayne **67** to *anti*-doublebent [5]phenylene **66** was investigated. Two previous efforts to affect this transformation using CpCo(CO)$_2$ had proven unsuccessful,[61,62] though a propyl-substituted *anti*-doublebent [5]phenylene (**68**) was made.[63] *anti*-Doublebent [5]phenylene **66** was chosen as a target because of the availability of silyl-protected hexayne **69** and its intrinsic theoretical interest.

anti-Doublebent [5]phenylene **66** can be viewed as the result of benzocyclobutadienofusion to the A ring of bent [4]phenylene (**70**) (Figure 2.6).[64] This fusion greatly reduces the aromaticity of ring A, which goes from being a terminal ring (the most aromatic ring in a phenylene) to the first internal benzene ring (the least aromatic benzene ring in an angular phenylene). This decrease in the aromaticity of A will in turn allow the B ring to be more aromatic. Thus, H$_a$ is be expected to be more deshielded than the protons on the B ring of **70**. H$_b$ and H$_c$ should be shielded relative to the protons on the A ring of **70** and should be in a similar environment to the protons on the C ring.
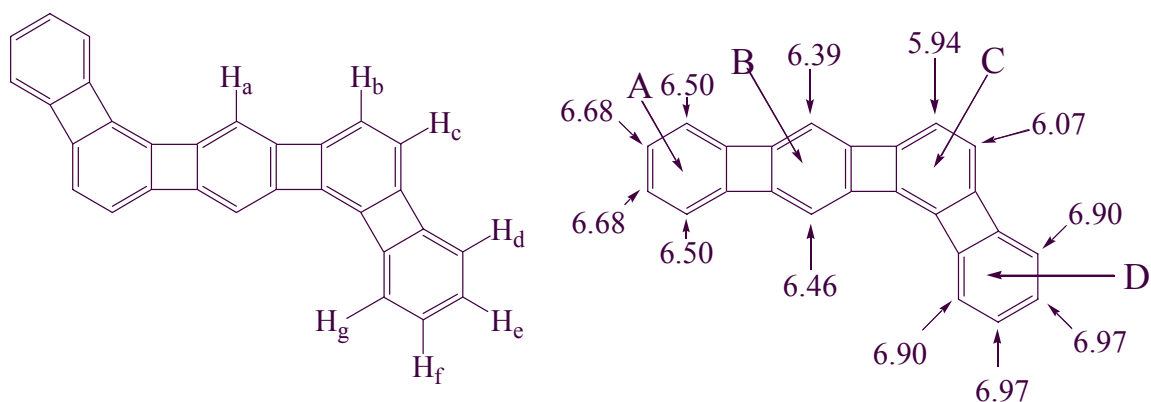
Figure 2.6 Labeling of the protons in **66** (left). Labeling of the benzene rings in **70** and ¹H NMR chemical shifts (CDCl₃, right).

67 **66**
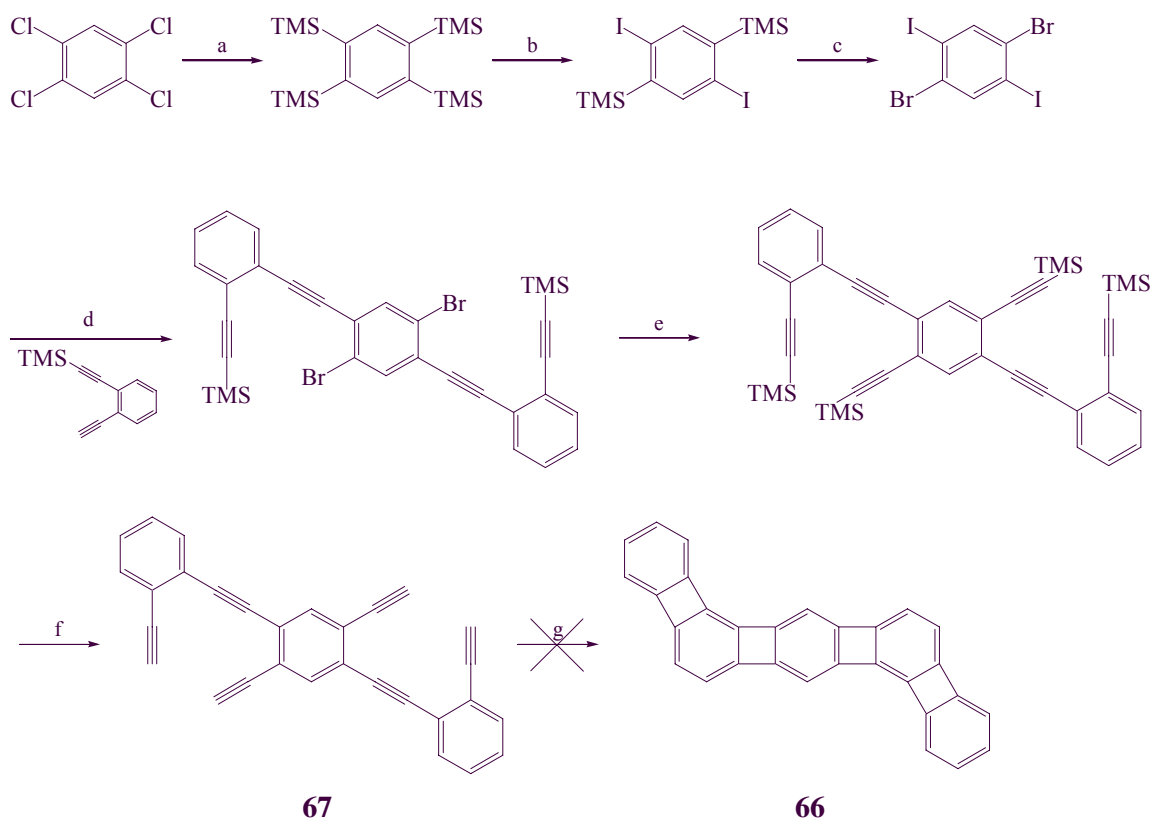
(a) Mg, TMSCl, HMPA, 56%; (b) ICl, CH₂Cl₂, 67%; (c) Br₂, FeBr₃, CCl₄, 99%;
(d) PdCl₂(PPh₃)₂, CuI, Et₃N, 61%; (e) TMSA, PdCl₂(PPh₃)₂, CuI, Et₃N, 60%;
(f) 35% KOH, Bu₄NBr, *o*-xylene; (g) CpCo(CO)₂, *o*-xylene, hν, Δ.

Scheme 2.10 The first attempted synthesis of *anti*-doublebent [5]phenylene **66**.

The first attempt to synthesize **66** was made in 1985. Triyne **67** was produced in six steps but could not be successfully cyclized with CpCo(CO)$_2$ (Scheme 2.10). Several years later, a more rapid synthesis was developed that allowed large amounts of silyl-protected hexayne **69** to be made (Scheme 2.11), but conditions capable of generating **66** could not be found.
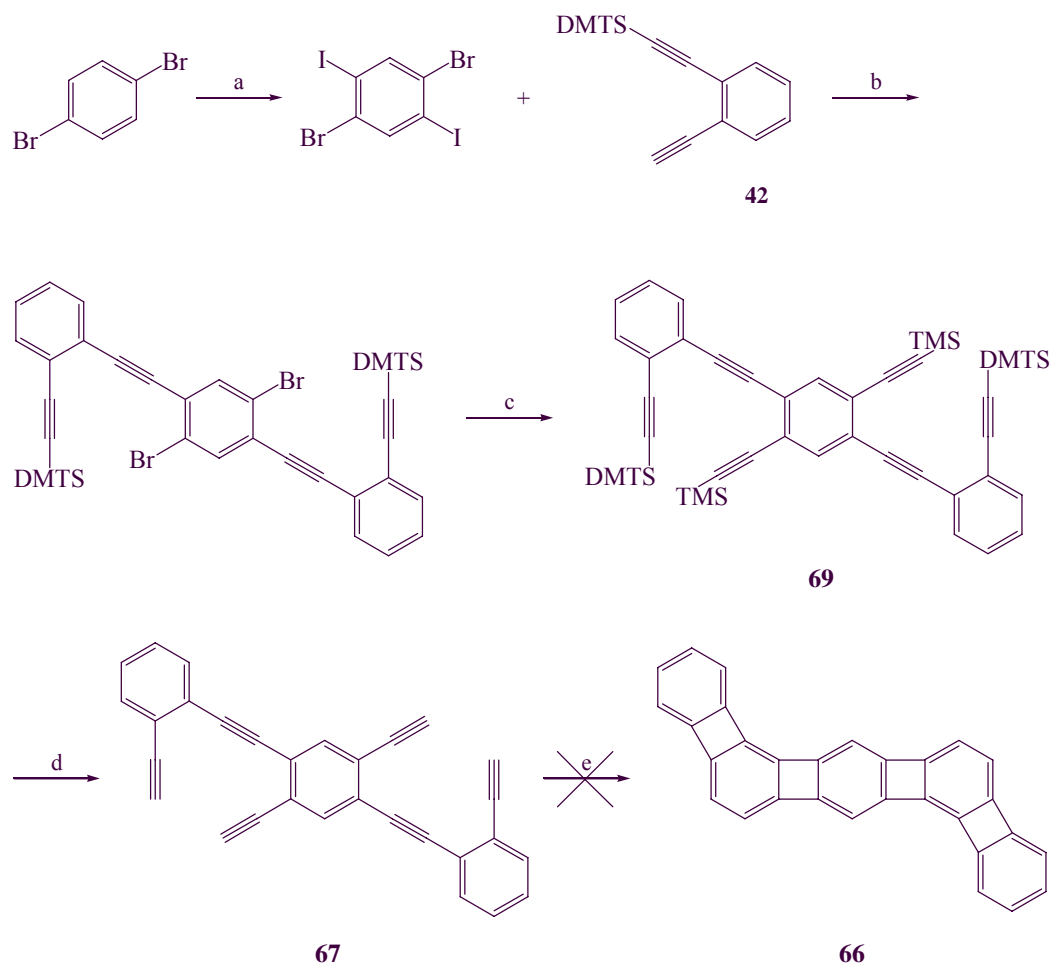
DMTS = Si(CH$_3$)$_2$C(CH$_3$)$_2$CH(CH$_3$)$_2$
(a) I$_2$, H$_2$SO$_4$, 70%; (b) PdCl$_2$(PPh$_3$)$_2$, CuI, Et$_3$N, 72%; (c) TMSA, PdCl$_2$(PPh$_3$)$_2$, CuI, Et$_3$N, 70%; (d) TBAF, THF, 95%; (e) CpCo(CO)$_2$, *m*-xylene, hν, Δ.

Scheme 2.11 Haley's attempted synthesis of *anti*-doublebent [5]phenylene **66**.

Because the insolubility of the product and intermediates was believed to be partially responsible for the failure to successfully cyclize **67**, the entire synthetic sequence was modified to incorporate propyl-solubilizing groups in a second approach to the system (Scheme 2.12). Cyclization of hexayne **71** generated propyl-substituted *anti*-doublebent [5]phenylene **68** in 2% yield. Enough **68** was produced to adequately characterize the compound, however, no crystal structure could be obtained.
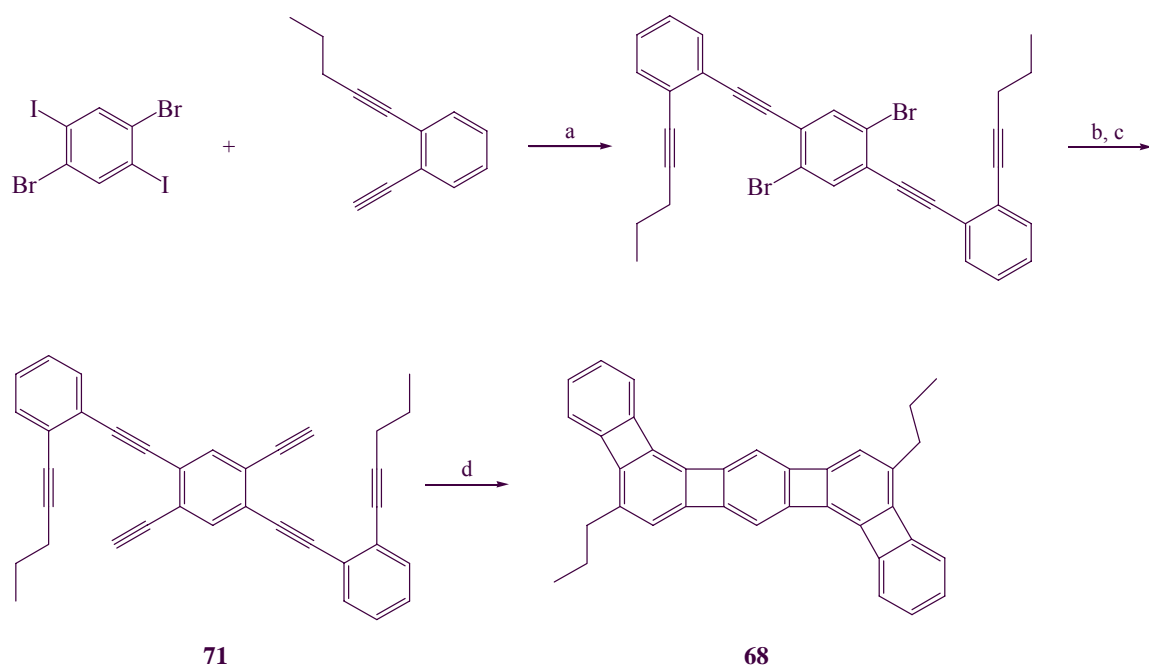
(a) PdCl$_2$(PPh$_3$)$_2$, CuI, Et$_3$N, 50 °C, 49%; (b) TMSA, PdCl$_2$(PPh$_3$)$_2$, CuI, Et$_3$N, 145 °C, 70%;
(c) NaOH, THF, CH$_3$OH, 85%; (d) CpCo(CO)$_2$, *m*-xylene, hv, Δ, 2%.

Scheme 2.12 Synthesis of propyl-substituted *anti*-doublebent [5]phenylene **68**.

Armed with this body of knowledge, **69** was desilylated to generate **67** in situ (Scheme 2.13). Treatment with CpCo(C$_2$H$_4$)$_2$ in THF at −25 °C led to the formation of a clear blood-red solution after 18 hours, typical of **57** and **59**. Subsequently, 1,3-cyclohexadiene was added and the solution heated to 105 °C for 90 minutes. After

purification by column chromatography, an orange solid was obtained. This material could not be redissolved at room temperature, thwarting initial attempts to acquire an NMR spectrum. However, a mass spectrum showed the desired M^+ at 374. Heating the solid in 1,2-dichlorobenzene dissolved enough material for a UV spectrum to be obtained. Peaks at 475, 485 and 505 nm match closely the peaks reported for propyl-substituted *anti*-doublebent [5]phenylene **68** (476, 486, and 508).
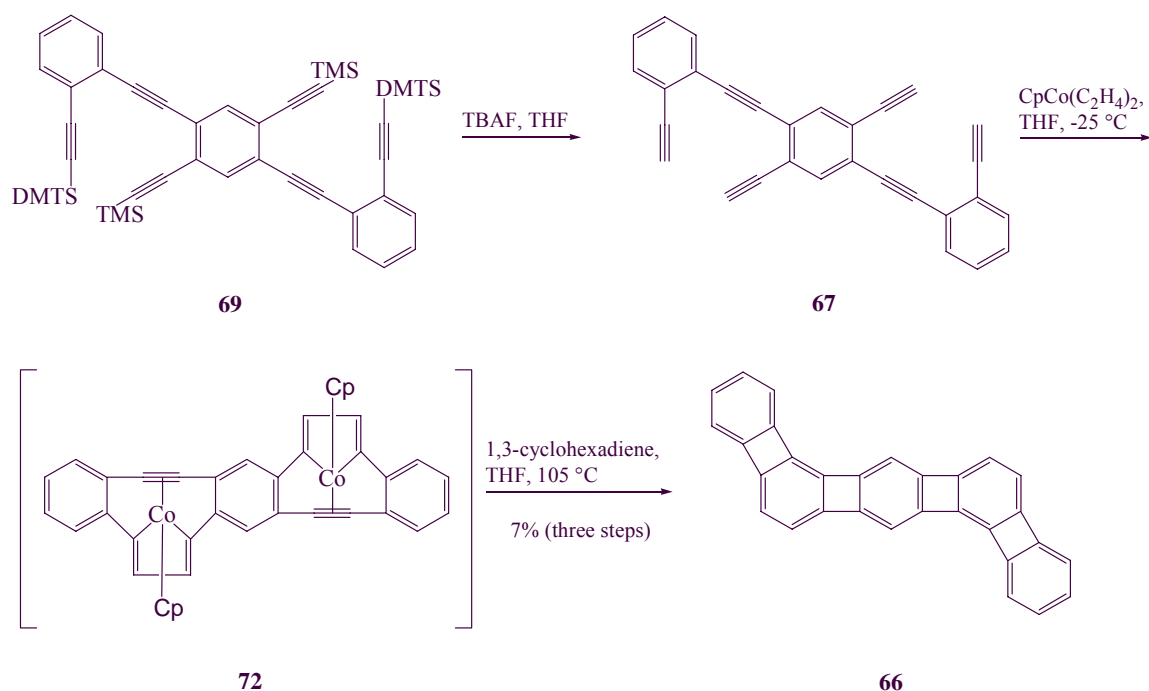
Scheme 2.13 Synthesis of *anti*-doublebent [5]phenylene **66**.

The increased solubility of the solid at elevated temperatures allowed the acquisition of ^1H NMR data. A spectrum taken at room temperature in d_4-1,2-dichlorobenzene showed only residual solvent peaks at δ 7.19 and 6.93 and their ^{13}C satellite peaks at δ 7.46 and 6.66 (Figure 2.8, top). A new set of peaks began to appear as the sample was heated. A spectrum taken at 115 °C (Figure 2.8, bottom) showed signals

consistent with **66** and compares well with a spectrum of **68** (taken at rt in CDCl$_3$).   The

multiplets at δ 6.98-6.83 (six protons) and δ 6.81-6.75 (two protons) can be assigned to

H$_d$-H$_g$ (δ 6.99-6.86 in **68**, see Figure 2.6 for labeling).   The singlet at δ 6.52 (two protons)

is due to H$_a$ (δ 6.61 in **68**).   The two doublets (two protons each) at δ 6.04 and 5.96 are

consistent with H$_b$ and H$_c$ (δ 5.91 in **68**).
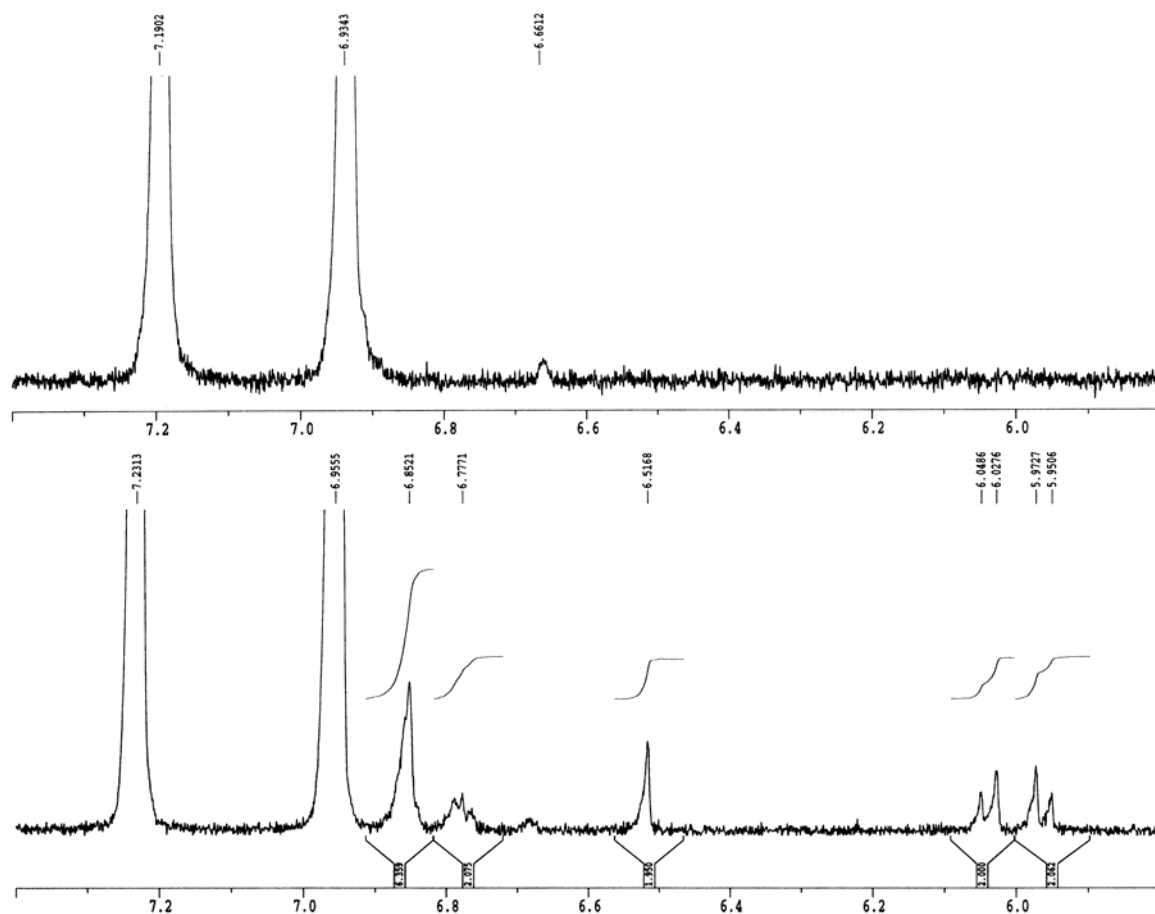
Figure 2.7 NMR spectrum of **66** at rt (top) and at 115 °C (bottom).

Small platelike crystals could be obtained by slowly cooling a dibutyl ether

solution of **66** from 190 °C to rt in a sealed tube.   The small size of these crystals

necessitated the employment of synchrotron radiation to obtain an X-ray structure (Figure 2.8). Like angular [4]phenylene (**47**), but in contrast to many other phenylenes,[49d] the geometry of **66** is essentially flat. The terminal benzene rings of **66** are highly aromatic, showing only 17% bond fixation, while the central ring shows a bisallyl system similar to that seen with **2** (Figure 1.10). Perhaps the most notable aspect of the crystal structure is that the bond fixation in the first internal rings of **66** (66%) is actually greater than that in the central ring of **3** (62%).[65] These data can be rationalized by noting that fusion of a biphenylene fragment to **3** such as to assemble **66**, increases the double bond character of the bond shown in bold in Figure 2.9, which will by relay increase the cyclohexatrienic character in the first internal benzene ring.
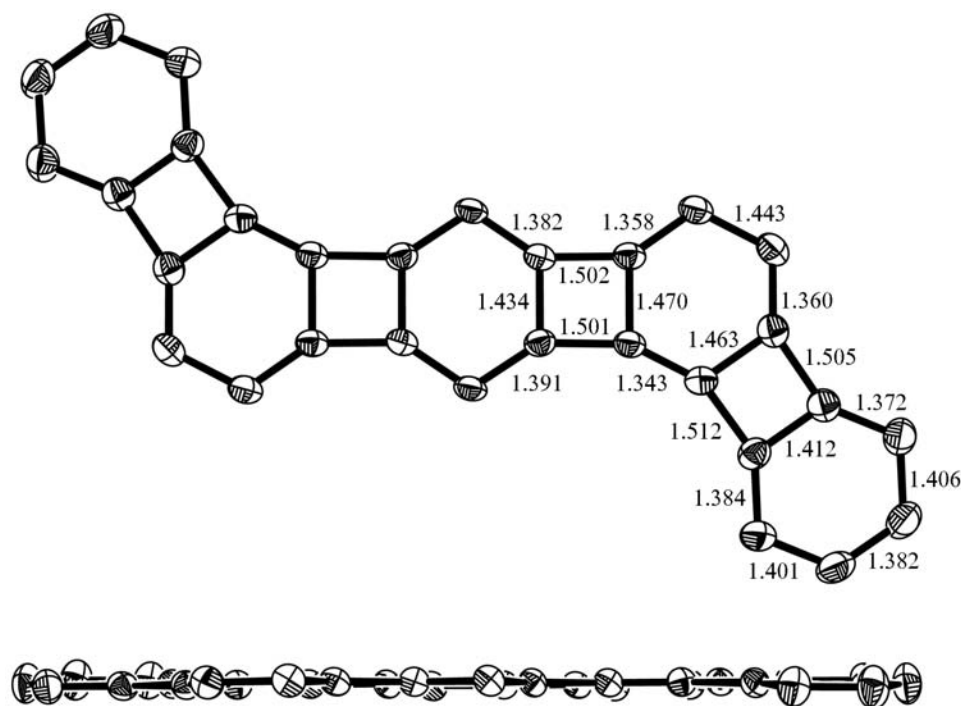
Figure 2.8 Crystal structure of **66**: views from above (top) and the side (bottom). Bond lengths (Å ; ±0.004).

60
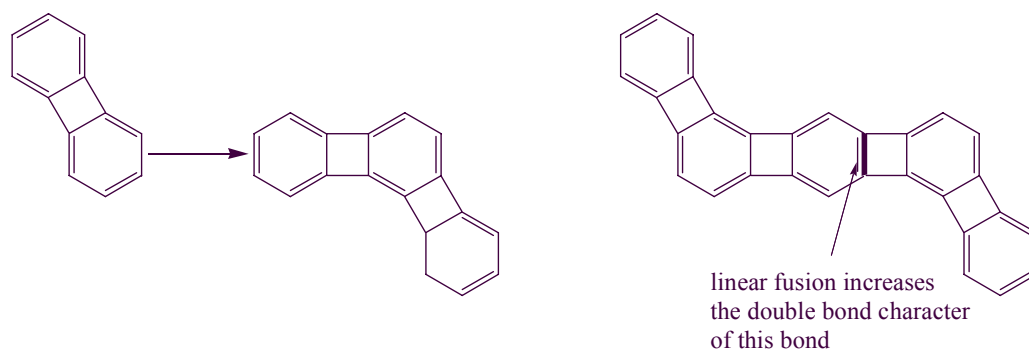
Figure 2.9. *anti*-Doublebent [5]phenylene 66 can be viewed as the result of fusion of biphenylene to angular [3]phenylene.

The CpCo(C$_2$H$_4$)$_2$-mediated cyclization methodology discussed in this chapter proved to be effective in synthesizing angular [3]-, angular [4]-, and *anti*-doublebent [5]phenylenes. Hopefully it will be used by future researchers to aid in the production of new phenylenes. A case in point are the helical members of the series. Thus, Han et al. found that the triple cyclization of nonayne 73 using CpCo(CO)$_2$ generated helical [7]phenylene 74 in only 2% yield (Scheme 2.14).[22d] This final cyclization could possibly be significantly improved by using CpCo(C$_2$H$_4$)$_2$.
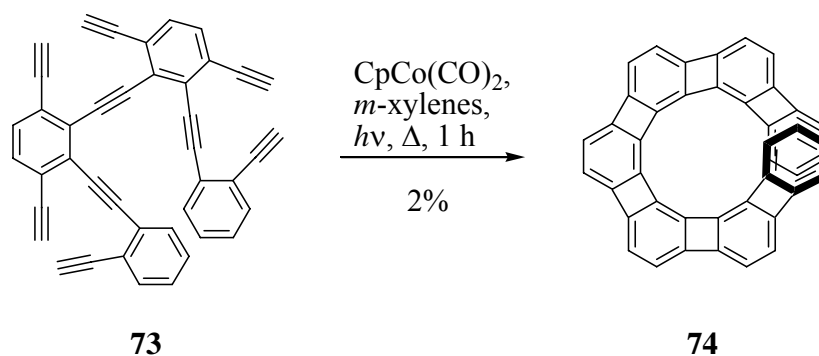
Scheme 2.14 Synthesis of helical [7]phenylene (74).

However, the ideal target molecules on which to use this methodology are the "holy grails" of phenylene research: antikekulene (**75**)[66] and circular [8]phenylene (**76**).[67] Attempts to make these molecules have thus far failed, presumably primarily due to solubility issues. These difficulties mirror those seen with *anti*-doublebent [5]phenylene **66**, which was successfully synthesized using a CpCo(C_2H_4)$_2$-mediated double cyclization.
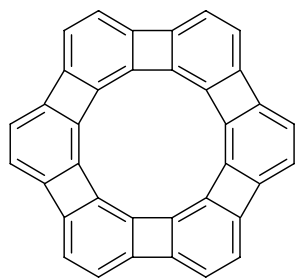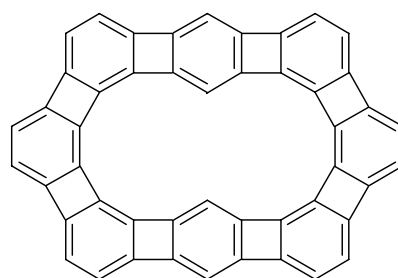
Antikekulene **75**   Circular [8]Phenylene **76**

Chapter Three

Isomerization of Linear to Angular [3]Phenylene and Polycyclic Aromatic Hydrocarbons Under Flash Vacuum Pyrolysis Conditions

3.1 Introduction

The phenylenes are high-energy potential precursors to polycyclic aromatic hydrocarbons (PAHs), including fullerene substructures.[68,69] The PAHs which are formed during their pyrolysis are often potent environmental pollutants,[70] and the phenylenes provide excellent starting materials for mechanistic research into the formation of these toxic substances. Their thermal chemistry is also of interest because of the possible isomerization of one phenylene to another, which holds the synthetic potential to access hitherto unknown isomers. Such an isomerization was recently demonstrated by Scott.[71]

There is a tremendous thermodynamic driving force behind the rearrangement of phenylenes to PAHs under flash vacuum pyrolysis (FVP) conditions. According to AM1 calculations, angular [3]phenylene (**3**) is 97 kcal/mol higher in energy than its isomer benzo[*ghi*]fluoranthene (**75**), the major product of its pyrolysis. This $\Delta H_f°$ difference is primarily due to the σ strain of the two four-membered rings in **3**, though the antiaromaticity of **3** also plays a role. In contrast, the $\Delta H_f°$ disparities between (isomeric) phenylenes, resulting from differences in σ strain and antiaromaticity, are relatively small, but are still large enough to drive isomerizations. For example, the $\Delta H_f°$ of linear

[3]phenylene (**2**) has been calculated at the BLYP/6-31G* level to be 2.4 kcal/mol greater than that of **3**.[72] One of the results discussed in this chapter, that **2** isomerizes under FVP conditions to **3**, but not vice versa, will provide experimental evidence in support of this energetic calculation.

This chapter will discuss the flash vacuum pyrolyses of linear [3]phenylene (**2**), angular [3]phenylene (**3**), and angular [4]phenylene (**47**). A ^{13}C labeling study, leading to a new mechanistic proposal for the isomerization of **3** and **2** into PAHs, will also be presented.

3.2 Flash Vacuum Pyrolysis of Phenylenes

A compound subjected to flash vacuum pyrolysis conditions is sublimed through a quartz tube that is heated by an external furnace. The products of this process, the pyrolysate, are captured in a cold trap located between the oven and the vacuum source. Figure 3.1 presents a guide to some common reactions that take place under FVP conditions.[73]
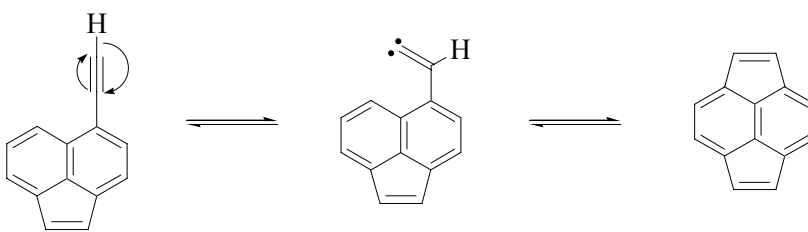
Isomerization of a terminal alkyne into a carbene, followed by insertion.
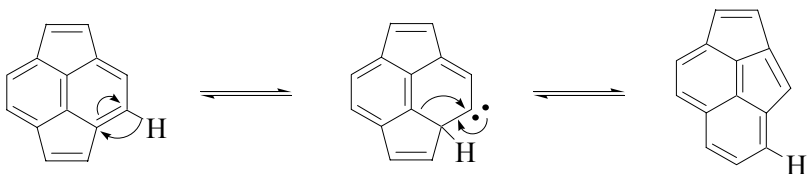
A benzene ring contraction rearrangement.
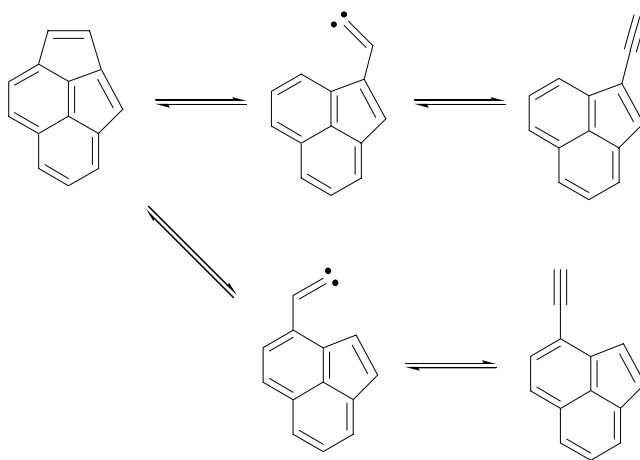
Carbene insertion is reversible in highly strained systems.

Figure 3.1 Some reactions that occur under FVP conditions.

Biphenylene (**1**) was the first phenylene subjected to flash vacuum pyrolysis conditions. At 900 °C, it isomerizes to form cyclopent[a]indene (**76**) and acenaphthylene (**77**). Upon standing in the solid phase or in solution, **76** dimerizes to form **78**. Jenneskens et al. proposed the mechanism in Scheme 3.1 to explain these results. Subsequently, Scott argued that **1** isomerizes to **76** via a benzene ring contraction rearrangement (Scheme 3.2).[71]
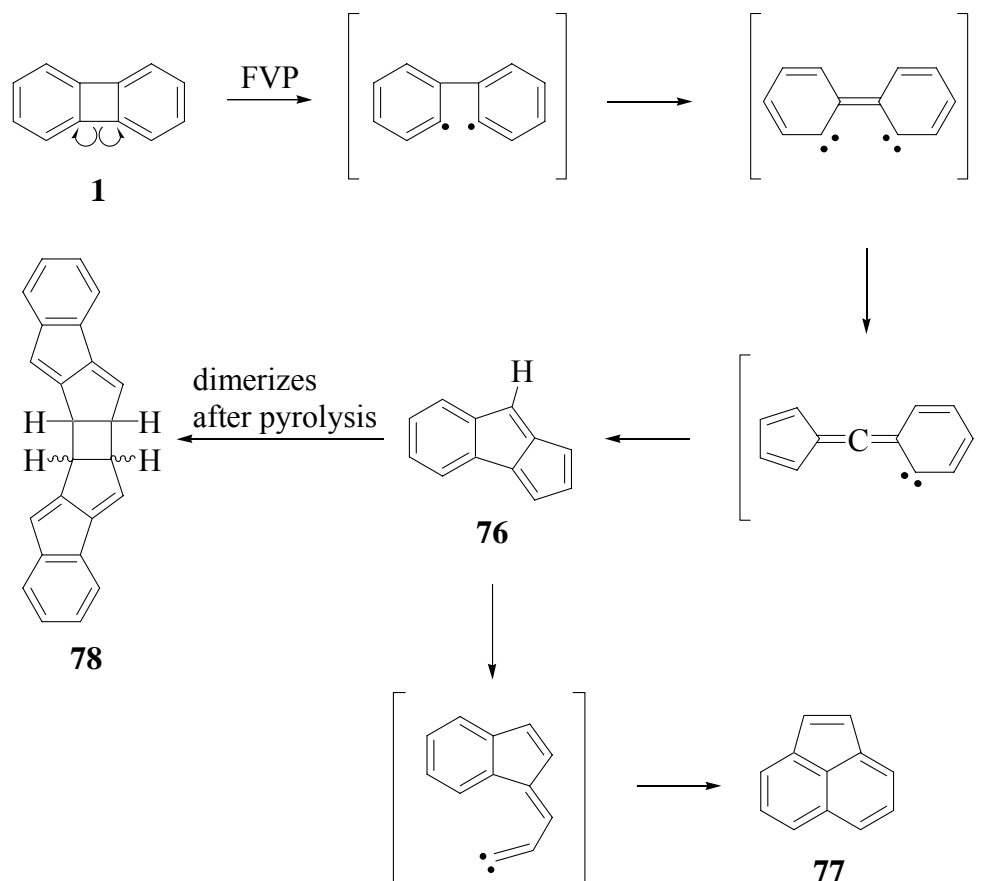
Scheme 3.1 Products of the FVP of biphenylene.
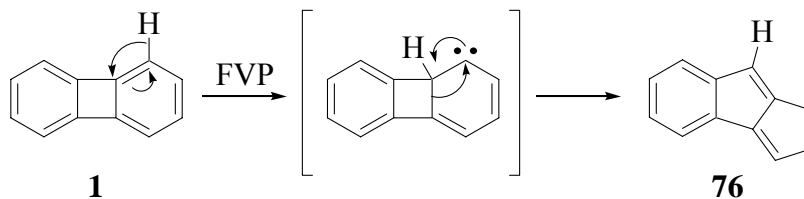
Scheme 3.2 Formation of **76** via a benzene ring contraction rearrangement.

Based on these results, it seemed likely that under FVP conditions **3** would undergo two benzene ring contractions to yield a benzopentalenopentalene like **79** (Scheme 3.3). However, in an initial study of this reaction by Vollhardt et al., no benzopentalenopentalenes were isolated. Instead, it was found that the FVP of angular [3]phenylene (**3**) at 1000 °C and 2 x 10^{-2} torr led to the formation of benzo[*ghi*]fluoranthene (**75**) in 10% yield. The initial step of the mechanism proposed at that time (Scheme 3.4) involved a Stone-Wales rearrangement. While such a reorganization has never been definitively observed and is calculated to be (normally) energetically too demanding,[74] the high strain (99.7 kcal/mol) in **3** may make this step feasible. Alternatively, a stepwise sequence may be followed. In either case, dibenzoacepentalene[75] (**80**) would be the first intermediate. According to the proposed mechanism, **80** undergoes cleavage followed by phenyl radical recombination to produce diethynyldibenzofulvene **81**. Under the conditions, **81** should undergo carbene formation followed by insertion to generate **75**.[73]
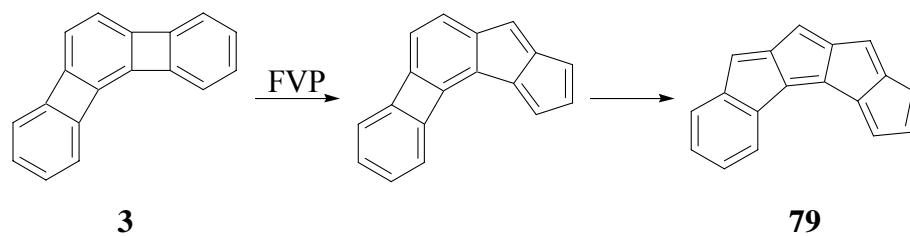
Scheme 3.3 FVP of **3** was expected to lead to **79** (or one of its isomers).
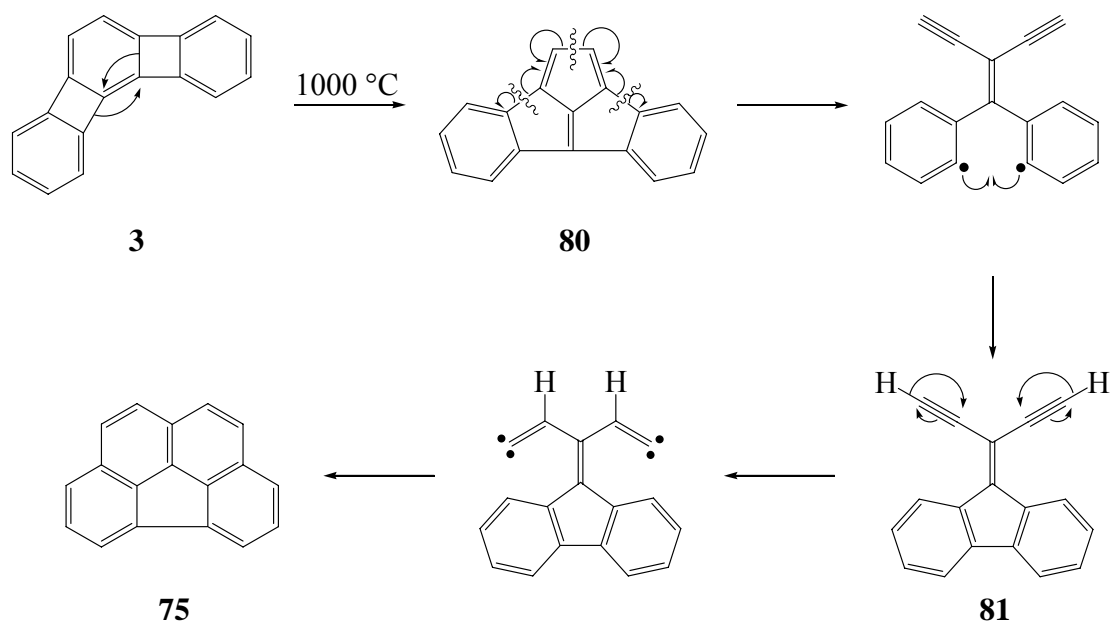
Scheme 3.4 Mechanism originally proposed for the formation of benzo[*ghi*]fluoranthene (**75**) from **3**.

3.3 Flash Vacuum Pyrolysis of Angular and Linear [3]Phenylenes

Repeating the flash vacuum pyrolysis of angular [3]phenylene (**3**) using a turbomolecular vacuum pump (5 x 10^{-7} torr) significantly improved the yield of benzo[*ghi*]fluoranthene (**75**) to 24% and facilitated the isolation and structural elucidation of three additional PAHs that were previously unidentified: acefluoranthylene (**82**, 11%), cyclopent[*hi*]acephenanthrylene (**83**, 3%), and the highly mutagenic cyclopenta[*cd*]pyrene (**84**, 7%). Traces of other PAHs, including fluoranthene and benz[*a*]anthracene, were also present. A small amount of **3** (4%) was recovered under these conditions. The products were separated by HPLC and their identities confirmed by comparison of their NMR and UV spectra with those published in the literature.[76] An NMR spectrum of the crude pyrolysate is shown in Figure 3.2 (bottom).

82   **83**   **84**
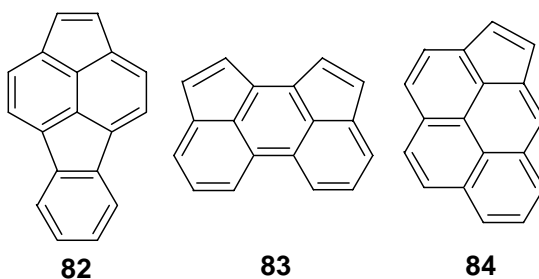
Next, the corresponding FVP of linear [3]phenylene (**2**) was explored. Several pathways are open to **2** under these conditions, including the formation of benzopentalenopentalenes and isomerization to **3**, which is thermodynamically more stable. Because of its topology, one option that was not available to **2** was a Stone-Wales rearrangement analogous to that proposed in Scheme 3.4. Thus it seemed likely that the pyrolysis of **2** would produce results markedly different than those obtained using **3**.

Instead, this pyrolysis produced a strikingly similar product mixture (Figure 3.2, top): **75** (10%), **82** (4%), **83** (1%), and **84** (2%), in addition to recovered **2** (17%) and, most significantly, its isomer **3** (1%). These results strongly imply the intermediacy of (the presumed to be more stable)[77] **3** in the FVP of **2**. A likely mechanism for this initial isomerization, paralleling that proposed by Scott for the conversion of benzo[*b*]biphenylene to benzo[*a*]biphenylene, is presented in Scheme 3.5.
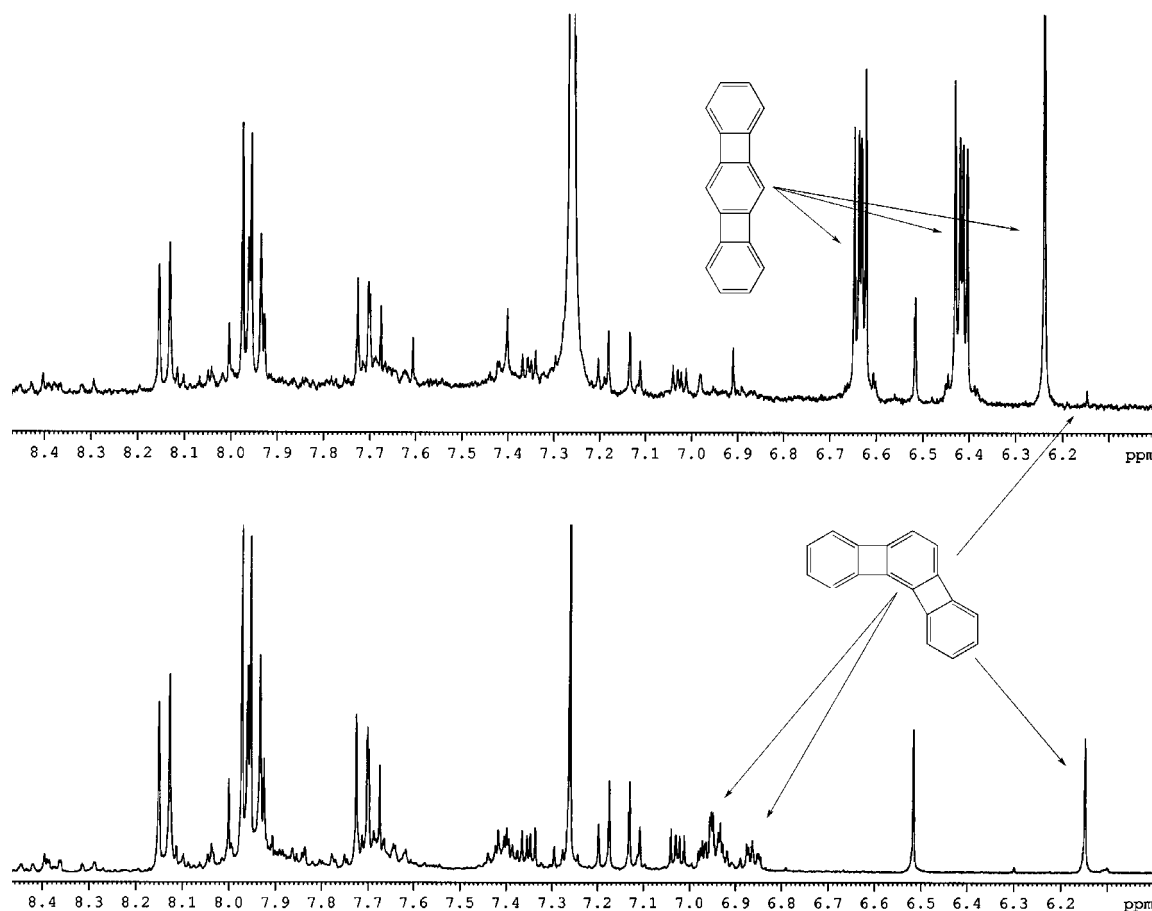
Figure 3.2 NMR spectra in CDCl$_3$ of the pyrolysates from the FVP of **2** (top) and **3** (bottom).

The isolation of **82-84**, in addition to **75**, is intriguing and suggested that the thermal conversion of **2** (and **3**) was more complicated than previously envisaged,

70

warranting further investigation. A series of control experiments demonstrated that **75**, **82**, **83**, and **84** did not interconvert under the reaction conditions.[78] To gain insight into the pathways that lead to the products, a mechanistic study employing ^{13}C-labeled angular [3]phenylene was undertaken.
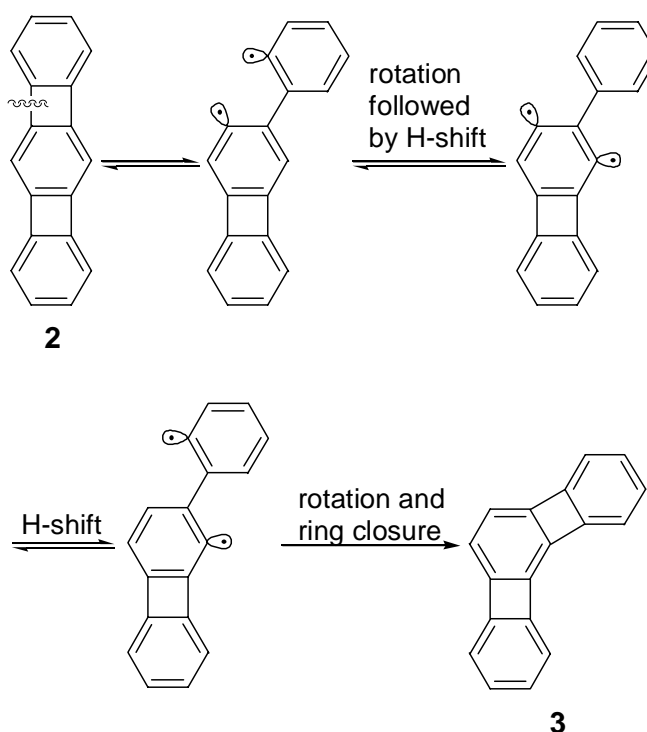
Scheme 3.5 Isomerization of **2** to **3** under FVP conditions.

For this purpose, the most reasonable commercially available source of ^{13}C proved to be acetylene-^{13}C$_2$. The methods used to synthesize unlabeled angular [3]phenylene (**3**) needed to be significantly modified to economically synthesize ^{13}C-labeled angular [3]phenylene. In order to introduce the ^{13}C-labeled material as late in the synthesis as possible, acetylene-^{13}C$_2$ was coupled with 1-iodo-2-trimethylsilylethynylbenzene (**85**). Initial efforts using Sonogashira conditions [unlabeled acetylene, **85**, Pd(PPh$_3$)$_4$, CuI, NEt$_3$], and an attempted Pd-catalyzed cross

coupling[79] of **85** with MgCl≡MgCl led to the formation of only trace amounts of the desired triyne **86**. Fortunately, a Negishi coupling proved to be more effective (48% yield based on acetylene-$^{13}C_2$, Scheme 3.6).

$^{13}C_2H_2$ → 1) BuMgCl (2 equiv), THF
2) ZnCl$_2$
3) **85**, Pd(PPh$_3$)$_4$, reflux
48%

TMS
TMS
86

KOH, methanol
95%

40f

● denotes ^{13}C-label
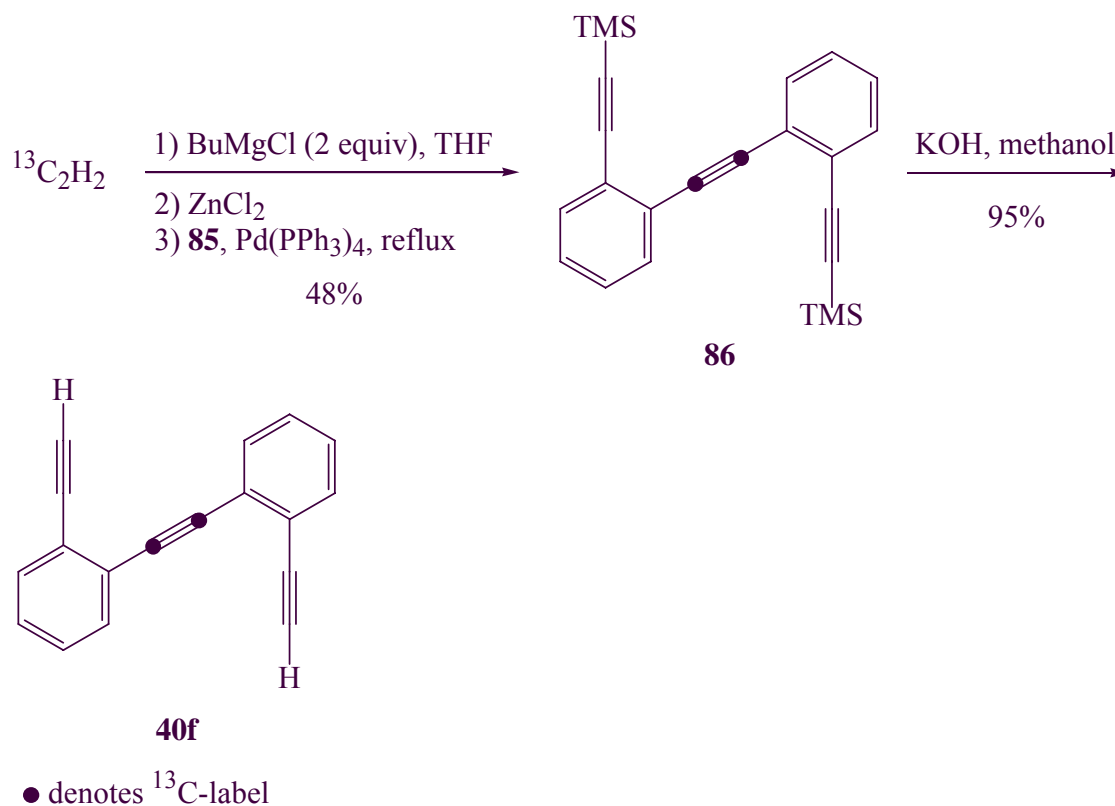
Scheme 3.6 Synthesis of $^{13}C_2$-labeled triyne **40f**.

The resulting triyne **86** was deprotected and cyclized in a stepwise protocol (see Section 2.2) to furnish **40f** (Scheme 3.7). According to the mechanism originally proposed for the formation of **75**, FVP of **40f** should lead to the formation of **75** with ^{13}C labels located only on the two carbons on the C$_2$-axis of the molecule (Scheme 3.8).
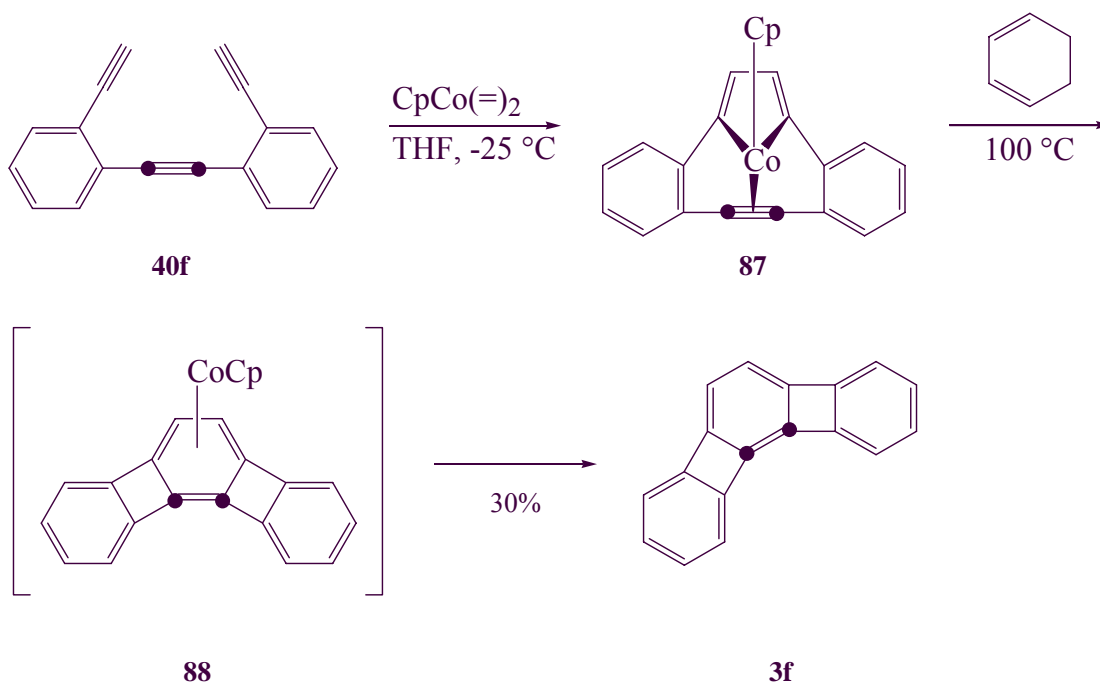
Scheme 3.7 Synthesis of $^{13}C_2$-labeled angular [3]phenylene **3f**.

● denotes ^{13}C-label
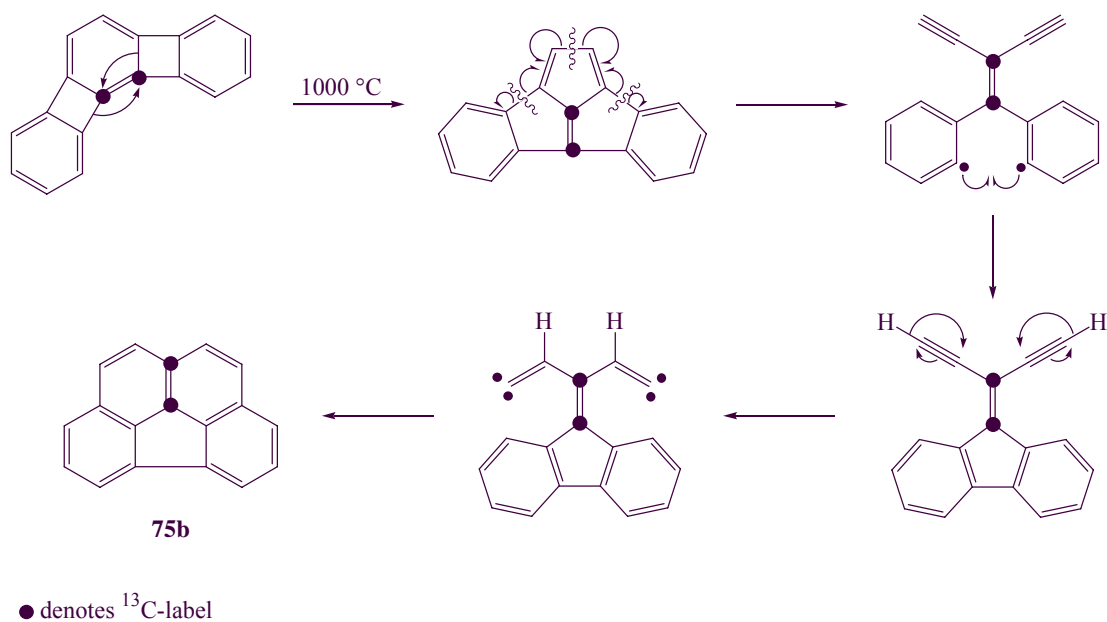
Scheme 3.8 According to the initially proposed mechanism, FVP of **3f** should lead to the formation of only isotopomer **75b** of **75**.

Pyrolysis of **3f** produced labeled **75**, **82**, **83**, and **84**, in addition to unchanged **3f**. The absence of scrambling in the starting material ruled out equilibration of **3** with **2** prior to rearrangement. The major label locations in the products (shown in Figure 3.3)[80] were determined by ^{13}C NMR analysis, which required the assignment of the ^{13}C NMR spectra of these compounds by HMQC, HMBC, and other NMR techniques (see Section 3.4). The vicinal nature of the label pairs in the products was evident from the observed strong carbon-carbon couplings, with *J* values between 50 and 69 Hz (except in the symmetrical case **83a**).

	75a	82a	83a	84a
	75b	82b	83b	84b
ratio **a/b**	2.4 to 1	2.4 to 1	1.8 to 1	1.4 to 1
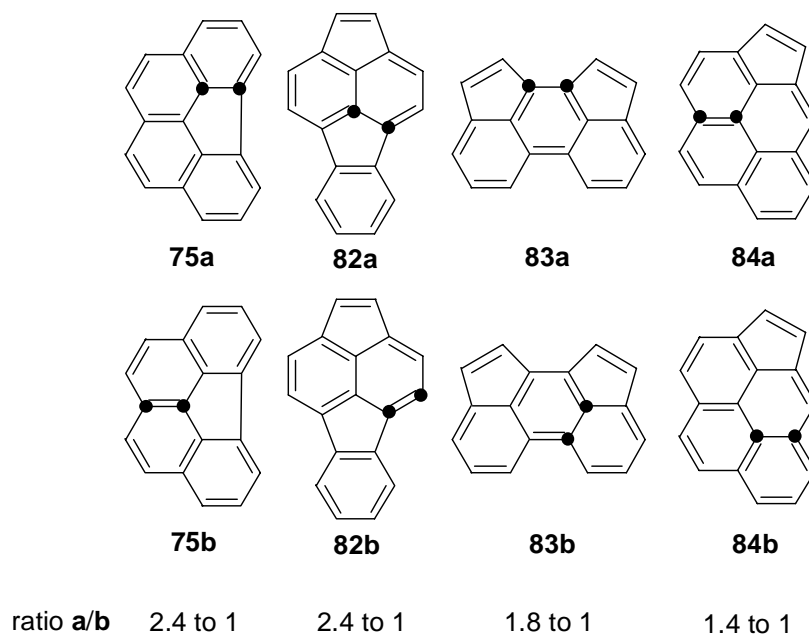
Figure 3.3 The major isotopomers isolated from the FVP of **3f** and their relative abundances, based on normalized ^{13}C NMR signal intensities.

These observations require a revision of the original mechanism proposed for the conversion of **3** to **75**, as it predicts the generation of only one isotopomer (**75b**) and cannot be readily adapted to explain the formation of **82-84**. While the literature provides several options, any reasonable mechanistic description must account for the

nature of the observed isotopomers of the products and the ratios in which they are

formed. The suggestions presented in Schemes 3.9 and 3.10 (leading to **75**, **82**, and **84**)

and in Scheme 3.11 (leading to **83**) do so and rely on precedented steps that are

thermodynamically reasonable according to AM1 ΔH_f° calculations. These steps include

the homolytic bond cleavage of strained rings followed by radical hydrogen shifts and

radical recombination, hydrogen shift/ring contractions,[73a] and carbene

formation/insertion reactions.[69,73c]
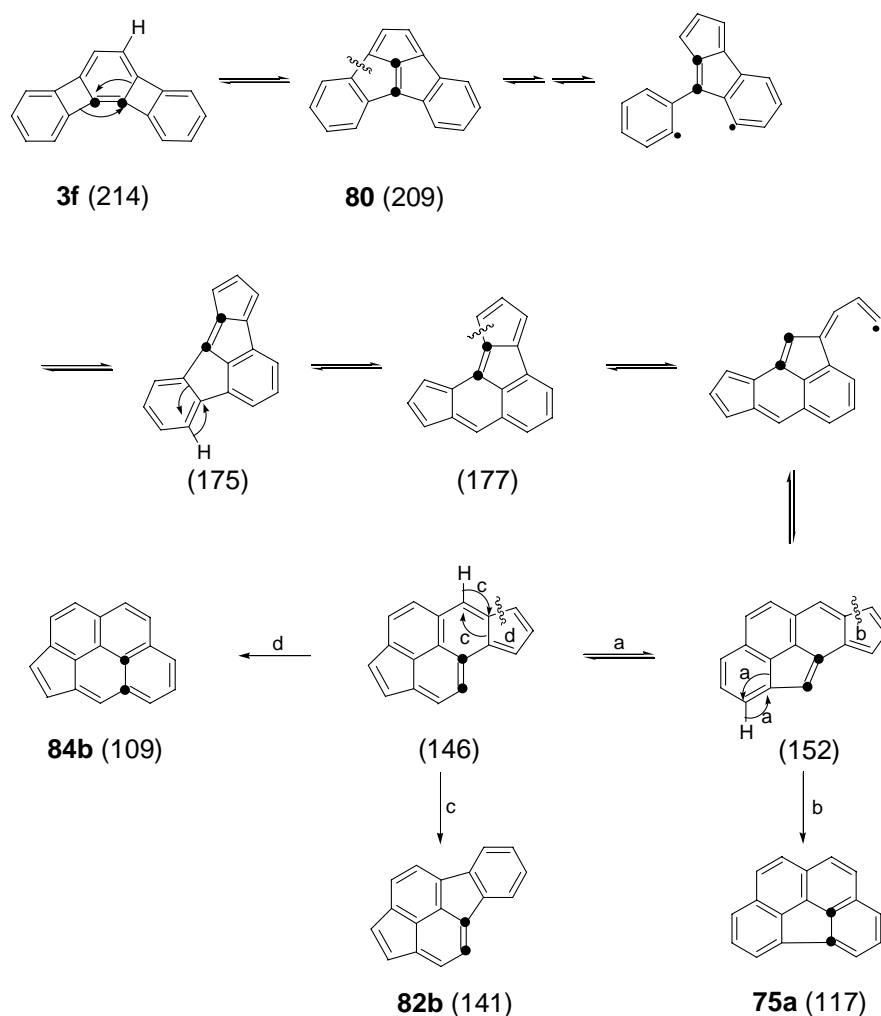
Scheme 3.9 Proposed mechanism for the formation of **75a**, **82b**, and **84b**. Numbers in parentheses are AM1 ΔH_f° values in kcal/mol.

The cornerstone of Schemes 3.9 and 3.10 is an initial Stone-Wales rearrangement

of **3f** to form **80**, as originally proposed. From **80**, two different pathways can be

followed. Thus, homolytic bond cleavage (Scheme 3.9), followed by hydrogen shifts and

bond formation, would result in **75a**, **82b**, and **84b** by a sequence of carbene

formation/insertion reactions and hydrogen shift/ring contractions. The preponderance of

75a in the total mixture of products would then be precipitated by its early appearance in

the scheme and the energetically favorable nature of step b.
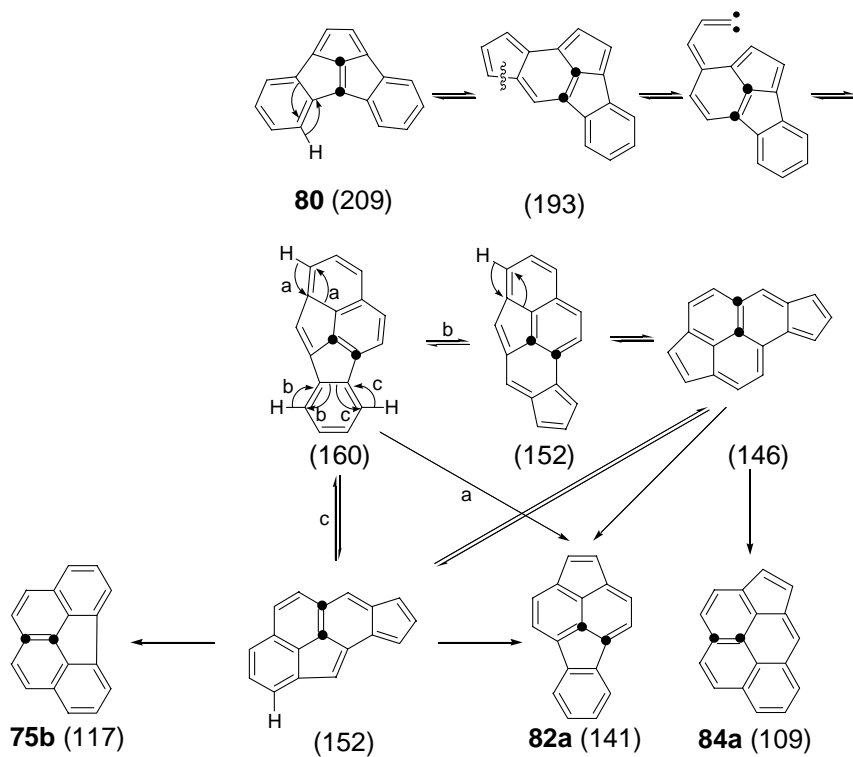
Scheme 3.10 Proposed mechanism for the formation of **75b**, **82a**, and **84a**. Numbers in parentheses are AM1 ΔH_f° values in kcal/mol.

Scheme 3.10 depicts an alternative (perhaps minor) reorganization of **80**, initiated

by a hydrogen shift/ring contraction at the benzene nucleus, followed by a combination of

carbene formation/insertion and further hydrogen shift/ring contractions to end up in **75b**, **82a**, and **84a**, all observed in roughly equal yields in the product mixture.

There appears to be no sequence of (precedented) steps that would connect the emergence of the isotopomers of **83**-$^{13}C_2$ directly with those of **75**, **82**, and **84**. It is, however, plausible to invoke an alternative (and evidently minor) migratory initial rearrangement fate of **3**, namely one that relies on a pathway traversed by biphenylene (**1**) itself (Scheme 3.11). Among the two options open to **3** which explain the isolation of **83a** and **b**, that resulting in the former would be expected to be more favorable as it disassembles the central, more activated ring,[22a] thus providing a tentative rationale for the preference for **83a**.
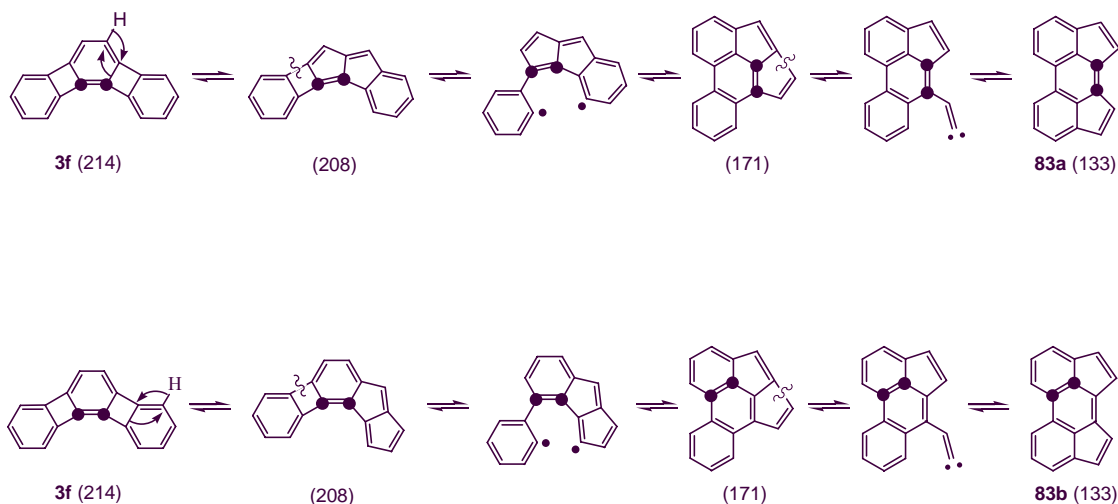
Scheme 3.11 Proposed mechanism for the formation of cyclopent[*hi*]acephenanthrylene (**83**). Numbers in parentheses are AM1 $\Delta H_f°$ values in kcal/mol.

In conclusion, the observed conversion of linear [3]phenylene (**2**) to angular [3]phenylene (**3**) demonstrates the potential of pyrolytic methods to convert phenylenes from one topology to another. This strategy might be applicable for the synthesis of new phenylenes by isomerization of known phenylenes. Moreover, the phenylenes represent

a high-energy entry into PAHs that may aid in developing a mechanistic understanding of PAH formation under extreme conditions.[81]   The extension of FVP studies to angular [4]phenylene (**47**), a larger molecule with more isomers that can potentially be reached under FVP conditions, will be discussed in the final section of this chapter.

3.4 ^{13}C NMR Assignments of the Polycyclic Aromatic Hydrocarbons Isolated From the FVP of Linear and Angular [3]Phenylene

Determining the label locations in the compounds (**75**, **82-84**) produced during the flash vacuum pyrolysis of ^{13}C$_2$-labeled angular [3]phenylene (**3f**) was an involved task. First, each of the products had to be separated by HPLC, allowing NMR spectra of the clean products to be acquired. Then, the ^{13}C NMR signals for each molecule were assigned based on spectral information obtained from both labeled and unlabeled materials. ^{13}C NMR literature assignments had already been published for **83**[82] and **84**,[83] but carbon-carbon coupling information obtained from ^{13}C$_2$-labeled **84** (Section 3.4.4) demonstrated that for this molecule they could not be correct. The following sections (3.4.1-3.4.4) contain new assignments for **75**, **82** and **84** and verification of those published for **83**.

3.4.1 Benzo[*ghi*]fluoranthene (75)
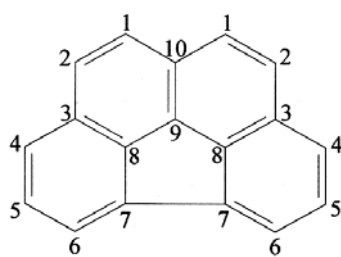
The ^{13}C NMR spectrum (Figure 3.4) of **75**-^{13}C$_2$ isolated from the FVP of **3f** exhibits two major labeling patterns:[80] a doublet at δ 137.3 (*J* = 53.1 Hz) correlated to a doublet at δ 133.2 (*J* = 53.1 Hz), and a smaller doublet at δ 133.0 (*J* = 56.0 Hz) correlated to a doublet at δ 126.7 (*J* = 55.9 Hz).
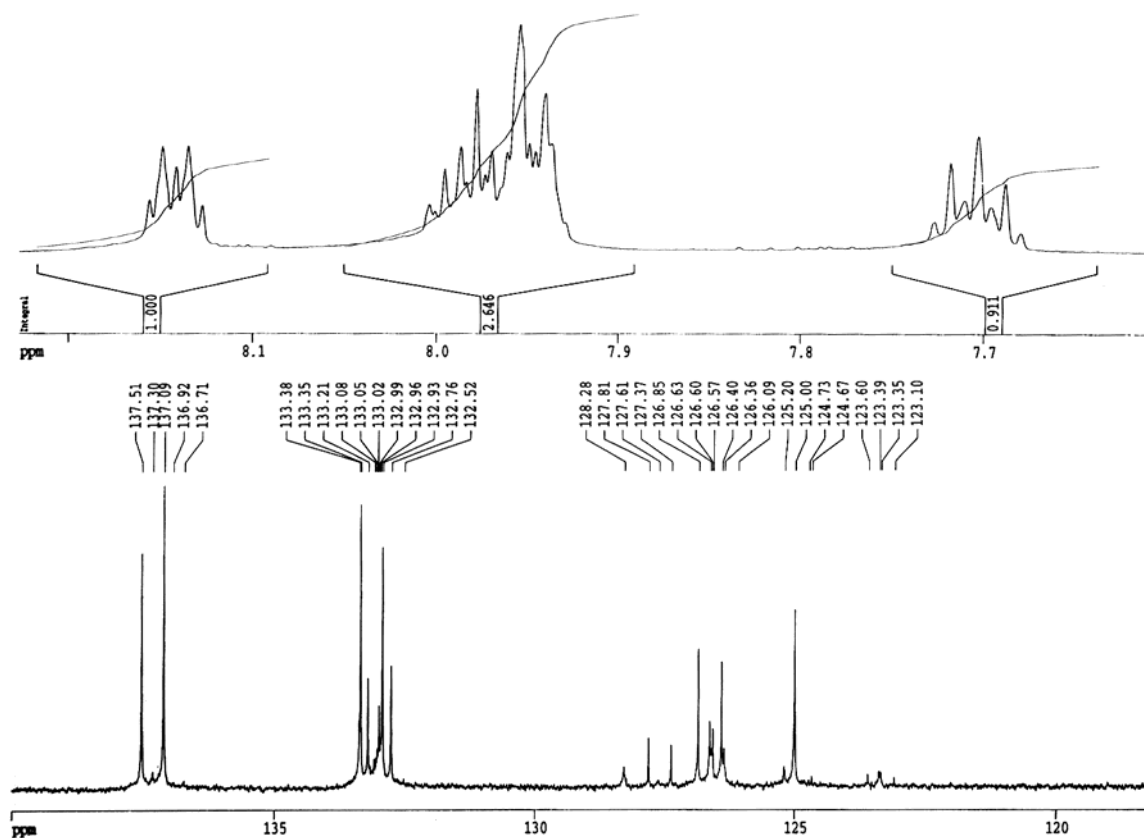
Figure 3.4 ^{1}H NMR (500 MHz, top) and ^{13}C NMR (125 MHz, bottom) of labeled **75** in CDCl$_3$.

Although **75** contains 18 carbons, because of the symmetry of the molecule there are only 10 signals in its ^{13}C NMR spectrum (Figure 3.5). Five of these (δ 128.3, 126.6, 126.3, 125.0, and 123.4) are due to tertiary carbon atoms (determined by HMQC, Figure 3.6) and five (δ 137.3, 133.2, 133.0, 127.6, and 126.7) are assignable to quaternary ones.
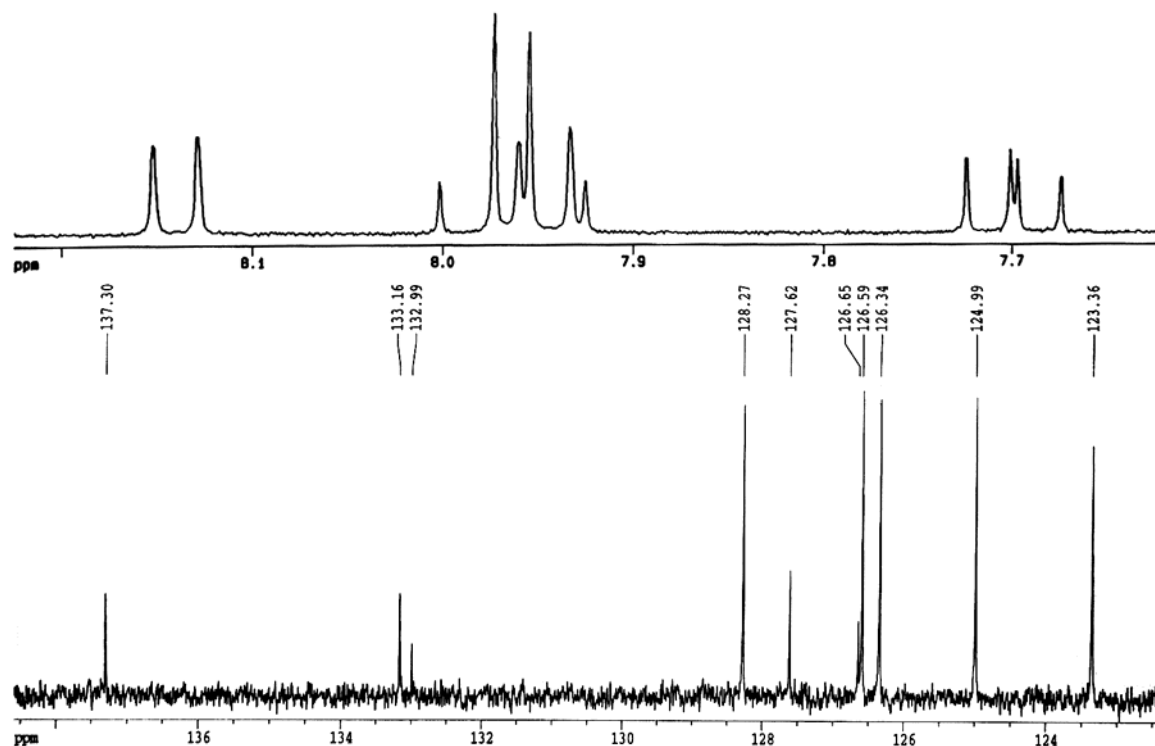
Figure 3.5 ^{1}H NMR (300 MHz, top) and ^{13}C NMR (125 MHz, bottom) of unlabeled **75** in CDCl$_3$.

The doublet at δ 8.15 ($J = 7.0$ Hz) in the ^{1}H NMR spectrum was assigned to H-6 based on the results of a deuterium labeling study conducted by Scott (and the location of H-6 in the deshielding bay region of **75**).[84] From the HMQC it can be determined that the ^{13}C NMR signal at δ 123.4 is from C-6. The doublet of doublets at δ 7.71 ($J = 8.0, 7.0$ Hz) arises clearly from H-5, and by HMQC the peak at δ 128.3 is due to C-5. This

allows the doublet at δ 7.96 (*J* = 8.0 Hz) to be assigned to H-4 (the ^{13}C signal at δ 126.3 is caused by C-4). Finally, the doublets at δ 8.00 (*J* = 8.7 Hz, HMQC correlated carbon signal at δ 126.6) and δ 7.95 (*J* = 8.7 Hz, correlated carbon signal at δ 125.0) have their origin in H-1 and H-2.

Further information was obtained from a long-range HMQC spectrum optimized to look for couplings of 7 Hz (Figure 3.7). H-5 correlates with carbon signals at δ 128.3 (C-5), 127.6, and 137.3. As this type of experiment most often shows three-bond or two-bond couplings,[85] it is highly likely that the quaternary carbon signals at δ 127.6 and 137.3 arise from C-3 and C-7.
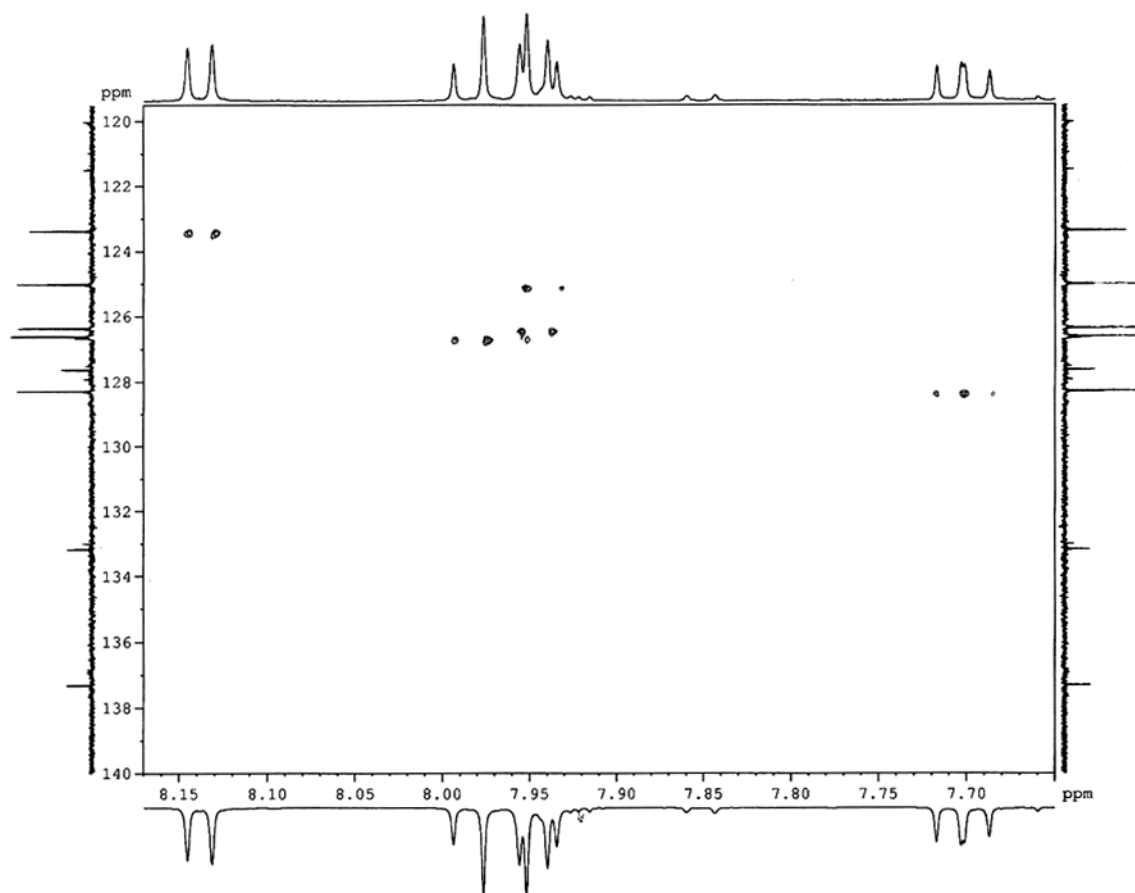
Figure 3.6 HMQC of **75** in CDCl₃.
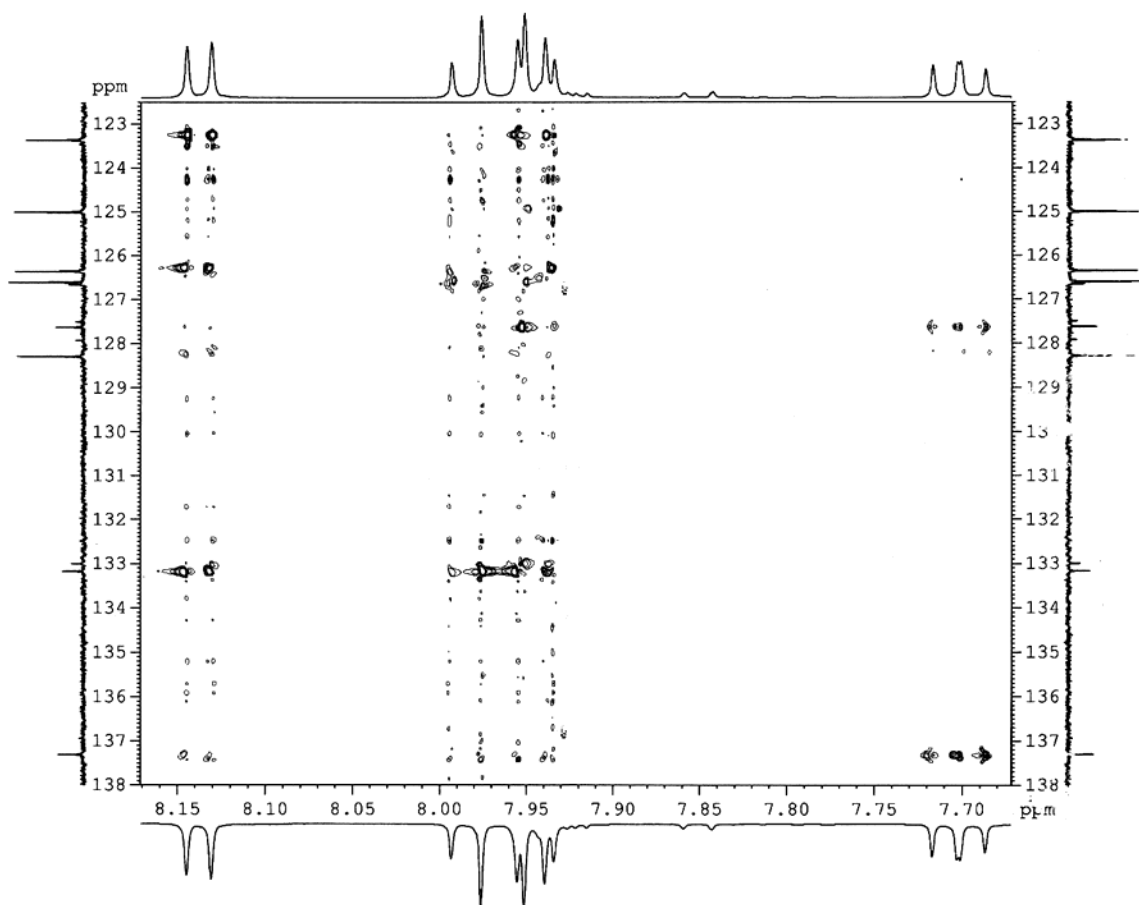
Figure 3.7 Long-range HMQC of **75** in CDCl₃.

H-6 correlates with carbon signals at δ 128.3 (C-5), 126.3 (C-4), 123.4 (C-6), 137.3 and 133.2. This leads to the conclusion that the signal at δ 137.3 belongs to C-7, because the two-bond coupling between H-6 and C-7 is much more likely to be observed than a four-bond coupling between H-6 and C-3. This allows the signal at δ 127.6 to be assigned to C-3. The observed correlation between H-6 and the signal at δ 133.2 suggests that this signal is due to C-8, as the three-bond coupling to C-8 is more likely to be observed than a long range coupling to C-9 or C-10. The only remaining unassigned signals (δ 133.0 and 126.7) are therefore due to C-9 and C-10.

C-8 shows a correlation with the proton signal at δ 8.00. Since the three-bond coupling between C-8 and H-2 is more likely to be observed than the four-bond coupling between C-8 and H-1, this leads to the conclusion that the signal at δ 125.0 is from C-1 and the signal at δ 126.6 is due to C-2.

These assignments are also consistent with the lesser intensity of the peaks at δ 126.7 and 133.0. Assigning these peaks to C-9 and C-10 is thus reasonable, as these carbons are quaternary and their relative abundance is half that of the other carbons.

To summarize, the ^{13}C NMR spectrum of **75** is as follows: δ 125.0 (C-1), 126.6 (C-2), 127.6 (C-3), 126.3 (C-4), 128.3 (C-5), 123.4 (C-6), 137.3 (C-7), 133.2 (C-8), 133.0 and 126.7 (C-9 and C-10). From these previously undetermined data, the conclusion can be drawn that the larger pair of doublets observed in the ^{13}C NMR spectrum of **75**-^{13}C$_2$ (*J* = 53.1 Hz) is due to C-7 and C-8, while the smaller pair of doublets (*J* = 56.0 Hz) can be assigned to C-9 and C-10.

3.4.2 Acefluoranthylene (82)
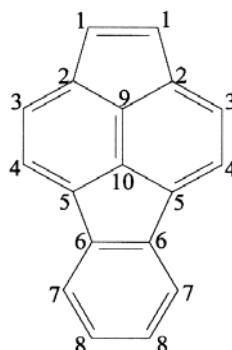
The ^{13}C NMR spectrum (Figure 3.8) of **82**-^{13}C$_2$ isolated from the FVP of **3f** exhibits two major labeling patterns: a doublet at δ 138.8 (J = 49.6 Hz) correlated to a doublet at δ 132.9 (J = 49.6 Hz), and a smaller doublet also at δ 138.8 (J = 68.5 Hz) correlated to a doublet at δ 121.1 (J = 68.5 Hz).
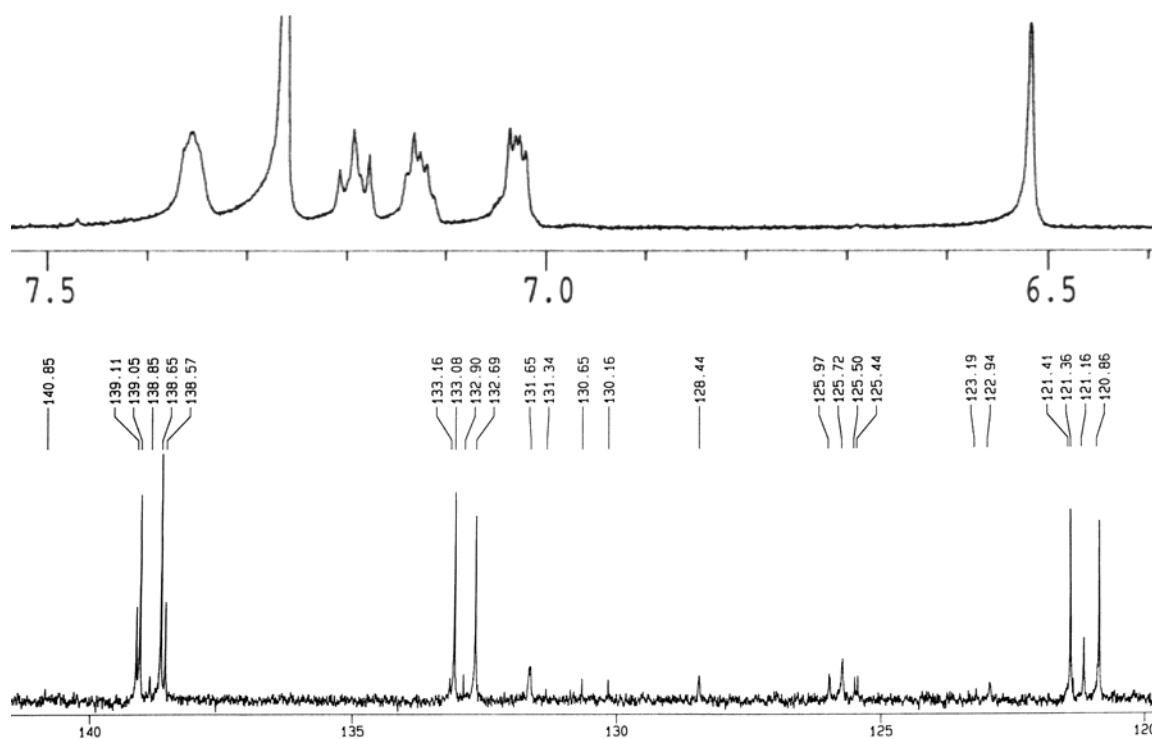
Figure 3.8 ^{1}H NMR (500 MHz, top) and ^{13}C NMR (125 MHz, bottom) of labeled **82** in CDCl$_3$.

Although **82** contains 18 carbons, because of the symmetry of the molecule there are only 10 signals in its ^{13}C NMR spectrum (Figure 3.9). Five of these (δ 131.6, 128.4, 125.7, 122.9, and 121.1) are due to tertiary carbon atoms (determined by HMQC, Figure 3.11) and five (δ 142.8, 140.6, 138.8, 132.9, and 130.4) are assignable to quaternary ones.
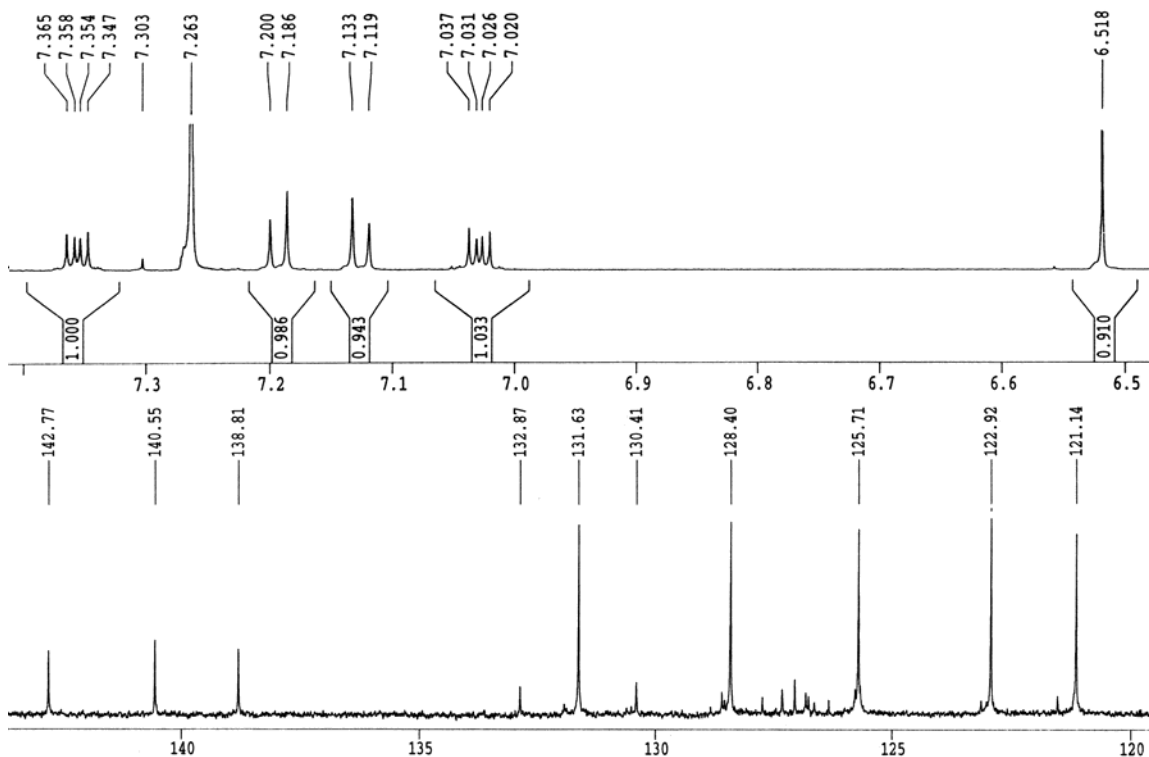
Figure 3.9 ^{1}H NMR (500 MHz, top) and ^{13}C NMR (125 MHz, bottom) of unlabeled **82** in CDCl$_3$.

The singlet at δ 6.52 in the ^{1}H NMR spectrum arises clearly from H-1. From the HMQC (Figure 3.10) it can be determined that the ^{13}C NMR signal at δ 131.6 is caused by C-1. The doublets at δ 7.19 and 7.13 arise from H-4 and H-3. A NOESY spectrum of **82** (Figure 3.11) reveals a cross peak between the singlet at δ 6.52 and the doublet at δ 7.13. This shows that the proton signal at 7.13 ppm is from H-3, and by HMQC the peak at δ 125.7 is due to C-3. By elimination, the doublet at δ 7.19 is caused by H-4

86

(δ 121.1 is due to C-4). The NOESY spectrum also shows a cross peak between H-4 and the multiplet at δ 7.36, consistent with this signal originating from H-7 (the signal at δ 122.9 belongs to C-7), allowing the multiplet at δ 7.03 to be assigned to H-8 (and δ 128.4 to C-8).
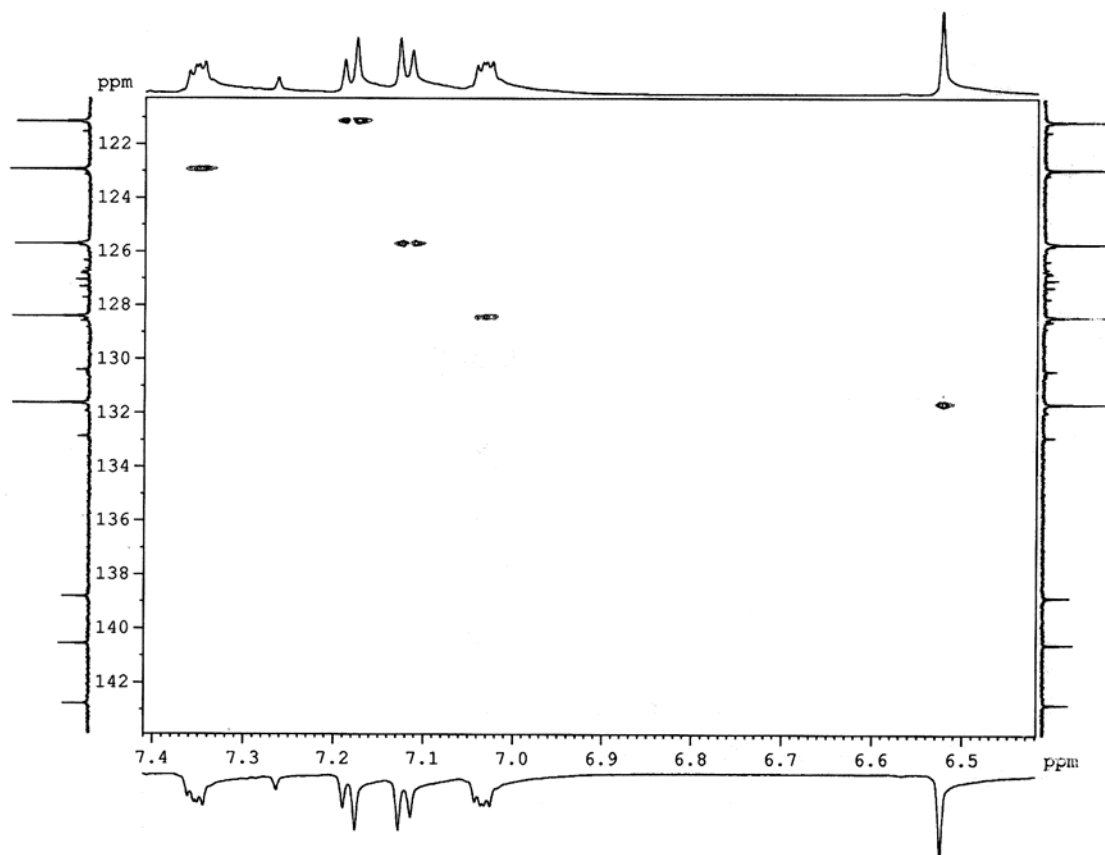
Figure 3.10 HMQC of **82** in CDCl₃.

Further information can be obtained from an HMBC spectrum (Figure 3.12). H-1 correlates with carbon signals at δ 131.6 (C-1), 130.4, and 140.6. As HMBCs most often show three-bond or two-bond couplings, it is highly likely that the quaternary carbon signals at δ 130.4 and 140.6 arise from C-2 and C-9.
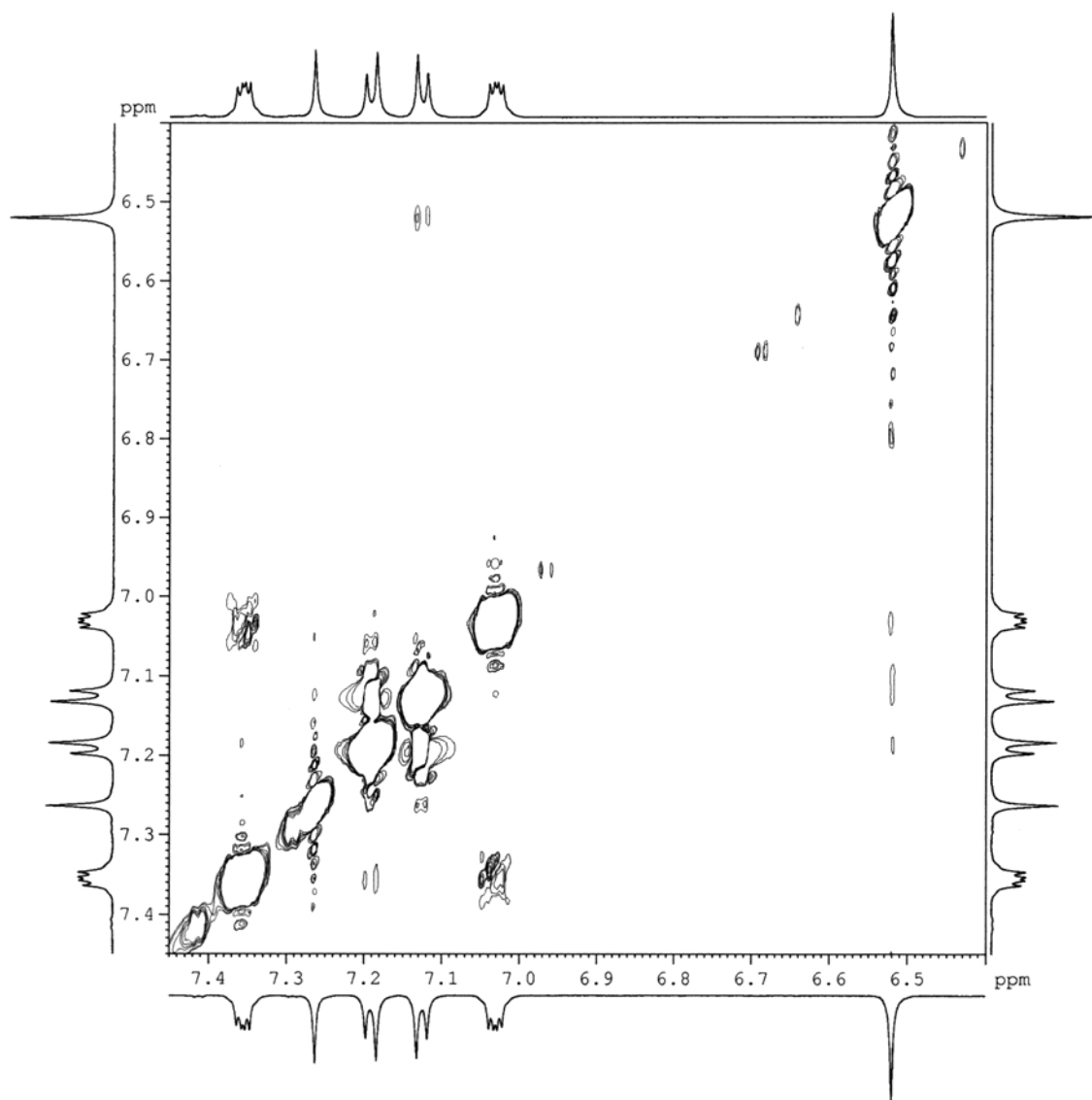
Figure 3.11 NOESY of **82** in CDCl$_3$.

H-3 correlates with carbon signals at δ 121.4 (C-4), 131.6 (C-1), 130.4, and 138.8. This leads to the conclusion that the signal at δ 138.8 belongs to C-5, as it is not from C-2 or C-9 (because they cause the signals at δ 130.4 or 140.6), and the three-bond coupling between H-3 and C-5 is much more likely to be observed in an HMBC than a four-bond coupling between H-3 and C-6 or C-10.
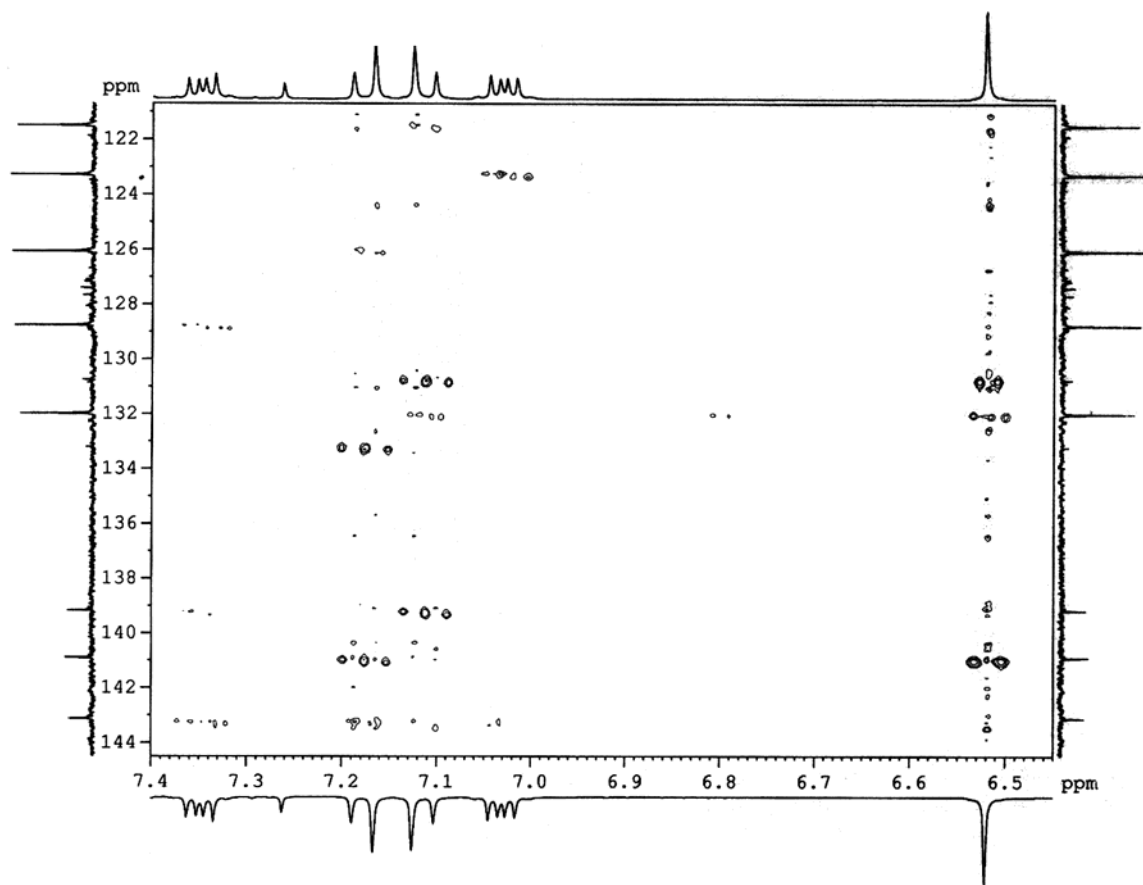
Figure 3.12 HMBC of **82** in CDCl₃.

H-4 correlates with carbons signals at δ 125.7 (C-3), 132.9, 140.6, and 142.8. From this and preceding data the conclusion can be drawn that the signal at δ 140.6 is due to C-2, as the correlation between H-4 and C-2 (a three-bond coupling) is much more likely to be observed in a HMBC than the correlation between H-4 and C-9 (a four-bond coupling). This means that the signal at δ 130.4 arises from C-9.

H-8 only correlates with signals at δ 122.9 (C-7) and 142.8. This strongly suggests that the signal at δ 142.8 is due to C-6 (a three-bond coupling to H-8).

H-7 correlates with signals at δ 128.4 (C-8), 138.8, and 142.8 (C-6). As the three-bond coupling between H-7 and C-5 is more likely to be observed than the four-bond

89

coupling between H-7 and C-10, the signal at δ 138.8 can be assigned to C-5. By elimination, the signal at δ 132.9 is due to C-10.

These assignments are also consistent with the lesser intensity of the peaks at δ 130.4 and 132.9. Assigning these peaks to C-9 and C-10 is thus reasonable, as these carbons are quaternary and their relative abundance is half that of the other carbons.

To summarize, the ^{13}C NMR spectrum on **82** is as follows: δ 131.6 (C-1), 140.6 (C-2), 125.7 (C-3), 121.1 (C-4), 138.8 (C-5), 142.8 (C-6), 122.9 (C-7), 128.4 (C-8), 130.4 (C-9), 132.9 (C-10). From these previously undetermined data, the conclusion can be drawn that the larger pair of doublets observed in the ^{13}C NMR spectrum of **82**-^{13}C$_2$ ($J =$ 49.6 Hz) is due to C-5 and C-10, while the smaller pair of doublets ($J = 68.5$ Hz) can be assigned to C-5 and C-4.

3.4.3 Cyclopent[*hi*]acephenanthrylene (83)
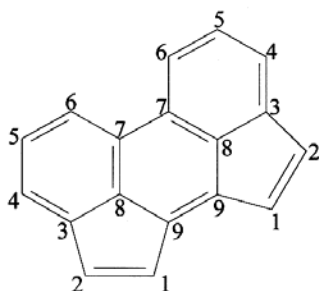
The ^{13}C NMR spectrum (Figure 3.13) of **83**-$^{13}C_2$ isolated from the FVP of **3f** exhibits two major labeling patterns: a singlet at δ 136.2, and a less intense doublet at δ 130.8 ($J = 61.0$ Hz) correlated to a doublet at δ 126.2 ($J = 61.0$ Hz).
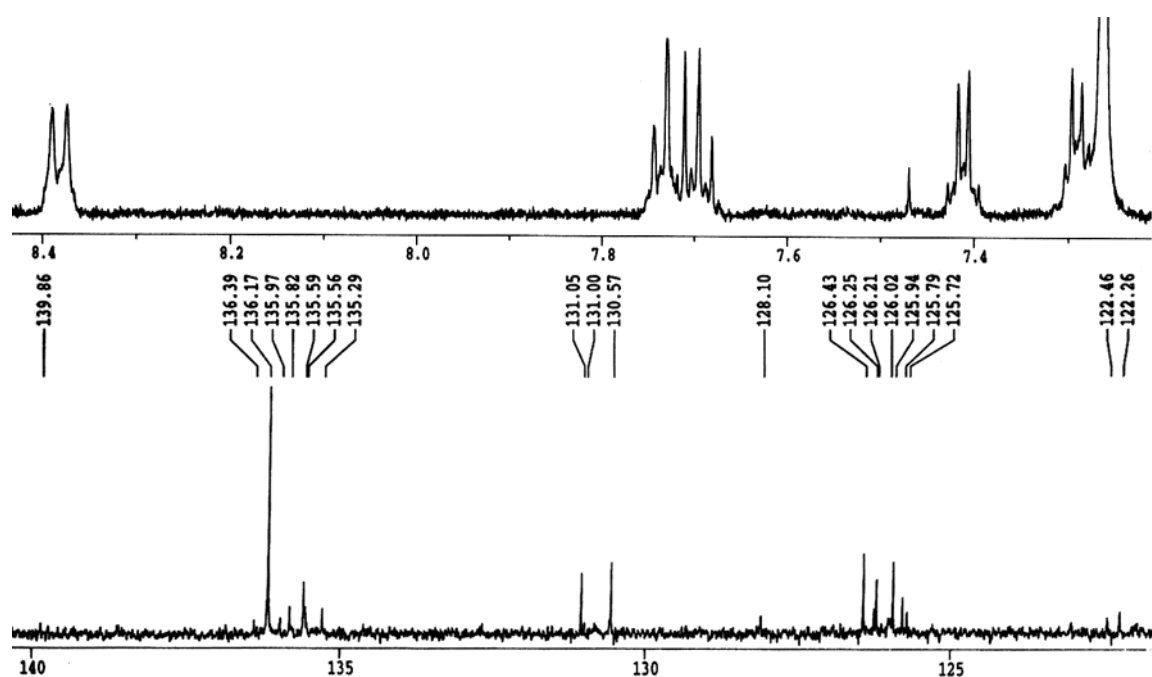
Figure 3.13 ^{1}H NMR (500 MHz, top) and ^{13}C NMR (125 MHz, bottom) of labeled **83** in CDCl₃.

The ^{1}H and ^{13}C NMR spectra of **83** have been previously assigned by Mulder et al. The authors first made ^{1}H NMR assignments by means of homodecoupling and NOE

experiments, and then used two CH COSY experiments (optimized to look for couplings of 7 Hz and 160Hz) to determine ^{13}C NMR assignments. As literature ^{13}C NMR assignments of PAH's have on occasion proven to be incorrect (see, for instance, Section 3.4.4), these assignments were redetermined. However, because independent confirmation of the ^{1}H NMR assignments made by Mulder was available,[86] these assignments were not reinvestigated.

Although **83** has 18 carbons, because of the symmetry of the molecule there are only 9 signals in its ^{13}C NMR spectrum (Figure 3.14). Five of these (δ 135.5, 128.0, 126.0, 123.0, and 122.2) are due to tertiary carbon atoms (determined by HMQC, Figure 3.15) and four (δ 139.6, 136.2, 130.8, and 126.2) are assignable to quaternary ones.
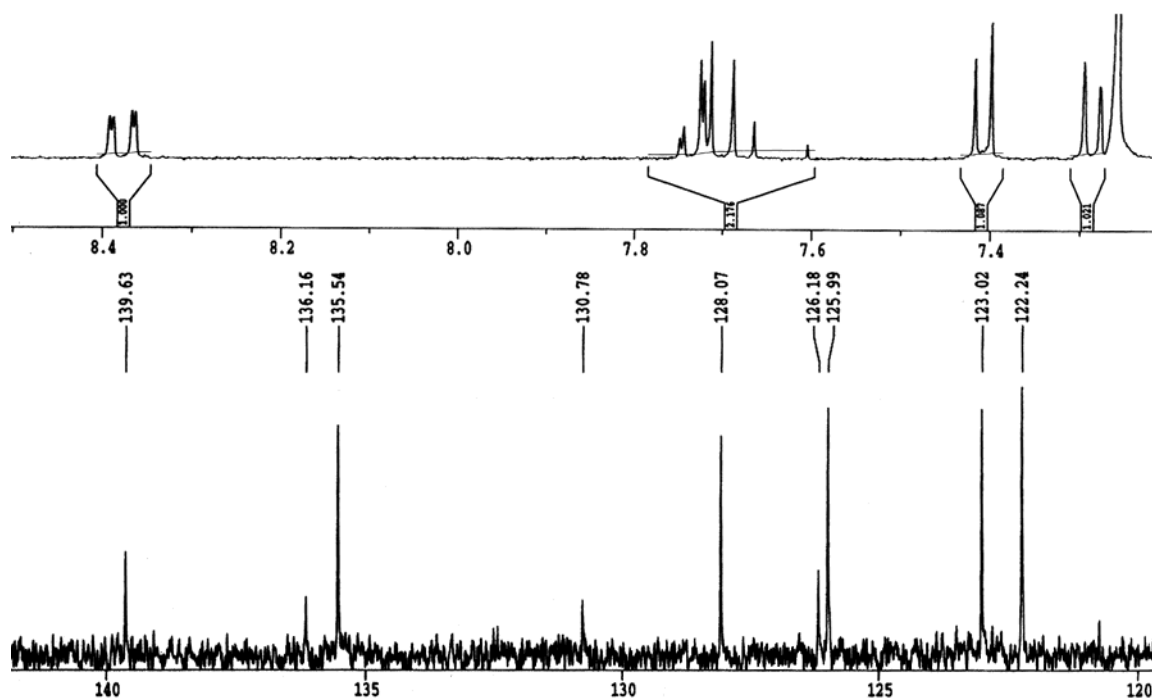
Figure 3.14 ^{1}H NMR (300 MHz, top) and ^{13}C NMR (125 MHz, bottom) of unlabeled **83** in CDCl$_3$.
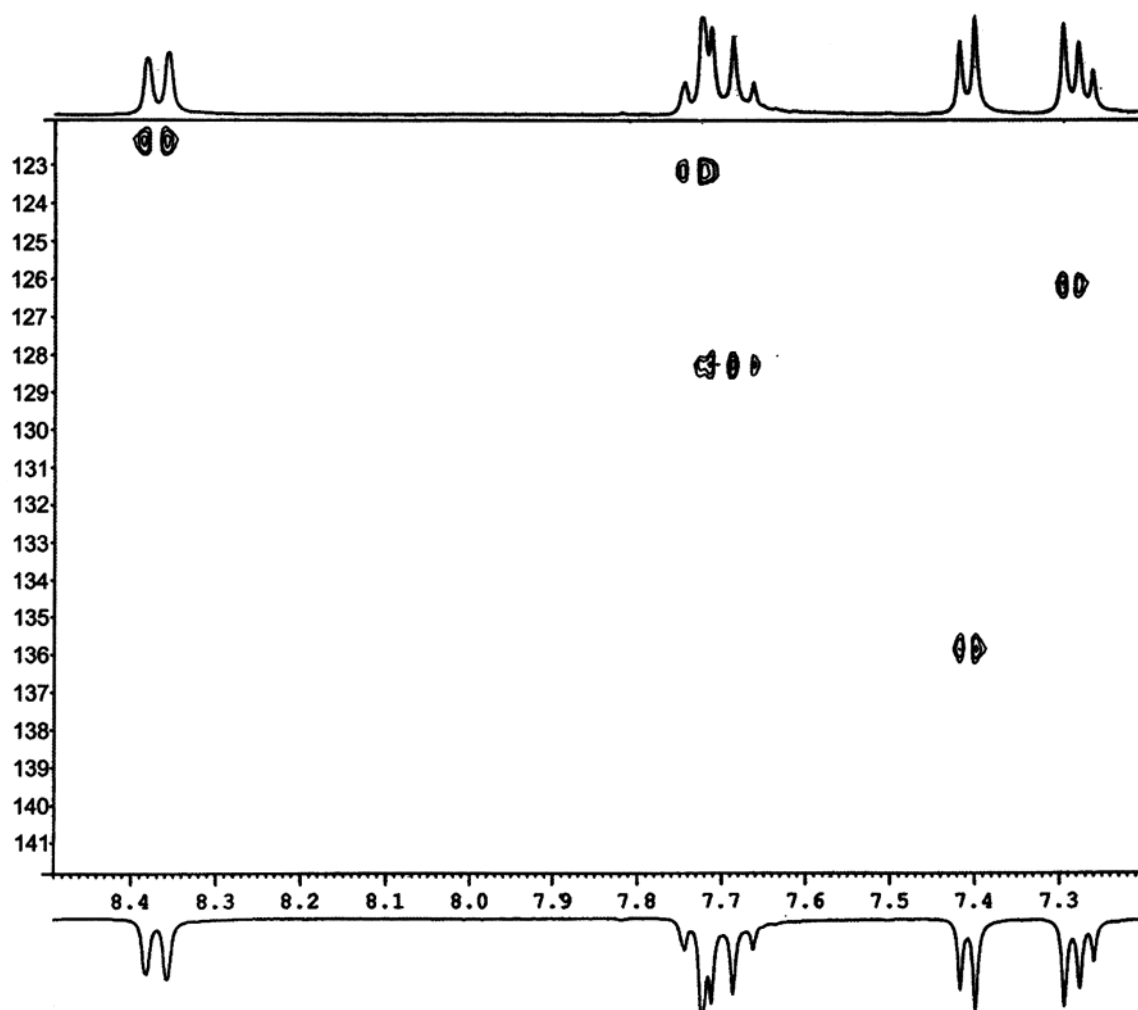
Figure 3.15 HMQC of **83** in CDCl₃.

The doublet of doublets at δ 8.38 is known to be due to H-6. From the HMQC it can be determined that the ^{13}C NMR signal at δ 122.2 ppm is from C-6. The doublet at δ 7.28 is caused by H-1 (δ 126.0 is from C-1) and the doublet at δ 7.40 arises from H-2 (δ 135.5 is from C-2). The doublet of doublets at δ 7.73 is due to H-4 (δ 123.0 is from C-4) and the doublet of doublets at δ 7.69 has its origin in H-5 (δ 128.0 is from C-5).

Further information can be obtained from an HMBC spectrum (Figure 3.16). H-6 correlates with carbon signals at δ 123.0 (C-4), 126.2, and 130.8. As HMBCs most often

show three-bond or two-bond couplings, it is highly likely that the quaternary carbon signals at δ 126.2 and 130.8 arise from C-7 and C-8.
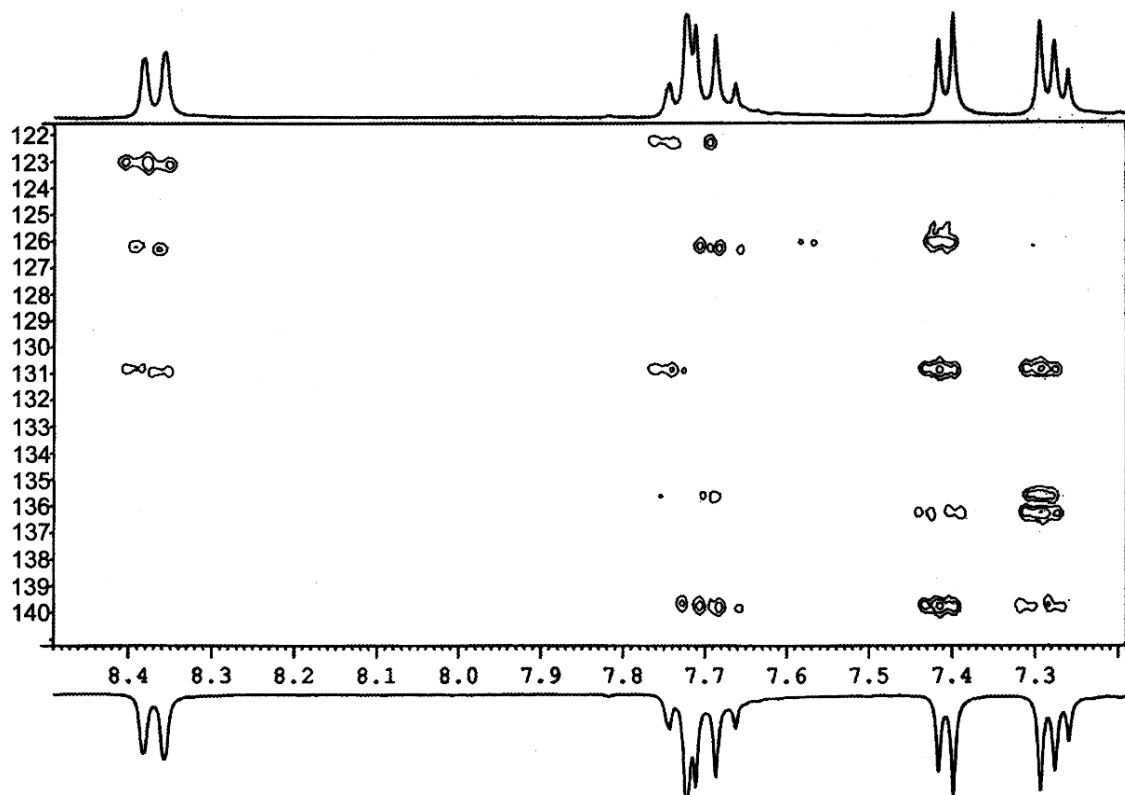
Figure 3.16 HMBC of **83** in CDCl$_3$.

H-1 correlates with carbon signals at δ 135.5 (C-2), 130.8, 136.2 and 139.6. This leads to the conclusion that the signal at δ 130.8 belongs to C-8, as this is the carbon most likely to correlate with both H-1 and H-6 (a three-bond coupling in each case). C-8 also shows the expected correlation with H-4 (another three-bond coupling). The signals at δ 136.2 and 139.6 are therefore from C-9 and C-3. H-5 correlates with the signal at δ 139.6, but not the signal at δ 136.2, leading to the conclusion that the peak at δ 139.6 is due to C-3 and that at δ 136.2 to C-9.

To summarize, the ^{13}C NMR spectrum of **83** is as follows: δ 126.0 (C-1), 135.5 (C-2), 139.6 (C-3), 123.0 (C-4), 128.0 (C-5), 122.2 (C-6), 126.2 (C-7), 130.8 (C-8), 136.2 (C-9). From these data, it can be concluded that the large singlet observed in the ^{13}C NMR spectrum of **83**-^{13}C$_2$ can be assigned to C-9, while the large pair of doublets is due to C-7 and C-8. The assignments obtained by HMQC and HMBC studies are identical to those previously published by Mulder based on CH COSY experiments.

3.4.4 Cyclopenta[cd]pyrene (84)
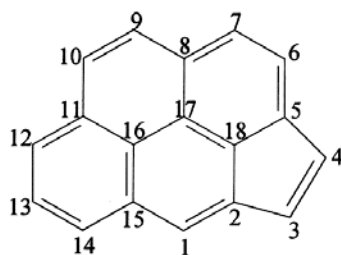
The ^{13}C NMR spectrum (Figure 3.17) of **84**-$^{13}C_2$ isolated from the FVP of **3f** exhibits two major labeling patterns: a doublet at δ 130.6 (J = 52.9 Hz) correlated to a doublet at δ 120.4 (J = 52.7 Hz), and a less intense doublet at δ 131.7 (J = 56.7 Hz) correlated to a doublet at δ 122.0 (J = 56.7 Hz).[80]
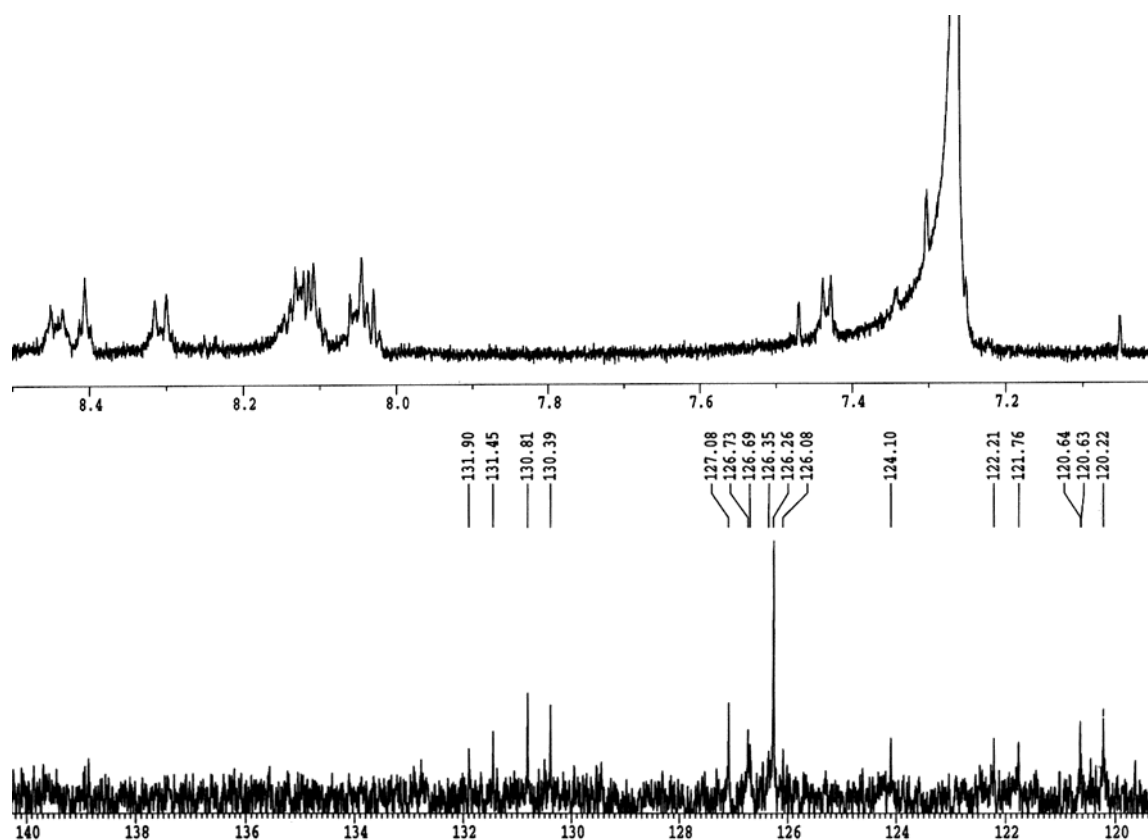
Figure 3.17 ^1H NMR (500 MHz, top) and ^{13}C NMR (125 MHz, bottom) of labeled **84** in CDCl$_3$.

An NMR study of **84** was published in 1986 by Jans et al. The authors used (and published the spectra of) a COSY experiment to assign the ^{1}H NMR spectrum, a ^{13}C-^{1}H shift correlation to locate the tertiary carbons, and a long-range ^{13}C-^{1}H shift correlation (optimized to look for couplings of 6 Hz) to ascertain some of the quaternary carbons. An H,C-COLOC experiment (the spectrum of which the authors chose not to publish) was used to verify the remaining quaternary carbons. Using the data of Jans, the signals can be assigned as follows: the peak at δ 131.7 is from C-15, that at δ 122.0 from C-17, at δ 130.6 from C-5, and at δ 120.4 from C-16. Inspection of the data above makes it clear that these assignments cannot be correct. The 57 Hz coupling constant is too large for a two-bond aromatic C-C coupling, and the 53 Hz coupling constant is far too large for a three-bond aromatic C-C coupling. It was thus necessary to subject this compound to renewed analysis, now aided by the presence of the labels. One piece of reliable literature information was available to help in this investigation, namely a synthesis of selectively deuterated **84** which was carried out in 1992 by Tannenbaum et al., proving that the doublet in the ^{1}H NMR spectrum at δ 7.25 (Figure 3.18) was due to H-3.[87]

Cyclopenta[*cd*]pyrene has 18 carbons (Figure 3.18). Ten of these (δ 133.2, 130.3, 128.3, 127.5, 126.70, 126.68, 126.4, 126.2, 124.1, and 122.4) are due to tertiary carbon atoms (determined by HMQC, Figure 3.19) and eight (δ 138.8, 135.3, 131.7, 130.6, 130.0, 127.1, 122.0 and 120.4) to quaternary ones, including the four signals of primary interest.
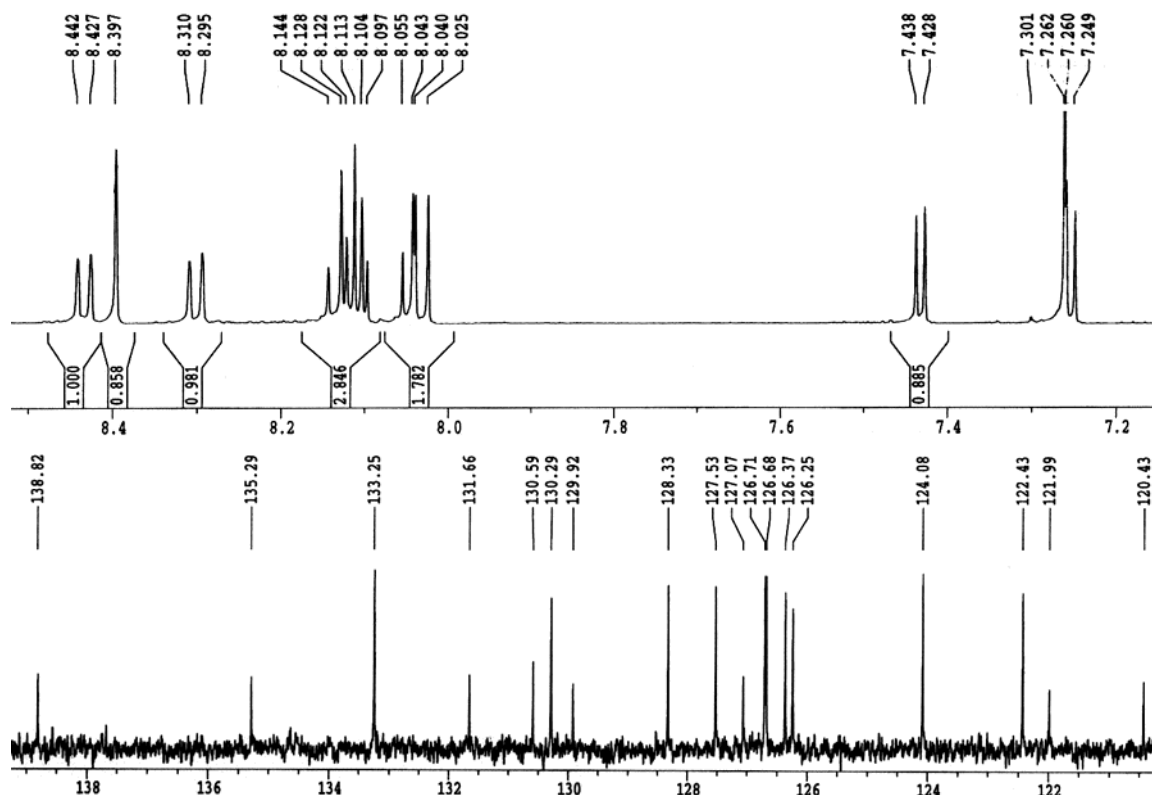
Figure 3.18 ^{1}H NMR (500 MHz, top) and ^{13}C NMR (125 MHz, bottom) of unlabeled **84** in CDCl$_3$.

The singlet at δ 8.39 in the ^{1}H NMR spectrum arises clearly from H-1. From the HMQC it can be determined that the ^{13}C NMR signal at 126.2 ppm is from C-1. The doublet at δ 7.25 (J = 5.1 Hz, HMQC correlated carbon signal at δ 127.5) is due to H-3, which means that the doublet at δ 7.43 is caused by H-4 (J = 5.1 Hz , the signal at δ 133.2 is from C-4). A NOESY spectrum of **84** (Figure 3.20) reveals a cross peak between the singlet at δ 8.39 and the signal at δ 8.43. This shows that the proton at 8.43 ppm is H-14 (δ 130.3 is due to C-14).

Further information can be obtained from a long-range HMQC optimized to look for couplings of 10 Hz (Figure 3.21). Both H-3 and H-4 clearly correlate with five carbons. Two of these (with signals at δ 127.5 and 133.2) are tertiary (C-3 and C-4) and

three are quaternary (with signals at δ 127.1, 135.3, and 138.8). As three-bond and two-

bond couplings are the most likely to be observed under these conditions, it is highly

probable that the three correlations to quaternary carbons that are observed are between

H-3 and H-4 and C-2, C-5, and C-18. This leaves C-8, C-11, C-15, C-16, and C-17 as

possible locations for the labels with signals at δ 131.7, 122.0, 130.6, and 120.4.
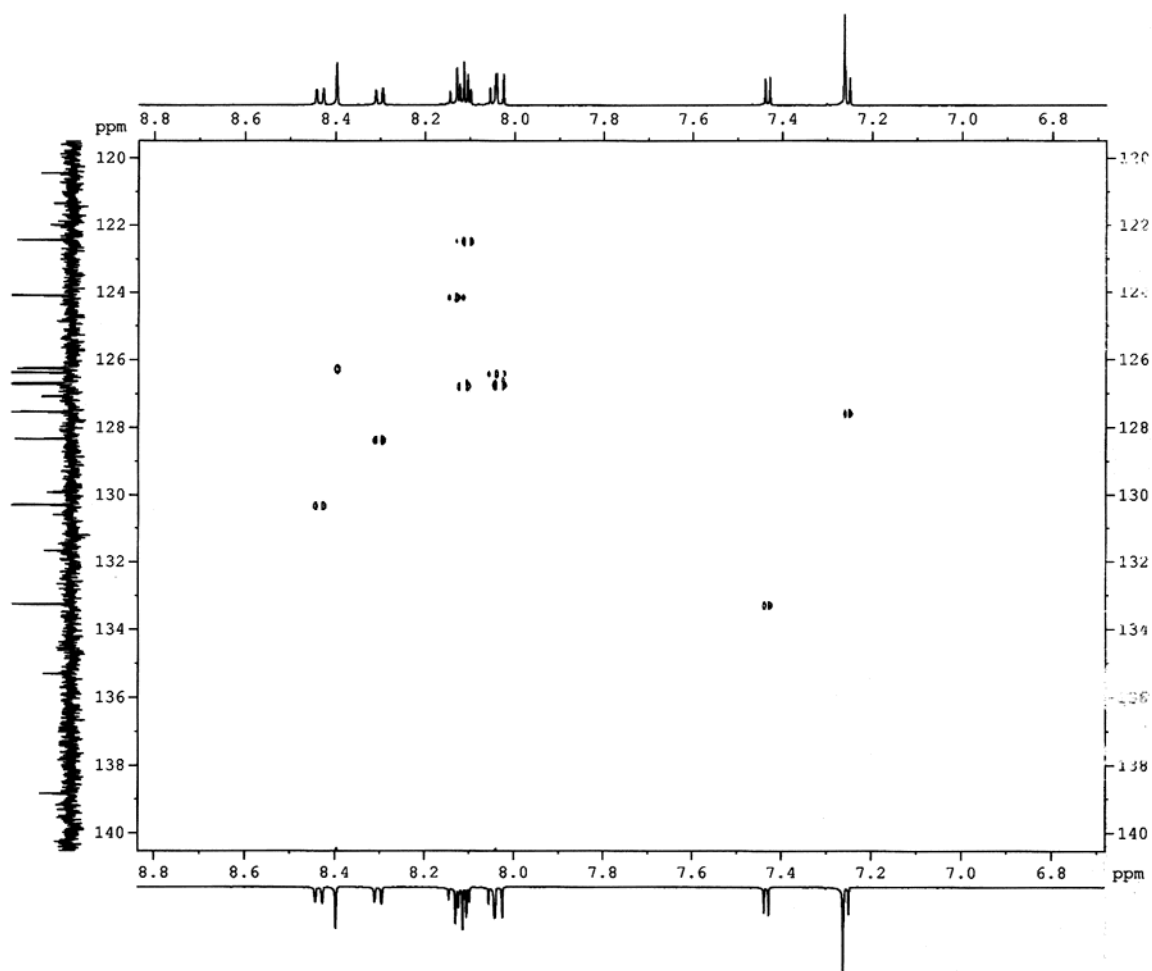
Figure 3.19 HMQC of **84** in CDCl₃.
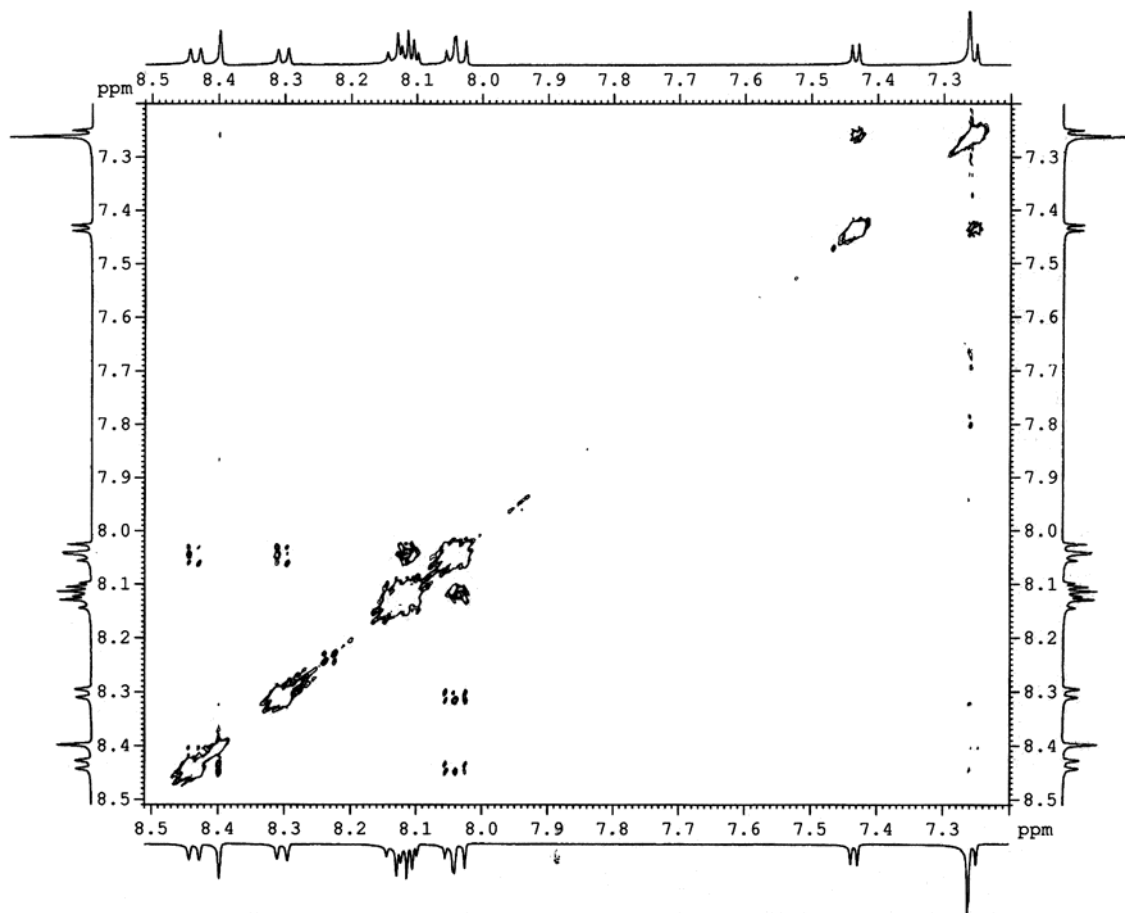
Figure 3.20 NOESY of **84** in CDCl$_3$.

H-1 correlates with one tertiary carbon (δ 130.3, C-14) and three quaternary carbons with signals at δ 122.0, 127.1 (arising potentially from either C-2, C-5, or C-18, C-5 being unlikely, as it would require a four-bond coupling), and 131.7. It is highly likely that the labeled signals at δ 122.0 and 131.7 are from C-15 and C-16, as the long range HMQC can be expected to show primarily three-bond and two-bond couplings, and C-2 and C-18 are already assigned. This leaves C-8, C-11, and C-17 as possible locations for the labels observed at δ 120.4 and 130.6. Because of the large coupling constants between the labeled signals at δ 120.4 and 130.6 (J = 53 Hz), it is clear that the two

labeled carbons must be adjacent and therefore be C-8 and C-17. By elimination, this also means that the signal at δ 130.0 is due to C-11.
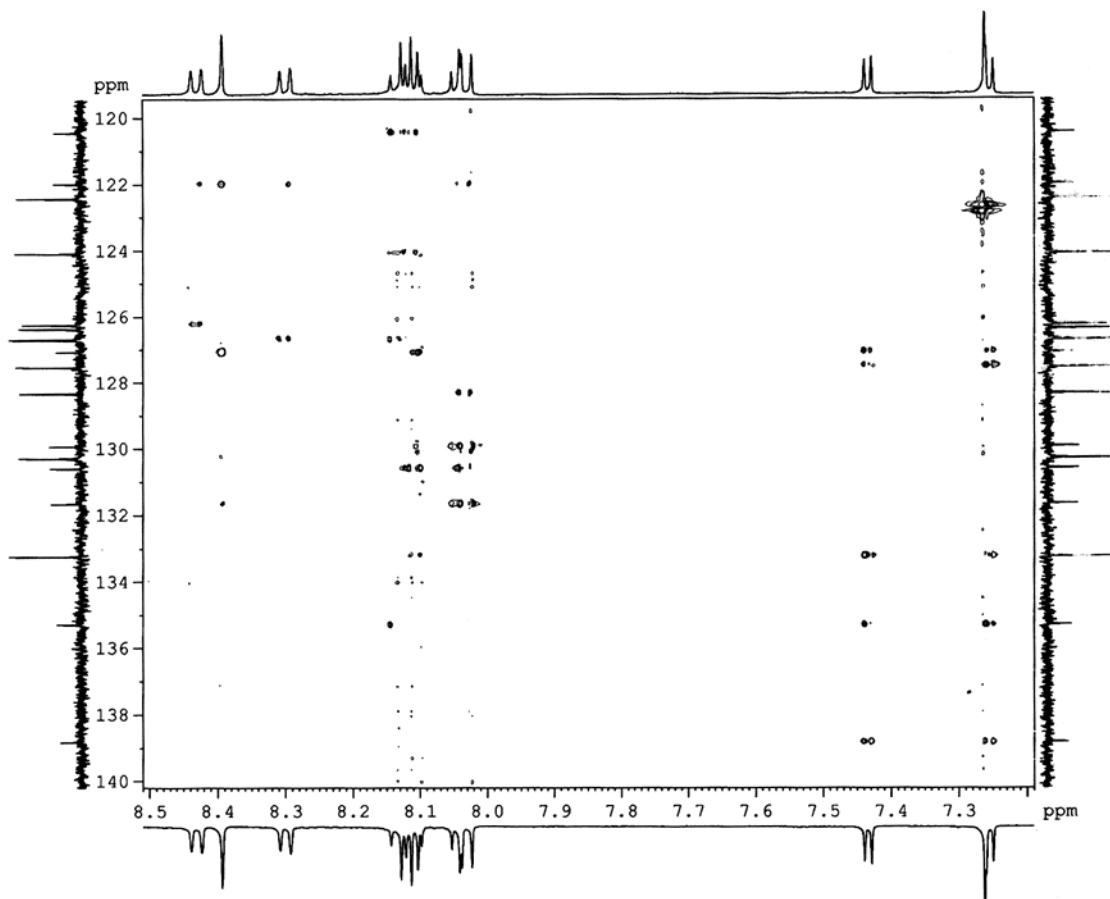
Figure 3.21 Long-range HMQC of **84** in CDCl₃.

There is further information that can be obtained from the spectra. The signal at δ 122.0 correlates with four protons, meaning that it is almost definitely C-16, because C-15 could only correlate with at most three protons by three-bond or two-bond couplings (H-1, H-13, and H-14) while C-16 can correlate with four (H-1, H-14, H-12, and H-10). This leaves the signal at δ 131.7 to be caused by C-15.

The signal at δ 127.1 (already determined to be either C-2 or C-18) correlates with four protons, indicating its origin as C-18, which can correlate by three-bond or two-

bond couplings with H-1, H-3, H-4, and H-6, instead of C-2, which can only correlate with three protons (H-1, H-3, and H-4). This means that the peaks at δ 135.3 and 138.8 are due to C-2 and C-5. The signal at δ 135.3 correlates with H-3, H-4, and a proton which is not H-1 (either H-6 or H-7). Therefore, the signal at δ 135.3 is from C-5, leaving the peak at δ 138.8 to be due to C-2.

To summarize the ^{13}C NMR assignments: δ 126.2 (C-1), 138.8 (C-2), 127.5 (C-3), δ 133.2 (C-4), δ 135.3 (C-5), 120.4 and 130.6 (C-8 and C-17), 130.0 (C-11), 130.3 (C-14), 131.7 (C-15), 122.0 (C-16), 127.1 (C-18). From these data, the conclusion can be drawn that the larger pair of doublets observed in the ^{13}C NMR spectrum of **84**-^{13}C$_2$ (J = 52.8 Hz) is due to C-8 and C-17, while the smaller pair of doublets (J = 56.7 Hz) can be assigned to C-15 and C-16. These conclusions fit better the large C-C couplings (>50 Hz) observed in the ^{13}C NMR spectrum of **84**-^{13}C$_2$ than do those made previously. While the spectra published in this reference appear to support the authors contentions, unfortunately the spectrum obtained from their most interesting study, the H,C-COLOC experiment, was not available. The correlation claimed in that spectrum between the signals at δ 8.00 and δ 135.3 (assigned to H9 and C8, respectively) seems erroneous, especially as the long-range HMQC spectrum shown in Figure 3.21 shows no such effect, but instead clear correlations between the carbon at δ 135.3 (C5) and H3 and H4.

3.5 Flash Vacuum Pyrolysis of Angular [4]Phenylene

After the study of the behavior of linear and angular [3]phenylenes under flash vacuum pyrolysis conditions was completed, angular [4]phenylene (**47**) was chosen as the next subject of investigation, because it is a high-energy potential precursor to both other phenylenes and numerous PAHs. Some of the molecules energetically "downhill" from **47** on the $C_{24}H_{12}$ manifold, along with their AM1 ΔH_f° values, are shown in Figure 3.22.

Unfortunately, **47** (Schemes 1.18 and 2.8) proved to be more difficult to work with than either **2** or **3**. Under the FVP conditions used (4.2 x 10^{-7} torr), **47** was difficult to sublime and care had to be taken not to overheat the sample to avoid unwanted reactions from occurring in the solid (or liquid) phase. The amount of recovered pyrolysate was very small; a large portion of the material never made it through the oven, but rather ended the FVP process as carbon residue on the quartz tube. Identification of the products was also complicated hindered by their low solubility, which made purification by HPLC unsuccessful despite extensive efforts.

Despite these difficulties, some progress was made in studying the behavior of **47** under FVP conditions. Figure 3.23 shows the ^{1}H NMR spectrum of the pyrolysate recovered from the FVP of **47** at 1000 °C. The largest constituent of this product mix is residual starting material **47**. Two other products could be identified, the biphenylene dimer **85**, recognized by comparison of its ^{1}H NMR spectrum [δ 6.72 (d, J = 8.6 Hz, 4H), δ 6.57 (dd, J_1 = 8.6 Hz, J_2 = 6.8 Hz, 4 H), δ 6.32 (d, J = 6.8 Hz, 4H)] with published data [δ 6.73 (d, J = 8.5 Hz, 4H), δ 6.57 (dd, J_1 = 8.5 Hz, J_2 = 7 Hz, 4H), δ 6.32 (d, J = 7 Hz,

4H)],[88] and coronene (**87**), responsible for the singlet at δ 8.93, whose presence was confirmed by HPLC (through comparison of retention times with commercially available material and UV spectroscopy).
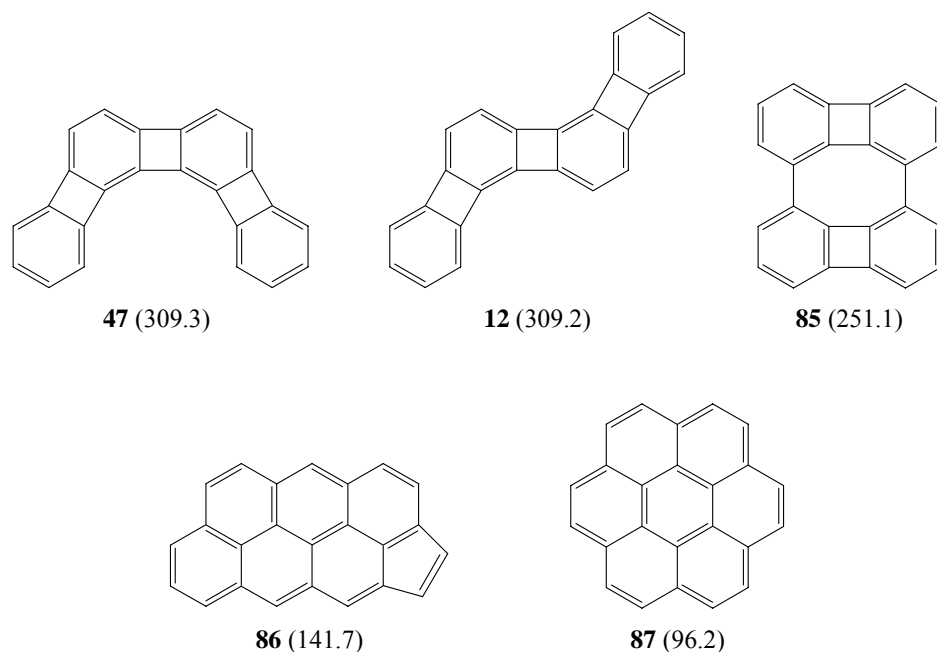
Figure 3.22 Some molecules on the $C_{24}H_{12}$ manifold. Numbers in parentheses are AM1 ΔH_f° values in kcal/mol.

The biphenylene dimer **85** is likely formed by a mechanism (Scheme 3.12) analogous to the one proposed for the isomerization of **2** to **3** (Scheme 3.5), namely bond cleavage to form the diradical **88**, followed by hydrogen shifts and radical recombination. AM1 calculations find that this rearrangement is energetically favorable by 58.2 kcal/mol. The formation of coronene (**87**), on the other hand, is favorable by 213.1 kcal/mol. The isolation of this molecule, the thermodynamic sink of the $C_{24}H_{12}$ manifold, provides further evidence for the ability of the phenylenes to isomerize to polycyclic benzenoid hydrocarbons. As of yet, a mechanism explaining the formation of **87** has not been formulated.
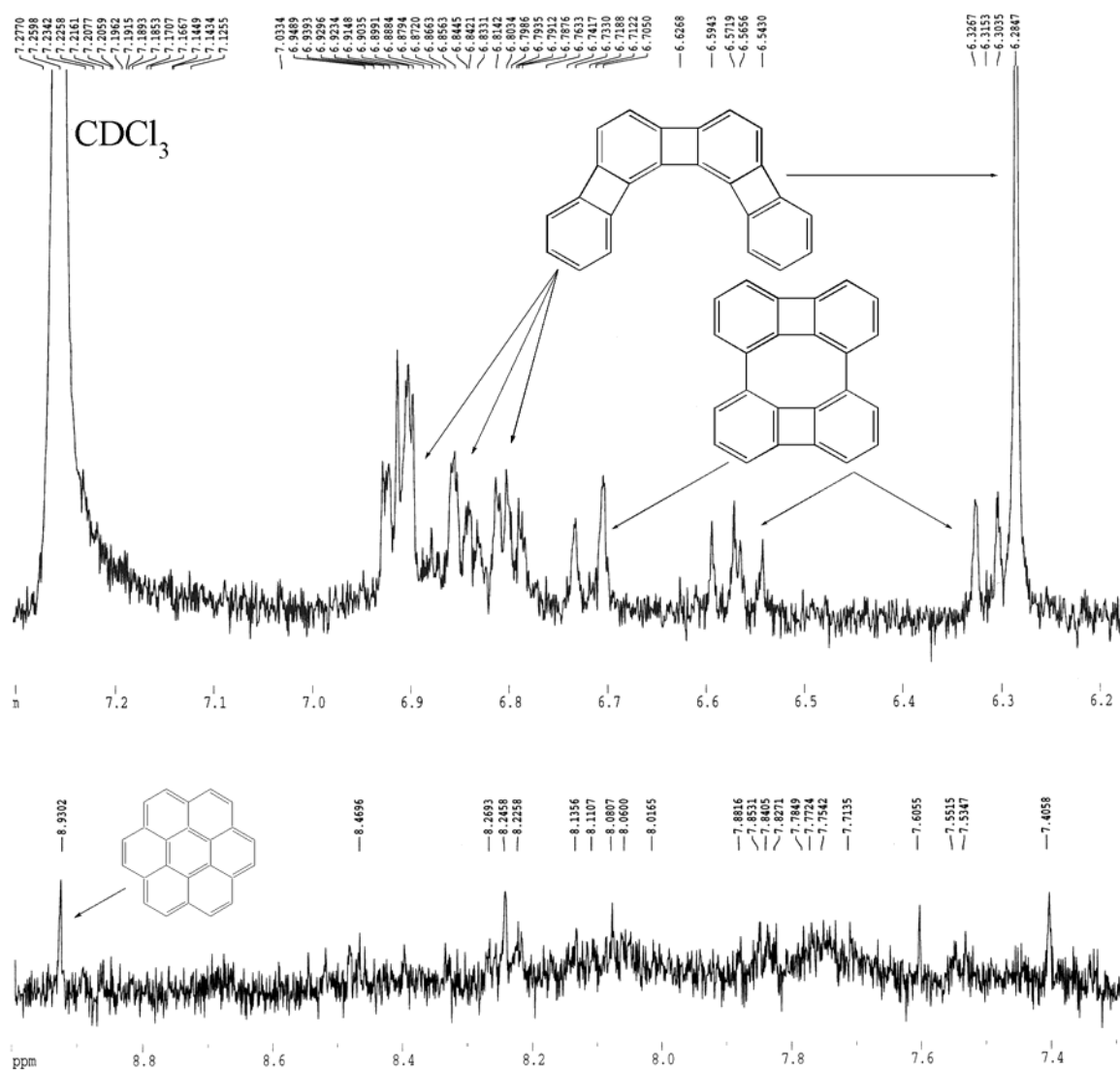
Figure 3.23 NMR spectrum in CDCl$_3$ of the pyrolysate from the FVP of angular [4]phenylene.

Any future work in this area should begin with finding a way to significantly improve the yields from the FVP of **47**. The most logical place to start would be to try a different pyrolysis method, possibly using a carrier gas. Such methods have on occasion proven to be superior to high vacuum conditions.[73a]
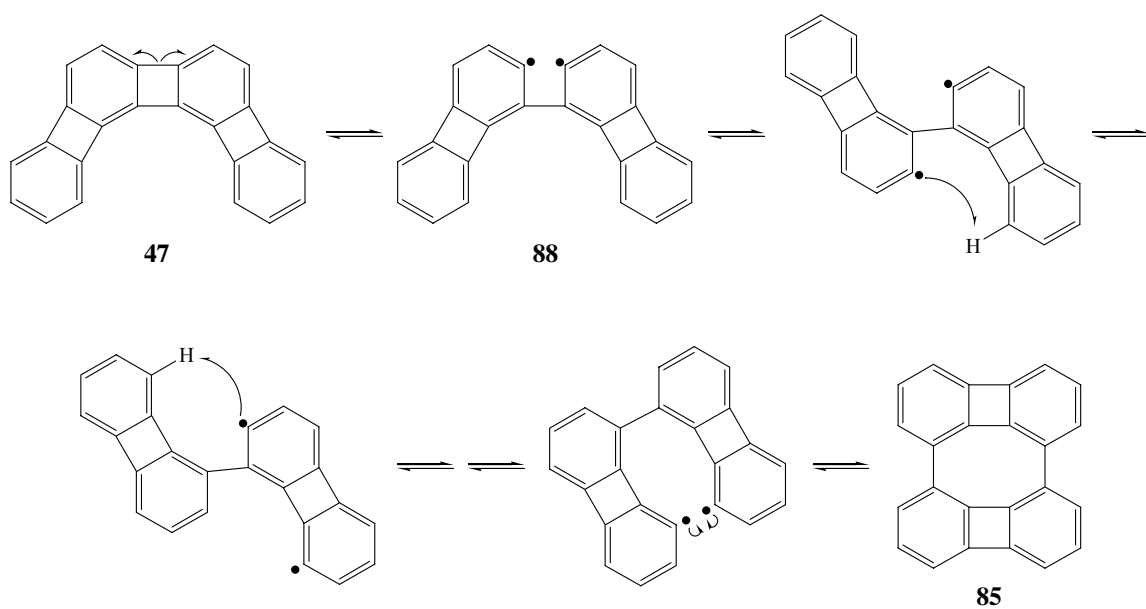
Scheme 3.12 Isomerization of **47** to **85** under FVP conditions.

Chapter Four

Approaches to an Alkyl-Solubilized Linear [5]Phenylene and a Kinetic Investigation of a Novel CpCo-Migration Along the Linear Phenylene Frame

4.1 Introduction

While the angular phenylenes have been studied extensively, comparatively little research has been conducted with their linear brethren. Among the reasons for this disparity are the relative air-sensitivity and insolubility of the larger linear phenylenes and their tendency to form CpCo complexes under cobalt-mediated [2+2+2]cycloaddition conditions. Because of these difficulties, only linear [3]-, [4]-, and [5]phenylenes[89] have been synthesized, and an X-ray crystal structure is only available for linear [3]phenylene (**2**). The original goal of the present study was to augment what is known about these molecules by obtaining an X-ray crystal structure of linear [5]phenylene **89**.

The synthesis of **89** was published in 1987 (Scheme 4.1) and follows the two triple cyclization approach used to make triangular [7]phenylene **35** (Scheme 1.15). Starting with 1,2,4,5-tetraethynylbenzene (**26**), cyclization with 1,6-bis[(triisopropylsilyl)ethynyl]-1,3,5-hexatriyne (**33**), followed by desilylation led to tetraethynyl linear [3]phenylene **90**. A second cyclization, this time with BTMSA, furnished the CpCo-complex **91**.
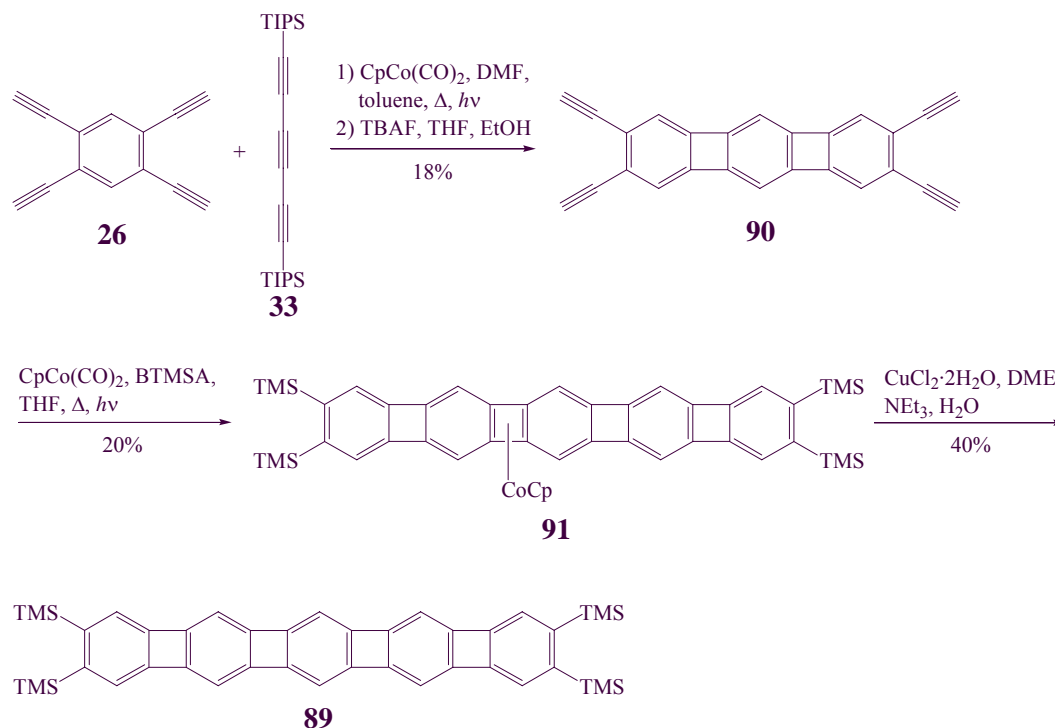
Scheme 4.1 Synthesis of TMS-substituted linear [5]phenylene **89**.

Attempted thermal demetallation of **91** with an external ligand, such as CO, successful in the case of the analogous Cp-complexed linear [4]phenylene **31**, failed. Evidently, the four-membered rings in **91** are sufficiently antiaromatic, as indicated by their relatively strong paratropism (an effect confirmed by NICS calculations), that binding to CpCo is too strong. Complexation "aromatizes" the molecule, as can be observed by ^{1}H NMR spectroscopy: the protons on the terminal rings of **91** resonate at δ 7.46 and 6.99, while the equivalent protons on **89** resonate at δ 6.81. In contrast, **31** can be readily demetallated with CO (Scheme 1.13), while decomplexation occurs spontaneously under the reaction conditions used to synthesize **2** (Scheme 1.12). Similarly, the relatively small antiaromatic character of the four-membered rings in angular phenylenes, evidenced in NICS calculations (Section 1.6), makes CpCo-binding

less energetically favorable, explaining why no analogous complex has been found with these molecules. (Note that in complex **58b**, the CpCo is bound to the central six-membered ring, see Section 2.1). Because attempted demetallation of **91** with CO in the original work failed, an oxidative approach with $CuCl_2$ was used to furnish **89**. Only a small amount of the material was synthesized, and neither a ^{13}C NMR spectrum nor an X-ray crystal structure was obtained.

This chapter will discuss the synthesis (Section 4.2) and attempted demetallation (Section 4.3) of a hexylsubstituted linear [5]phenylene derivative complexed to CpCo. A kinetic study of a novel migration of CpCo along the frame of this molecule will be presented in Section 4.4.

4.2 Synthesis of an Alkyl-Substituted Linear [5]Phenylene CpCo Complex

A serious difficulty frequently encountered during the synthesis of large polycyclic aromatic hydrocarbons like **89** is the insolubility of the products and synthetic intermediates, a problem that can be countered by incorporating solubilizing groups. This tactic has been used successfully with phenylenes on several occasions. For instance, monocyclization of hexayne **92** (Scheme 4.2) and double cyclization of hexayne **94** (Scheme 4.3)[22b] both occur with higher yields when solubilizing groups are utilized. For the present study, a synthesis incorporating hexyl solubilizing groups into the linear [5]phenylene frame was developed.

92a, R = H
92b, R = *i*-Pr

CpCo(CO)$_2$,
toluene, *h*ν, Δ

93a (trace amounts)
93b (5%)
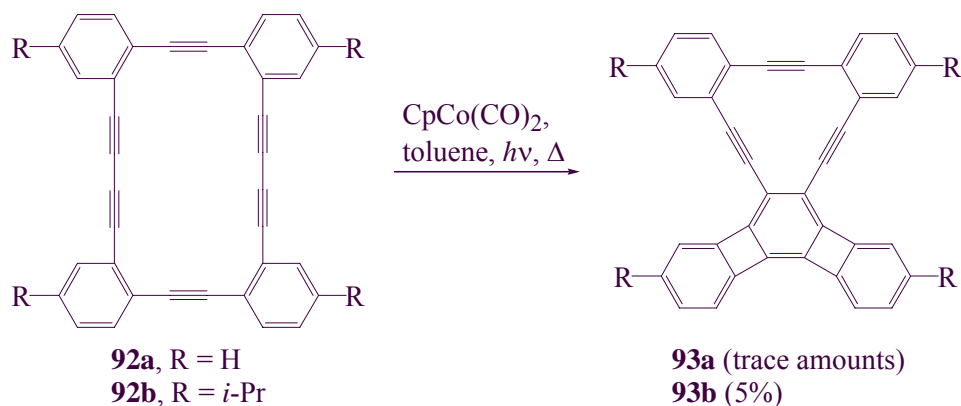
Scheme 4.2 Adding solubilizing groups to **92** resulted in better cyclization yields.
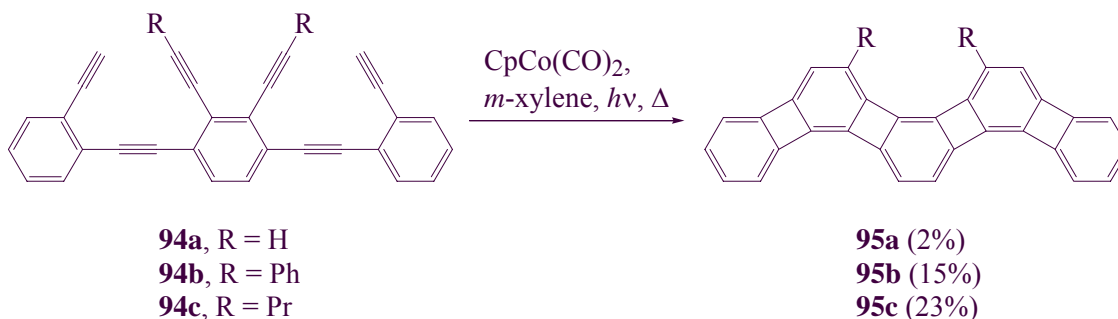
Scheme 4.3 Yields of zigzag [5]phenylene (**95**) increase when solubilizing substituents are present.

Hexylsubstituted 1,2,4,5-tetraethynylbenzene **96** was produced in good yields (86%) by palladium-catalyzed Sonogashira coupling of tetraiodobenzene **29** with 1-octyne at 80 °C (Scheme 4.4). The conditions for this reaction were important, as at lower temperatures the reaction rate was very low, while at higher temperatures decomposition occurred. Cyclization of **96** with **33** generated silylprotected tetrayne **97**, which, after desilylation, was subjected to a cobalt-mediated [2+2+2]cycloaddition to BTMSA to yield the highly air-sensitive CpCo-complexed linear [5]phenylene **99**. Gratifyingly, the yields of both cyclizations in this route were higher than that in the original synthesis (Scheme 4.1), probably due to both the increased solubility of the products and the decreased potential for unwanted polymerization of the starting materials.
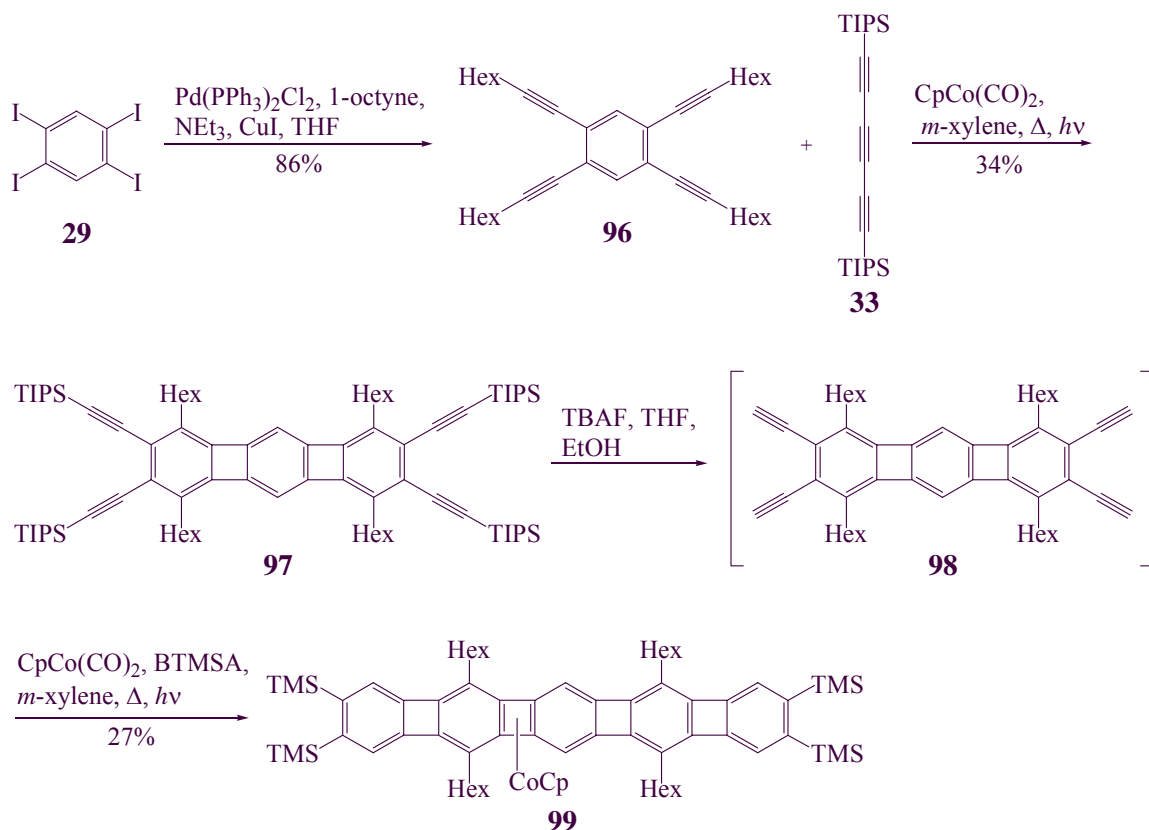
Scheme 4.4 Synthesis of CpCo-complexed linear [5]phenylene **99**.

Exhaustive attempts were made to acquire an X-ray crystal structure of **99**, but ironically these efforts were hindered by the high solubility of **99** in common organic solvents. Low-quality crystals were eventually obtained by slow evaporation from hexane. Synchrotron radiation was necessary to solve the X-ray structure (Figure 4.1). Unfortunately, the low resolution (R = 16.8%) prevents a detailed analysis of the bond lengths in **99** (Figure 4.2). Even so, the X-ray crystal structure unambiguously determines the point of CpCo attachment to the linear [5]phenylene fragment. A search of the Cambridge Structural Database found no other structurally characterized example of a CpCo bound to a cyclobutadiene ring of a phenylene.

Figure 4.1 Two views of the X-ray crystal structure of **99**. One of the hexyl groups is disordered over two positions.

Figure 4.2 Bond lengths in **99** (Å).

4.3 Attempted Demetallation of CpCo-Linear [5]Phenylene

The cobalt-mediated [2+2+2]cycloaddition used to synthesize **99** also produced trace amounts of what appeared to be uncomplexed linear [5]phenylene **100**. Unfortunately, this material could not be separated from **99** by either crystallization or chromatography on alumina. Because it could not be isolated, the tentative assignment of this compound as **100** is based primarily on ^{1}H NMR data (Figure 4.3) and the observation of the similar presence of small amounts of **89** in samples of crude **91**.[90]
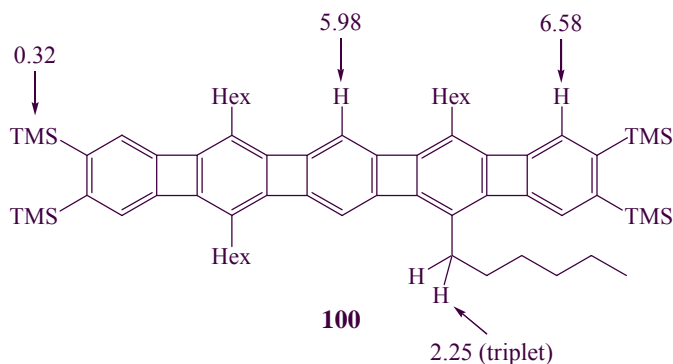
Figure 4.3 ^{1}H NMR data (δ, in CD$_2$Cl$_2$) of material believed to be **100**.

Regrettably, these traces of putative **100** were the only evidence for its existence. Oxidative demetallation, which was successful in generating **89** from **91**, led only to decomposition of **99** (Scheme 4.5). Heating **99** in the presence of the potential external ligands hexamethylbenzene (to 185 °C) and 1,5-cyclooctadiene (to 160 °C) furnished only recovered starting material (Scheme 4.6). Several other attempts at demetallation, including oxidation with ferrocenium hexafluorophosphate or irradiation of **99** in the presence of 1,2-bis(diphenylphosphino)ethane resulted in decomposition.
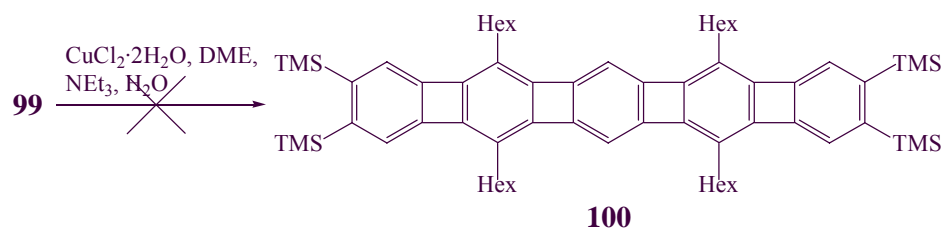
Scheme 4.5 Oxidative demetallation of **99** led to decomposition.
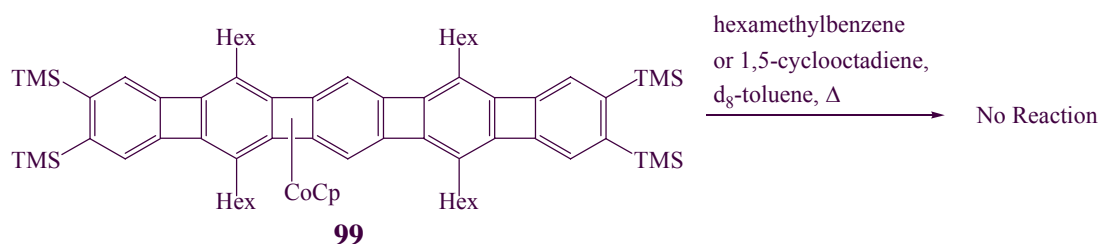
Scheme 4.6 Thermolysis of **99** in the presence of external ligands had no effect.

Another approach that initially seemed to hold promise was based on recent work by Sekiguchi and coworkers, who found that reduction of the CpCo-cyclobutadiene complex **101** with lithium, followed by oxidation with 1,2-dibromoethane, furnished the free cyclobutadiene **103** (Scheme 4.7).[91] Subjecting **99** to this series of reactions had no effect, while decomposition occurred when potassium was used as a reducing agent instead of lithium.
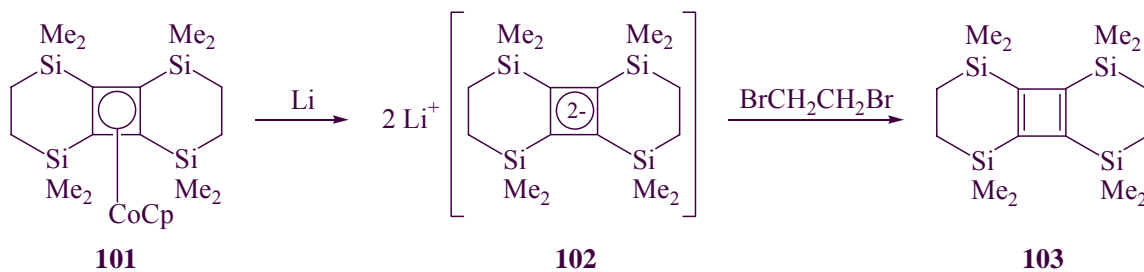
Scheme 4.7 Reductive removal of CpCo from **101** with lithium, followed by oxidation with 1,2-dibromoethane, generated the free cyclobutadiene **103**.

While the isolation of pure **100** was never achieved, efforts to demetallate **99** under irradiative conditions led to an interesting discovery that will be the subject of the next section: migration of the CpCo unit along the linear phenylene frame.

4.4 Thermal and Photochemical CpCo-Migration Along the Linear [5]Phenylene Frame

In an attempt to decomplex the linear [5]phenylene derivative **100**, CpCo-complex **99** was subjected to UV irradiation (Rayonet, 300 and 350 nm light). Interestingly, an ^{1}H NMR spectrum revealed a new set of aromatic and Cp singlets at δ 7.97, 6.88, 6.33, and 4.44 with relative integrations of 2:2:2:5. These signals slowly disappeared over a two week period. The amount of new material (relative to **99**) increased on continuing irradiation until a steady-state was reached (about 1:5) after a few hours.
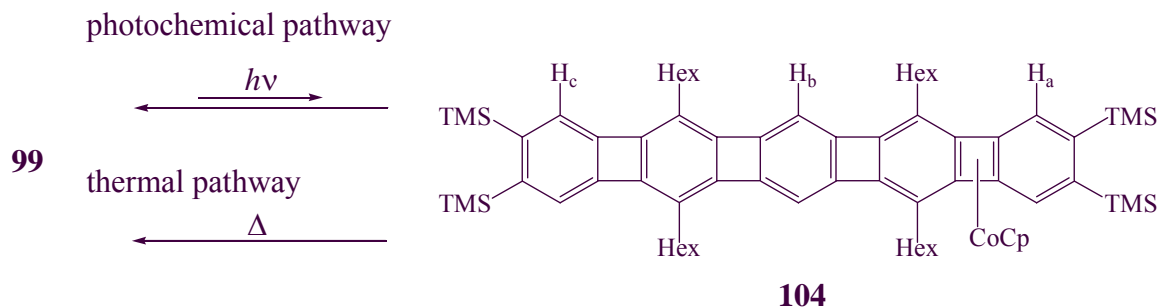
Scheme 4.8 Irradiation causes the CpCo-moiety to shift. The process is thermally and photochemically reversible.

By comparing the ^{1}H NMR spectrum with data from known CpCo-complexes (Figure 4.4),[24,89,92] the new compound was assigned the structure **104** (Scheme 4.8). In each of the molecules shown in Figure 4.4, the CpCo-moiety divides the phenylene into two units, one of which is a biphenylene. The locations of the signals from the protons on this segment (H$_1$ and H$_2$), vary only slightly with the length of the phenylene fragment on the other side of the CpCo, suggesting that to a first approximation, each "side" can be

considered separately. The chemical shift of the highly deshielded proton on **105** (δ 7.95) is almost identical with one of those for **104** (δ 7.97), providing key support for the proposed structure if this signal is assigned to H$_a$. Unfortunately, there is no known linear [4]phenylene fragment that can be used for comparison (see, however, below); nevertheless, likely chemical shifts can be extrapolated from the data in Figure 4.4. As the number of rings (and paratropism in the four-membered rings) in a fragment grows, the protons on the terminal rings become increasingly shielded (δ 7.45 with **31** and δ 6.99 with **91**). The signal from **104** at δ 6.88 is consistent with the value expected for H$_c$. This would leave the peak at δ 6.33 as being due to H$_b$. This value seems reasonable on the basis of the following argument. Using H$_4$ on **91** (δ 6.32) as an initial reference, addition of another phenylene unit (between the rings containing H$_4$ and H$_5$) should shield the proton by about 0.2-0.3 ppm. This effect is apparently canceled by that of alkyl substitution, as evidenced by the deshielding of H$_2$ on **99** relative to H$_3$ on **91** by 0.23 ppm.

105

H$_3$ H$_2$ H$_1$
TMS   TMS
TMS   TMS
7.95   6.90   7.45
CpCo

91

H$_5$ H$_4$ H$_3$ H$_2$ H$_1$
TMS   TMS
TMS   TMS
6.99   6.32   6.36   6.75   7.46
CpCo

31

H$_1$ H$_2$ H$_2$ H$_1$
TMS   TMS
TMS   TMS
7.45   6.72   6.72   7.45
CpCo

99

H$_3$ Hex H$_2$ Hex H$_1$
TMS   TMS
TMS   TMS
7.03   Hex   6.59   Hex   7.47
CpCo
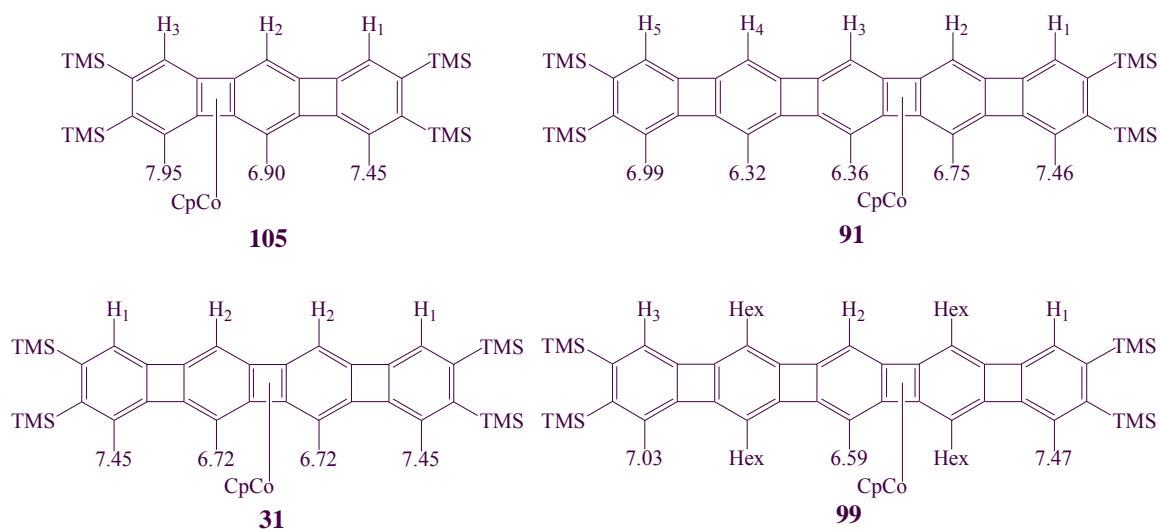
Figure 4.4. ^{1}H NMR chemical shifts (in δ) of **31**, **91**, **105** (in C$_6$D$_6$), and **99** (in d$_8$-toluene).

To probe the generality of this "CpCo-walk" and corroborate structural assignments, **91** was examined. Subjecting a sample of **91** in C_6D_6 to the same irradiative conditions as those used for **99** led to five new aromatic signals in the ^1H NMR spectrum (δ 8.00, 6.88, 6.48, 6.31, and 5.95), as well as a new Cp signal (δ 4.45). The new compound reverted thermally to **91** (Scheme 4.9). The signals at δ 8.00 and 6.88 can be assigned to H_a and H_e, by analogy to H_a and H_c on **104**. The remaining signals, at δ 6.48, 6.31 and 5.95, are tentatively assigned to H_d, H_b, and H_c, respectively, based on the following arguments. As discussed above, without the shielding neighboring alkyl groups, the protons on the central ring of **106**, H_c, are expected to resonate significantly downfield of H_4 on **91**, consistent with the signal at δ 5.95. Like H_3 on **91**, H_b on **106** is adjacent to the highly deshielding CpCo-moiety, but should be upfield (δ 6.31) because it is attached to a longer phenylene fragment. This leaves the remaining signal at δ 6.48 to be due to H_d, a reasonable value for this proton.

photochemical pathway

$h\nu$

91

thermal pathway

Δ

H_e H_d H_c H_b H_a

TMS   TMS

TMS   TMS

CoCp

106
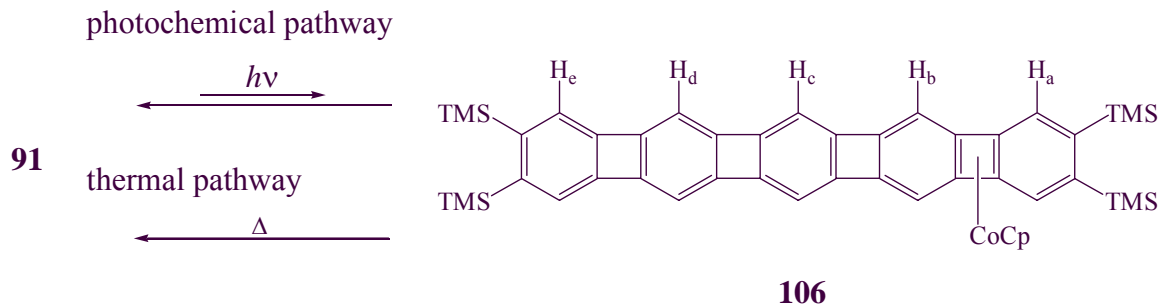
Scheme 4.9 The same CpCo-shift occurs in the absence of hexyl-solubilizing groups.

While haptotropic shifts of a metal from one cyclobutadiene to another appears to be unprecedented,[93] a related "CpCo-walk" along 1,3,5-hexatriene has been reported (Scheme 4.10).[94] King et al. proposed that the degenerate isomerization of **106** occurs via the η^2-intermediate **107**, a mechanistic pathway of this type may also be followed during the rearrangement of **104** to **99**, though several intermediates would be necessary (Scheme 4.11).
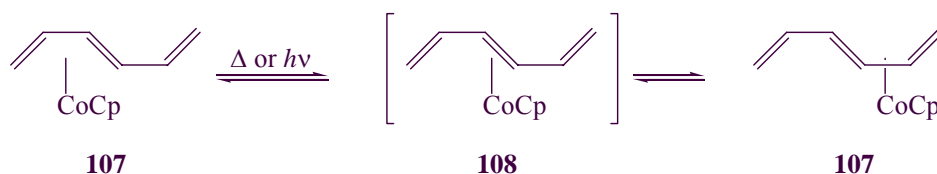
Scheme 4.10 "CpCo-walk" along 1,3,5-hexatriene.

M = CpCo
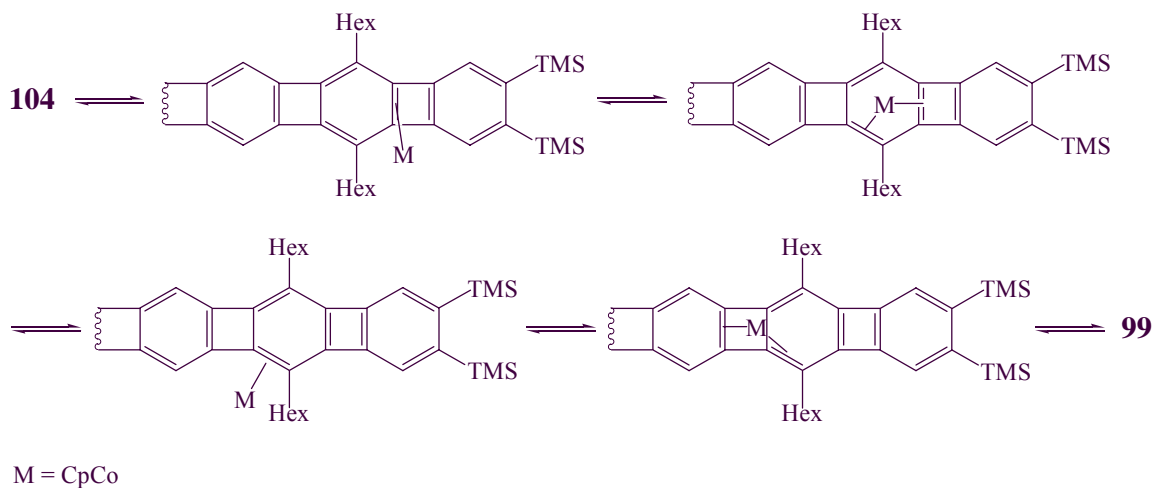
Scheme 4.11 A "CpCo-walk" mechanism converting **104** to **99** would require several intermediates.

Alternatively, a more complicated route may be taken, analogous to the one proposed for the degenerate migration of $Cr(CO)_3$ along naphthalene.[95] Albright et al. found a barrier of 43.7 kcal/mol if $Cr(CO)_3$ crossed over the central point of naphthalene,

while a much lower energy pathway of 27.4 kcal/mol was available if the metal fragment followed a more circuitous route. In several other examples, including the degenerate migration of $Fe(CO)_3$ along 1,3,5-hexatriene (analogous to the shift shown in Figure 4.10), Albright's molecular orbital analysis showed that a more direct route may be taken.

Because of the novelty of this shift, a series of kinetic experiments was performed to further investigate this process. A sample of **99** in d_8-THF was subjected to UV light for twelve hours, leading to the formation of **104**. The sample was heated and the disappearance of **104** (relative to an internal standard) followed by ^{1}H NMR spectroscopy. The reaction proved to be first-order, consistent with an intramolecular process. The rate constant (k) at each temperature was obtained from the slope of a plot of -ln([**104**]/initial [**104**]) versus time (Figures 4.5-4.8).[96] This information was used to calculate the activation energy (E_a) by plotting ln k versus 1/T (Figure 4.9) and multiplying the slope by R (1.99 cal/K•mol). Using this method, a value of 28.2 kcal/mol was determined for E_a. In a similar fashion, multiplying the slope of a plot of log(k/T) versus 1/T (Figure 4.10) by -4.576 yields a value for $\Delta H^{\ddagger}$ of 27.6 kcal/mol. $\Delta S^{\ddagger}$ (7.7 eu) can be obtained from the formula $\Delta S^{\ddagger} = 4.575$ log A - 60.53, where ln A is equal to the intercept from Figure 4.9 (-34.391).
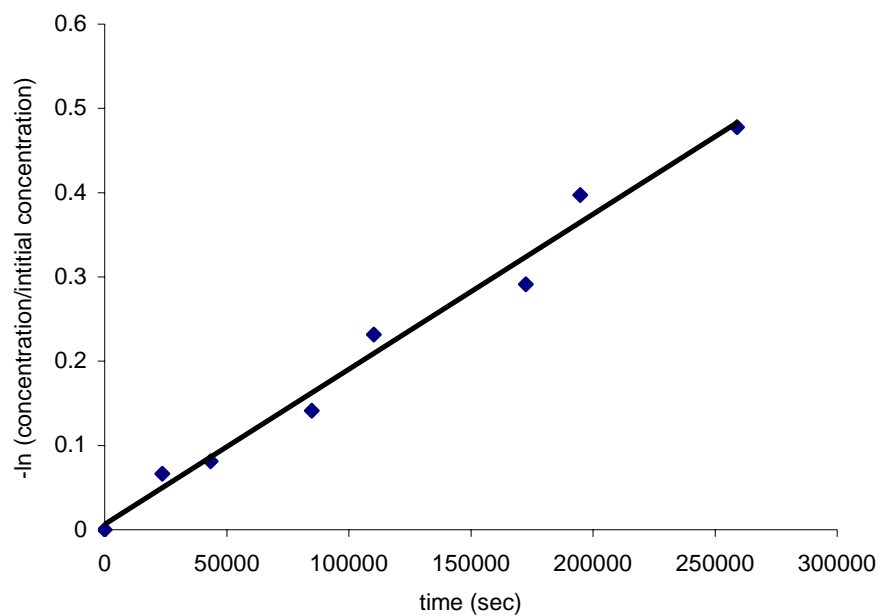
Figure 4.5 Plot of -ln([**104**]/initial [**104**]) versus time at 25.5 °C (k = 1.841 x 10^{-6} sec^{-1}, R^2 = 0.9828).
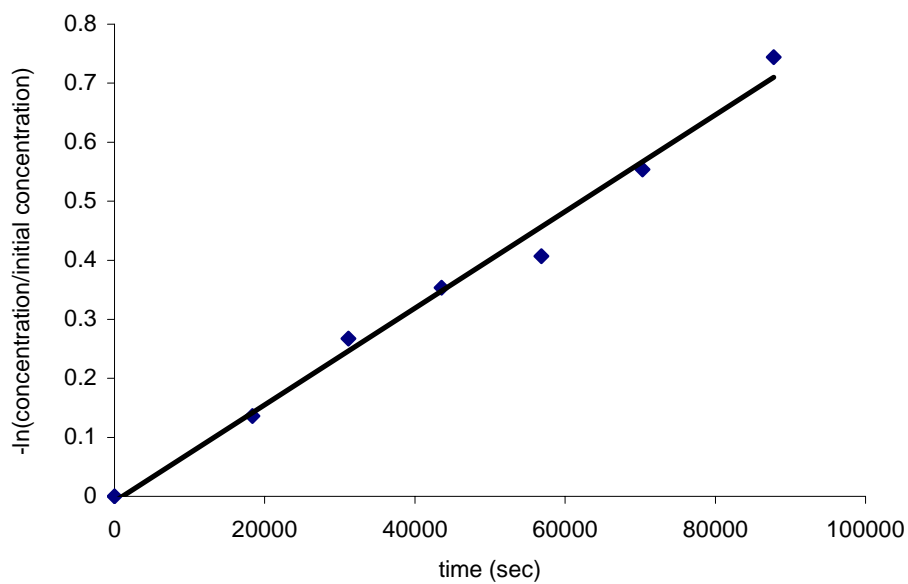
Figure 4.6 Kinetics experiment with **104** at 35 °C (k = 8.189 x 10^{-6} sec^{-1}, R^2 = 0.9883).
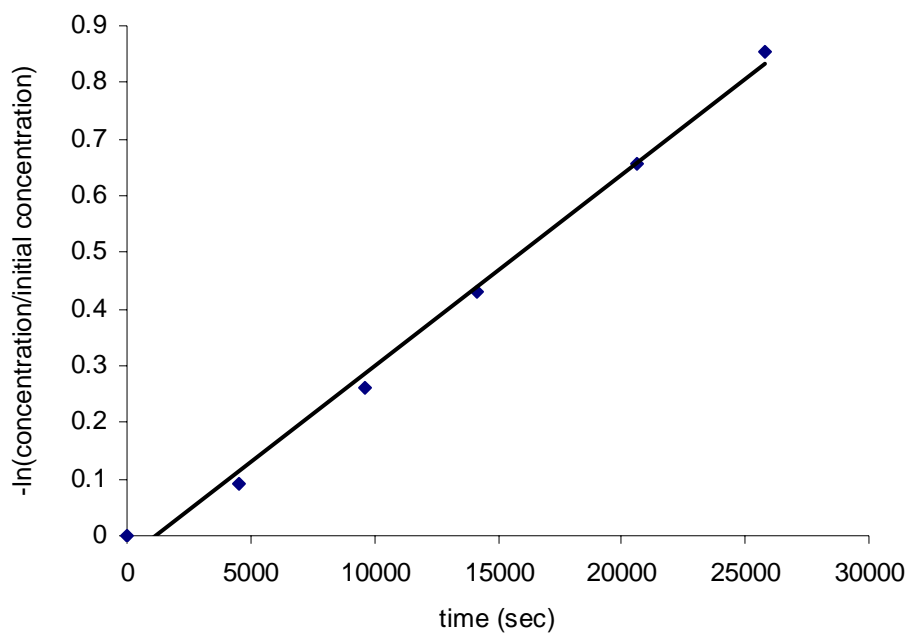
Figure 4.7 Kinetics experiment with **104** at 45 °C ($k = 3.39$ x 10^{-5} sec^{-1}, $R^2 = 0.994$).
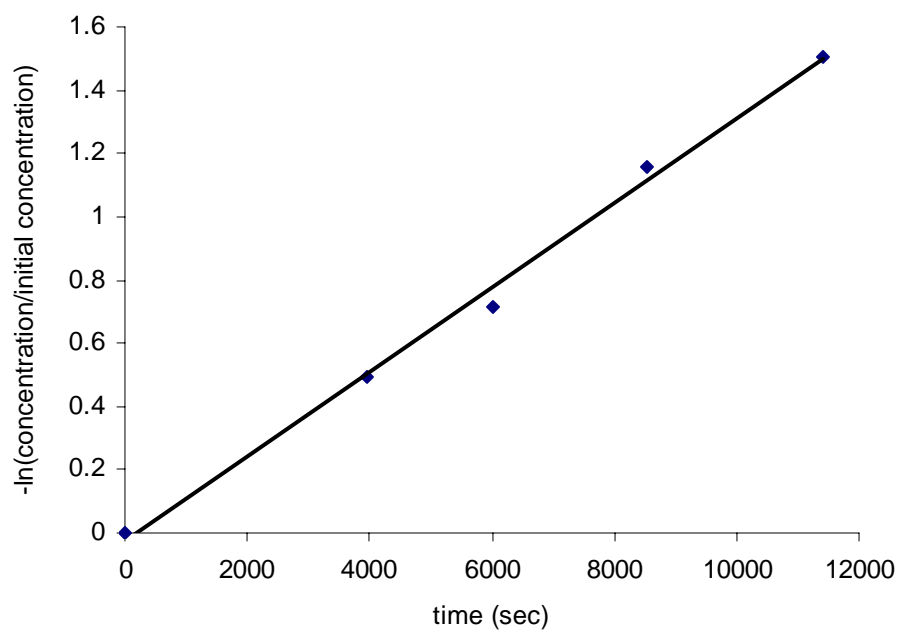
Figure 4.8 Kinetics experiment with **104** at 55 °C ($k = 1.34$ x 10^{-4} sec^{-1}, $R^2 = 0.9947$).
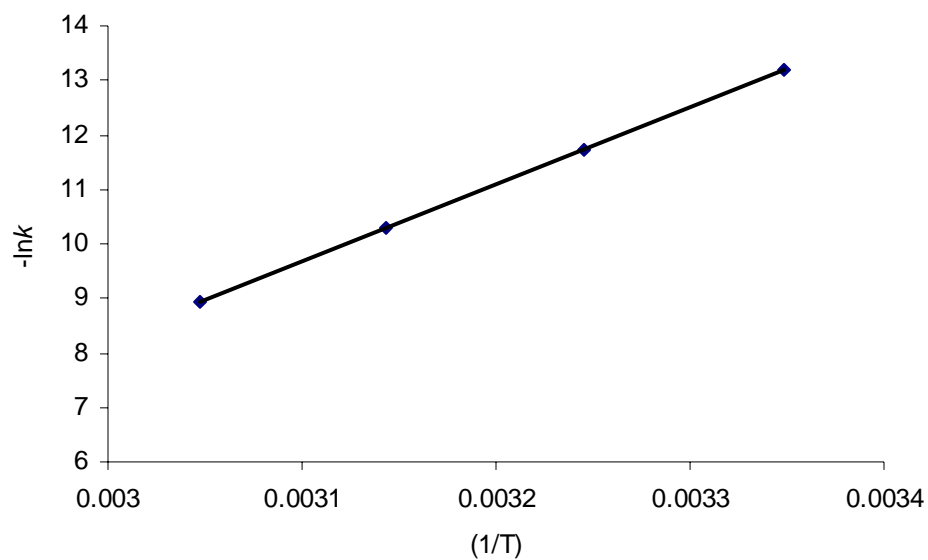
Figure 4.9 Plot of $-\ln k$ vs. $(1/T)$. The slope of this plot can be used to calculate the activation energy (slope $= 14212$, $R^2 = 1.000$, $E_a = 28.3$ kcal/mol).
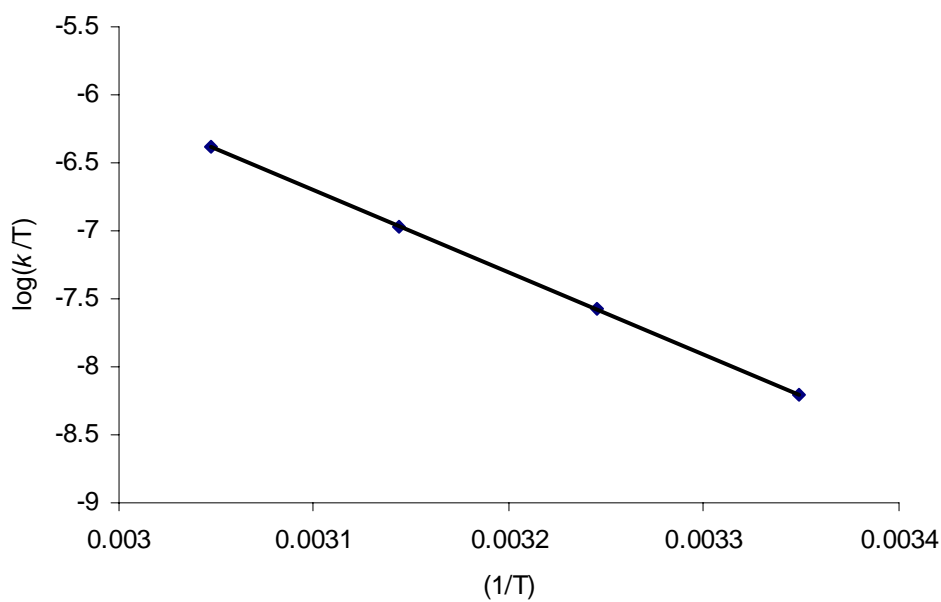
Figure 4.10 Plot of $\log (k/T)$ vs. $(1/T)$. Multiplying the slope of this plot by -4.576 yields $\Delta H^{\ddagger}$ (slope $= -6036$, $R^2 = 1.000$, $\Delta H^{\ddagger} = 27.6$ kcal/mol).

124

The barrier to CpCo-migration along the linear [5]phenylene frame (from **104** to **99**) is 2.7 kcal/mol greater than that found for the similar "CpCo-walk" along 1,3,5-hexatriene (Scheme 4.10). This energy difference is most likely a ground state effect, reflecting the preference of CpCo to bind to cyclobutadiene rather than 1,3-butadiene (though the situation may be more complicated, as binding to CpCo causes significant changes to the electronic structure of the entire phenylene which will effect both the ground and transition states). This process should be an excellent subject for a molecular orbital study like those conducted by Albright et al.

A second CpCo-migration along the linear phenylene frame could conceivably be taking place under thermal conditions, the degenerate shift shown in Scheme 4.12. If the barrier to this isomerization is low enough, it can be calculated via NMR by measuring the temperature at which the signals from H_a and H_c (or TMS_a and TMS_c) coalesce. No change in the ^{1}H NMR spectrum was observed when **99** was heated to 125 °C, experimentally the maximum that could be attained (Figure 4.11, top). A minimum value for the activation energy can be estimated by using this temperature. The rate constant (k_c) at the coalescence temperature (T_c) equals to $\pi\Delta v/2^{1/2}$, where v is the frequency difference between the two resonances at slow exchange (11.6 Hz for TMS_a and TMS_c, k_c = 25.8 sec^{-1}). Using the expression $\Delta G^{\ddagger} = 2.3RT_c[10.32 + \log (T_c/k_c)]$, the minimum barrier ($\Delta G^{\ddagger}$) for the process in Scheme 4.12 is 21.0 kcal/mol.[97]
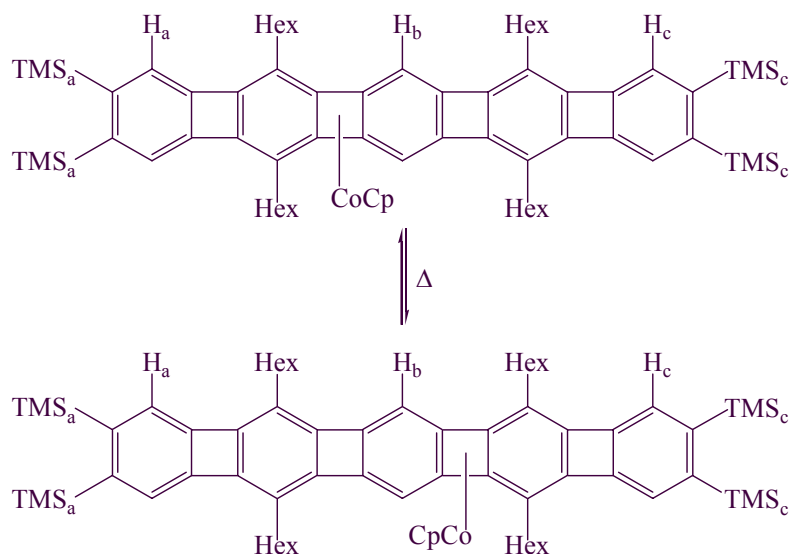
Scheme 4.12 A degenerate CpCo-shift is also possible.

Because a saturation transfer experiment is capable of detecting chemical exchange processes that are too slow to be observed by means of coalescence,[98] the sample was heated to 125 °C and one of the potentially exchanging ^{1}H NMR signals was saturated by preirradiation for 15 seconds (Figure 4.11, bottom). If an exchange were taking place between H_a and H_c, this irradiation would lead to a reduced signal from H_c. However, no change in signal strength from H_c was observed, meaning that the barrier to this process is significantly greater than 21 kcal/mol.[98]
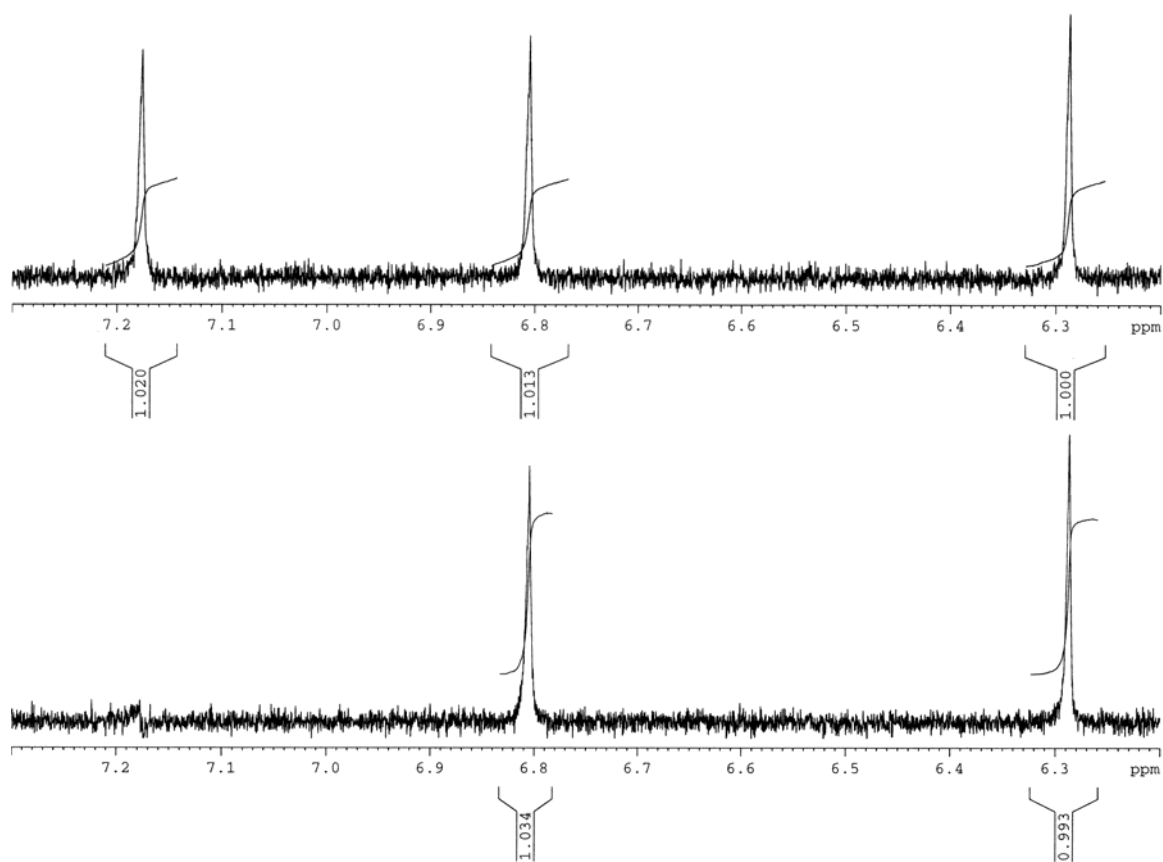
Figure 4.11 ^{1}H NMR spectrum of **99** (in d_{14}-diglyme) at 125 °C taken before (top) and after (bottom) irradiation of the signal at δ 7.18.

4.5 Conclusions and Future Directions

The use of hexyl-solubilizing groups facilitated the synthesis of the linear [5]phenylene frame but had several negative aspects, in particular, the isolated products were less crystalline and demetallation was more difficult. The first problem can be solved by using a smaller alkyl group, while, in the future, the latter dilemma can hopefully be avoided by using a catalytic cobalt reagent that does not form strong complexes with linear phenylenes. Research into developing such a catalyst is currently ongoing.

Chapter Five

Experimental Details

General: All reactions were carried out under a nitrogen atmosphere in oven-dried glassware with magnetic stirring, unless otherwise indicated. The term "concentrated *in vacuo*" refers to removal of solvents by rotary evaporation. Tetrahydrofuran (THF), *m*-xylenes, and toluene were distilled from sodium/benzophenone ketyl immediately prior to use. Methanol (Fischer), $Pd(PPh_3)_4$ (Strem), 2.0 M butylmagnesium chloride in THF (Aldrich), $^{13}C_2$-acetylene (Cambridge Isotope Laboratories), 1,3-cyclohexadiene (Aldrich), and $ZnCl_2$ (Strem) were used without further purification. Column chromatography was carried out with ICN SiliTech 32-63 D 60 Å silica gel.

The ^1H NMR data are reported as follows: chemical shift in parts per million downfield from tetramethylsilane (TMS), multiplicity (s = singlet, d = doublet, t = triplet, q = quartet, and m = multiplet), integration, and coupling constant (Hz). The ^{13}C spectra were determined with complete proton decoupling. Infrared spectra were obtained on a Perkin-Elmer System 2000 FT-IR spectrophotometer. Melting points were determined in sealed capillary tubes using a Thomas-Hoover Unimelt apparatus and are uncorrected.
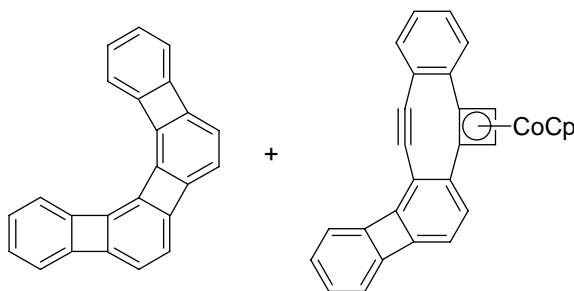
Angular [4]Phenylene (47) and Complex 65. A 200 mL Schlenk flask was charged with triyne **46** (27.1 mg, 0.090 mmol) in THF (120 mL) and chilled to –25 °C. Similarly, a 50 mL round-bottomed flask containing cyclopentadienylbis(ethene)cobalt (17.2 mg, 0.095 mmol) in THF (10 mL) was cooled to –25 °C. This solution was added by cannula to the Schlenk flask and the reaction mixture left to stir at –25 °C. After 16 h, the cooling bath was allowed to warm slowly during 3 h. As soon as the bath had reached a temperature of -10 °C, 1,3-cyclohexadiene (1.0 mL, 0.84 g, 10.5 mmol) in THF (10 mL) was added by cannula. The flask was sealed and the solution heated to 105 °C for 90 min. The mixture was concentrated in vacuo and the residue chromatographed eluting with CH_2Cl_2/hexanes (1:6) to afford **47** (13.8 mg, 51%) as a yellow solid, followed by **65** (6.0 mg, 16%) as an orange solid. Crystals of **47** suitable for single crystal X-ray diffraction were obtained from CH_2Cl_2/hexanes.

Data for **65**: IR (NaCl) 2917, 2850, 1478, 1468, 1243, 811 cm^{-1}; EI-MS (70 eV) (*m/z*, rel intensity) 425 (33), 424 (M^+, 100), 363 (37), 359 (19), 300 (57), 298 (63), 124 (14); ^{1}H NMR (500 MHz, CD_2Cl_2): δ 7.13-7.00 (m, 4), 6.85-6.77 (m, 2), 6.76-6.73 (m, 1), 6.68-6.66 (m, 1), 6.61 (d, 1, $J = 7.3$), 6.36 (d, 1, $J = 7.3$), 4.69 (s, 1), 4.67 (s, 5), 4.60 (s, 1); ^{13}C NMR (100 MHz, CD_2Cl_2): δ 151.3, 150.2, 150.0, 148.4, 148.2, 147.3, 129.4, 128.9, 128.8, 126.6, 125.9, 125.7, 124.9, 119.1, 118.3, 117.7, 117.4, 110.1, 108.4, 102.8, 81.61, 74.2, 72.8, 60.0, 59.4. HRMS Calcd for $C_{29}H_{17}Co$: 424.0662. Found: 424.0668.
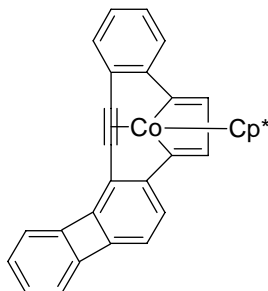
Complex 60. A 50 mL round-bottomed flask was charged with **46** (29.5 mg, 0.098 mmol) and Cp*Co(C$_2$H$_4$)$_2$ (28.2 mg, 0.11 mmol) in THF (25 mL). After 3 d of stirring at rt, the solution had become deep red in color. It was concentrated in vacuo and the residue recrystallized from CH$_2$Cl$_2$/hexanes to obtain **60** (45.0 mg, 93%) in three crops as a red solid. Crystals suitable for single crystal X-ray diffraction were obtained by slow evaporation from toluene. IR (KBr) 2974, 2914, 1414, 1264, 778, 734 cm^{-1}; EI-MS (70 eV) (*m/z*, rel intensity) 495 (38), 494 (*M*$^+$, 100), 359 (4), 300 (45), 247 (5); ^{1}H NMR (500 MHz, C$_6$D$_6$): δ 7.29 (br d, 1, *J* = 7.6), 7.07 (br d, 1, *J* = 7.6), 6.96 (td, 1, *J* = 7.6, 1.2), 6.75 (d, 1, *J* = 7.1), 6.71 (td, 1, *J* = 7.5, 1.1), 6.68 (d, 1, *J* = 2.4), 6.65 (d, 1, *J* = 2.4), 6.57 (br d, 1, *J* = 6.7), 6.55-6.50 (m, 1), 6.49 (m, 2), 6.36 (d, 1, J = 7.1), 1.30 (s, 15); ^{13}C NMR (100 MHz, CD$_2$Cl$_2$): δ 208.1, 207.1, 160.2, 159.8, 152.3, 150.4, 144.93, 144.88, 140.8, 139.7, 129.2, 128.8, 128.3, 128.1, 125.4, 123.6, 119.1, 118.8, 117.8, 117.5, 116.0, 115.9, 97.1, 86.9, 80.7, 8.25. HRMS Calcd for C$_{34}$H$_{27}$Co: 494.1445. Found: 494.1434.

Synthesis of Angular [4]Phenylene (47) from 60. A 5 mL flask was charged with **60** (11.0 mg, 0.022 mmol) in a mixture of toluene (3 mL), DMSO (1 mL), and 1,3-cyclohexadiene (0.5 mL) and sealed. The flask was heated to 150 °C for 7 min in a SmithSynthesizer microwave instrument. Ether was added (100 mL), the solution washed with brine (100 mL), dried with Na$_2$SO$_4$, and concentrated in vacuo. The residue was

chromatographed eluting with CH_2Cl_2/hexanes (1:6) to afford **47** (1.5 mg, 22%) as a yellow solid.
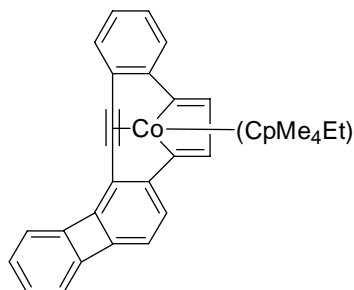
Complex 61. A 50 mL round-bottomed flask was charged with **46** (20.3 mg, 0.068 mmol) and $(CpMe_4Et)Co(C_2H_4)_2$ (15.1 mg , 0.057 mmol) in THF (15 mL). After 3 d of stirring at rt, the solution had become deep red in color. It was concentrated in vacuo and the residue purified by column chromatography on alumina eluting with hexanes/ether (10:1) to obtain **61** (23.3 mg, 80%) as a red solid. IR (CH_2Cl_2) 3054, 2959, 1422, 1266, 1056, 848, 730, 706 cm^{-1}; EI-MS (70 eV) (*m/z*, rel intensity) 509 (2), 508 (M^+, 6), 300 (100); ^{1}H NMR (400 MHz, CD_2Cl_2): δ 7.32 (br d, 1), 7.24 (br d, 1), 7.15 (td, 1, J = 7.6, 1.2), 6.94 (td, 1, J = 7.5, 1.1), 6.79-6.72 (m, 4), 6.65-6.62 (m, 1), 6.49 (d, 1, J = 7.1), 6.41 (d, 1, J = 2.4), 6.40 (d, 1, J = 2.4), 1.75 (q, 2, J = 7.6), 1.282 (s, 3), 1.277 (s, 3), 1.272 (s, 3), 1.264 (s, 3), 0.83 (t, 3, J = 7.6); ^{13}C NMR (100 MHz, CD_2Cl_2): δ 207.7, 205.7, 160.2, 159.8, 152.3, 150.4, 144.9, 144.8, 140.9, 139.7, 129.2, 128.9, 128.3, 128.1, 125.3, 123.5, 119.2, 118.7, 117.8, 117.4, 116.0, 115.8, 102.2, 97.7, 97.5, 96.1, 96.0, 86.6, 80.5, 30.3, 17.2, 13.7, 8.29, 8.26, 8.03. HRMS Calcd for $C_{35}H_{29}Co$: 508.1601. Found: 508.1601.
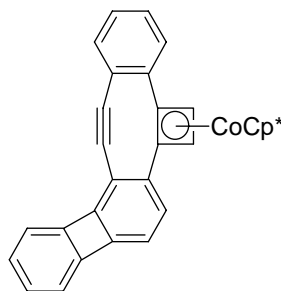
Complex 62. An NMR tube was charged with **60** (50.2 mg, 0.102 mmol) in d_8-THF (1 mL). The tube was irradiated with a slide projector lamp until all the starting material had disappeared by NMR (12 h). The solution was concentrated in vacuo and the residue chromatographed eluting with CH_2Cl_2/hexanes (1:4) to afford **62** (29.2 mg, 58%) as an orange solid. Crystals suitable for single crystal X-ray diffraction were obtained from THF/hexane, mp 247-249 °C. IR (KBr) 3059, 2964, 2904, 1478, 1467, 1378, 1239, 748, 737 cm^{-1}; EI-MS (70 eV) (*m/z*, rel intensity) 495 (38), 494 (M^+, 100), 359 (6), 300 (22), 247 (7); ^{1}H NMR (500 MHz, CD_2Cl_2) δ 7.12-7.07 (m, 1), 7.03-6.98 (m, 2), 6.87 (br d, 1, $J = 8.0$), 6.81-6.74 (m, 2), 6.72-6.69 (m, 1), 6.64-6.61 (m, 1) 6.43 (d, 1, $J = 7.4$), 6.37 (d, 1, $J = 7.4$), 4.19 (s, 1), 4.08 (s, 1), 1.57 (s, 15) ppm; ^{13}C NMR (125 MHz, CD_2Cl_2) δ 151.6, 150.3, 149.7, 148.2, 147.1, 146.6, 129.2, 128.5, 128.3, 126.4, 124.6, 124.5, 123.2, 118.1, 118.0, 117.3, 117.2, 109.7, 108.0, 102.1, 90.4, 72.3, 71.0, 63.7, 63.2, 9.39. HRMS Calcd for $C_{34}H_{27}Co$: 494.1445. Found: 494.1445. Anal. Calcd for $C_{34}H_{27}Co\bullet\frac{1}{2}THF$: C, 81.50; H, 5.89. Found: C, 81.87; H, 5.89.
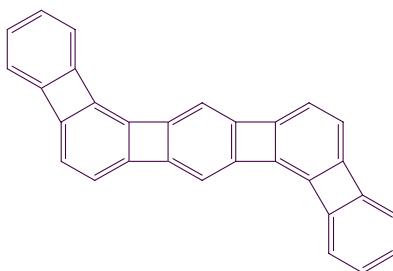
Anti-Doublebent [5]Phenylene (66). To a solution of **69** (104.3 mg, 0.130 mmol) in THF (25 mL) was added TBAF (0.7 mL of 1M in THF, 0.7 mmol). After 30 min, 1.5 mL of ethanol was added by syringe. The reaction was stirred for an additional 1 h, diluted with ether (200 mL), and quenched by washing with water (2 x 150 ml). The organic layer was dried with anhydrous Na_2SO_4, filtered through a short plug of silica, and concentrated. The hexayne was dissolved in THF (100 mL), transferred to a 200 mL Schlenk flask, degassed and chilled to -25 °C. Similarly, a 50 mL round-bottomed flask containing cyclopentadienylbis(ethene)cobalt (45.5 mg, 0.253 mmol) in THF (15 mL) was cooled to –25 °C. This solution was added by cannula to the Schlenk flask and left to stir at –25 °C. After 18 h, the cooling bath was allowed to warm slowly during 2 h. As soon as the bath had reached a temperature of -15 °C, 1,3-cyclohexadiene (1.0 mL, 0.84 g, 10.5 mmol) in THF (10 mL) was added by cannula. The flask was sealed and the solution heated to 105 °C for 90 min. The mixture was concentrated in vacuo and the residue chromatographed eluting with CH_2Cl_2/hexanes (1:3). Crystallization from 1,2-dichlorobenzene yielded 3.3 mg (7%) of **66** as a red solid, mp > 330 °C. Crystals of **66** suitable for single crystal X-ray diffraction were obtained from dibutyl ether. A ^{13}C NMR spectrum could not be obtained because of the low solubility of the compound. UV-VIS (1,2-dichlorobenzene, rel absorbance) 475 (0.200), 485 (0.186), 505 (0.204) nm; IR (KBr) 2958, 2925, 1735, 1451, 1378, 1108, 862 cm^{-1}; EI-MS (70 eV) (*m/z*, rel intensity) 375 (35), 374 (M^+, 100), 372 (22); ^1H NMR (300 MHz, 1,2-diclorobenzene-d_4, 116 °C): δ 6.89-6.82 (m, 6), 6.80-6.74 (m, 2), 6.52 (s, 2), 6.04 (d, 2, $J = 6.3$), 5.96 (d, 2, $J = 6.6$). HRMS Calcd for $C_{30}H_{14}$: 374.1096. Found: 374.1106.
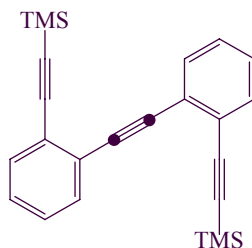
Bis(2-trimethylsilylethynylphenyl)-$^{13}C_2$-ethyne (86). A Schlenk flask was connected by tubing (containing a magnetic stir bar) to a sealed flask containing 34 mL (1.52 mmol) of $^{13}C_2$-acetylene. The Schlenk flask was charged with 15 mL of THF, which was degassed with nitrogen, chilled to −78 °C, and 1.52 mL (3.04 mmol) of 2.0 M butylmagnesium chloride in THF were added. It was then placed in liquid nitrogen, evacuated, and the exit port closed. The magnetic stir bar in the hose was used to break the seal on the flask containing the acetylene. The Schlenk flask was left open to the acetylene for 10 min, after which it was sealed and left at −78 °C for 25 min. The solution was then allowed to warm to rt for 70 min. The flask was placed under nitrogen, and 414 mg (3.04 mmol) of $ZnCl_2$ were added under strong nitrogen purge. After the cloudy reaction mixture had been stirred for 30 min, 0.980 g (3.26 mmol) of 1-iodo-2-trimethylsilylethynylbenzene[99] in 5 mL of THF was injected by syringe. $Pd(PPh_3)_4$ (200 mg, 0.17 mmol) was added under strong nitrogen purge and the vessel fitted with a condenser. After heating to reflux for 3 d, 100 mL of saturated NH_4Cl solution were added and the mixture extracted with ether (2 x 150 mL). The organic layer was dried with Na_2SO_4 and concentrated *in vacuo*. The residue was chromatographed with 99:1 petroleum ether/diethyl ether. Crystallization from ethanol yielded 269 mg (48%) of **86** as a yellow solid. IR (KBr) 2959, 2897, 2158, 1486, 1445, 1245, 875, 845, 760 cm^{-1}; MS (70 eV) (*m/z*, re intensity): 372 (*M*$^+$, 3), 358 (11), 357 (30), 342 (35), 341 (100), 300 (10), 285 (20); ^{1}H NMR (500 MHz, CDCl$_3$): δ 7.58-7.52 (m, 2), 7.52-7.47 (m, 2), 7.33-7.23

135

(m, 4), 0.26 (s, 18); ^{13}C NMR (125 MHz, CDCl$_3$): δ 132.2 (t, J = 2.2), 131.9 (t, J = 2.0),128.1 (t, J = 2.7), 128.0, 126.1 (t, J = 53.4), 125.6 (t, J = 1.7), 103.4, 98.7, 92.0 (^{13}C-enriched), -0.02.
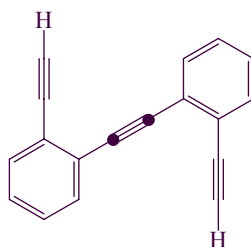
Bis(2-ethynylphenyl)-^{13}C$_2$-ethyne (40f). A round-bottomed flask was charged with 955 mg (2.57 mmol) of bis(2-trimethylsilylethynylphenyl)-^{13}C$_2$-ethyne (**86**), 724 mg (18.1 mmol) of sodium hydroxide, and 40 mL of methanol. After 18 h, 100 mL of 0.5 M HCl were added and the solution extracted with ether (2 x 100 mL). The organic layer was dried with Na$_2$SO$_4$ and concentrated *in vacuo*. The residue was chromatographed with 9:1 hexanes/diethyl ether to afford 557 mg (95%) of **40f** as a white solid. IR (KBr) 3282, 3059, 1484, 1445, 761, 666, 636 cm^{-1}; MS (70 eV) (*m/z* rel intensity): 229 (19), 228 (*M*$^+$, 100), 227 (34), 226 (55), 225 (14), 202 (10), 114 (10), 113 (17); ^{1}H NMR (500 MHz, CDCl$_3$): δ 7.60-7.55 (m, 2), 7.55-7.50 (m, 2), 7.35-7.25 (m, 4), 3.33 (s, 2); ^{13}C NMR (125 MHz, CDCl$_3$): δ 132.6 (t, J = 2.2), 132.3 (t, J = 2.0), 128.5 (t, J = 2.7), 128.2, 126.2 (t, J = 53.3), 124.5 (t, J = 1.6), 91.7 (^{13}C-enriched), 82.1 (t, J = 1.5), 81.3.
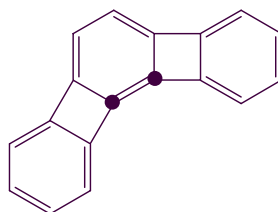
$^{13}C_2$-Angular [3]Phenylene (3f). A 100 mL Schlenk flask was charged with 99 mg (0.43 mmol) of **40f** and 20 mL of THF and chilled to –25 °C. Similarly, a 50 mL round-bottomed flask containing 86 mg (0.48 mmol) of cyclopentadienylbis(ethene)cobalt and 10 mL of THF was cooled to –78 °C. This solution was added by cannula to the Schlenk flask and left to stir at –25 °C. After 19 h, 0.80 mL of 1,3-cyclohexadiene was injected by syringe, the flask sealed, and the solution heated to 100 °C for 45 min. The mixture was concentrated *in vacuo* and the residue chromatographed with hexanes to afford 30 mg (30%) of **3f** as a yellow solid. IR (KBr) 3051, 1415, 1376, 1157, 933, 831, 744 cm^{-1}; MS (70 eV) (*m/z* rel intensity): 229 (19), 228 (M^+, 100), 227 (31), 226 (37), 225 (9); ^{1}H NMR (500 MHz, CD$_2$Cl$_2$): δ 7.03-6.93 (m, 6), 6.93-6.87 (m, 2), 6.18 (dd, 2, J = 4.1, 3.4); ^{13}C NMR (125 MHz, CD$_2$Cl$_2$): δ 151.0 (t, J = 2.4), 149.6 (dd, J = 18.8, 17.6), 149.5 (dd, J = 25.0, 24.4), 136.1 (^{13}C-enriched), 129.4, 128.8 (t, J = 2.2), 119.8, 118.7 (t, J = 4.5), 114.6 (t, J = 1.9).
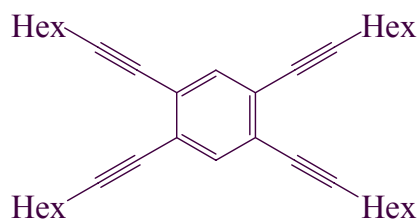
1,2,4,5-Tetraoctynylbenzene (96). A 500 mL round-bottomed flask was charged with 1,2,4,5-tetraiodobenzene[100] (1.56g, 2.68 mmol), Pd(PPh$_3$)$_2$Cl$_2$ (94 mg, 0.13 mmol), CuCl (26 mg, 0.14 mmol), THF (50 mL), and triethylamine (200 ml). After the addition by syringe of 1-octyne (4.0 mL, 27 mmol), the reaction mixture was stirred at 80 °C for 22 h. The resulting dark mixture was diluted with hexanes (250 mL) and washed with a

0.7 M solution of HCl (8 x 250 mL). The organic layer was dried with Na$_2$SO$_4$ and concentrated *in vacuo*. The residue was chromatographed with hexanes to afford 1.18 g (86%) of **96** as a yellow brownish oil. IR (NaCl) 2956, 2930, 2858, 2230, 1488, 1466, 1429, 1397, 1378, 1328, 890, 725 cm^{-1}; MS (70 eV) (*m/z* rel intensity): 511 (40), 510 (M$^+$, 100), 241 (17), 239 (15), 229 (14); ^{1}H NMR (400 MHz, CDCl$_3$): δ 7.37 (s, 2), 2.43 (t, 8, *J* = 10.0), 1.59 (quint, 8, *J* = 10.0), 1.46 (m, 8), 1.31 (m, 8), 1.30 (m, 8), 0.90 (t, 12, *J* = 9.2); ^{13}C NMR (100 MHz, CDCl$_3$): δ 134.9, 125.1, 95.3, 78.8, 31.4, 28.7, 28.5, 22.5, 19.6, 14.0. HRMS Calcd for C$_{38}$H$_{54}$: 510.4226. Found: 510.4231.
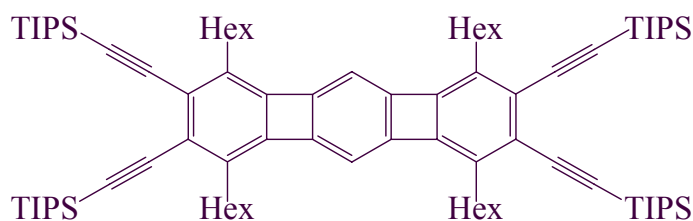
Tetrahexyltetrakis[(triisopropylsilyl)ethynyl] Linear [3]Phenylene (97). Tetrayne **96** (120 mg, 0.236 mmol) and CpCo(CO)$_2$ (90 mg, 0.470 mmol) were dissolved in degassed *m*-xylene (30 mL). The resulting mixture was injected over 12 h into a solution of bis[(triisopropylsilyl)ethynyl]-1,3,5-hexatriyne (**33**, 270 mg, 0.698 mmol) in boiling *m*-xylene (60 mL). During addition and for an additional 10 h, the reaction mixture was irradiated with a slide projector lamp and maintained at reflux. The reaction solution was allowed to cool and concentrated *in vacuo*. The black residue was chromatographed with hexanes to afford 103 mg (34%) of **97** as a red wax. IR (NaCl) 3055, 2987, 2866, 2686, 2411, 2306, 2130, 1422, 1266, 896, 740, 706 cm^{-1}; MS (70 eV) (*m/z* rel intensity): 1286 (38), 1285 (70), 1284 (100), 1283 (M$^+$, 95); ^{1}H NMR (500 MHz,

CD$_2$Cl$_2$): δ 6.30 (s, 2), 2.56 (t, 8, J = 7.7), 1.59 (quint, 8, J = 7.6), 1.38-1.27 (m, 16),

1.19-1.11 (m, 20), 1.14 (d, 72, J = 2.5) 0.89 (t, 12, J = 6.9); ^{13}C NMR (125 MHz,

CD$_2$Cl$_2$): δ 151.5, 146.7, 131.4, 127.8, 111.9, 105.1, 100.5, 32.4, 31.4, 29.9, 29.8, 23.2,

19.2, 14.4, 12.1. HRMS Calcd for C$_{86}$H$_{138}$Si$_4$: 1282.9876. Found: 1282.9860.
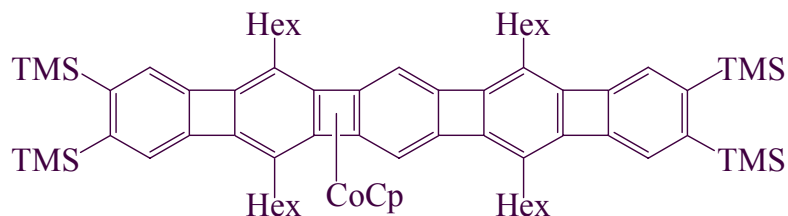
CpCo-Linear [5]phenylene (99). To a solution of **97** (99.3 mg, 0.077 mmol) in

THF (25 mL) were added successively ethanol (50 μL, 0.88 mmol) and TBAF (0.50 mL

of 1M in THF, 0.50 mmol). After 2h, the solution was filtered through a short plug of

silica (washing with ether). *m*-Xylene (40 mL) was added, and the volatile solvent was

removed by rotary evaporation. The round-bottomed flask was placed under vaccum

until 30 mL of solvent remained. CpCo(CO)$_2$ (25 mg, 0.14 mmol) in *m*-xylene (1 mL)

was added by syringe. The resulting mixture was injected over 18 h into a solution of

BTMSA (2 mL, 0.88 mmol) in boiling *m*-xylene (100 mL). During addition and for an

additional 2 h, the reaction mixture was irradiated with a slide projector lamp and

maintained at reflux. The reaction solution was allowed to cool and concentrated *in

vacuo*. The black reddish residue was chromatographed under nitrogen on alumina with

pentane/ether (1:7) to afford 24 mg (27%) of **99** as a red solid, mp 129-132 °C. UV-VIS

(hexanes) λ$_{max}$ (log ε) = 296 (4.60), 321 (4.61), 349 (4.68), 415 (4.71); IR (in ether) 2986,

2940, 2849, 1445, 1383, 1351, 1153, 1109, 1077, 846 cm^{-1}; MS (70 eV) (*m/z* rel

intensity): 1125 (4), 1124 (12), 1123 (M$^+$, 17), 1122 (22), 207 (45), 128 (26), 75 (42), 57 (100); ^{1}H NMR (500 MHz, CD$_2$Cl$_2$): δ 7.23 (s, 2), 6.85 (s, 2), 6.35 (s, 2), 4.54 (s, 5), 2.69 (t, 4, J = 7.5), 2.41 (t, 4, J = 7.5), 1.91 (quint, 4, J = 7.5), 1.67 (quint, 4, J = 7.5), 1.58-1.30 (m, 24), 0.98-0.85 (m, 12), 0.37 (s, 18), 0.34 (s, 18); ^{13}C NMR (125 MHz, CD$_2$Cl$_2$): δ 152.0, 149.9, 149.6, 148.5, 148.2, 147.1, 141.6, 139.7, 130.0, 126.6, 125.0, 122.3, 112.1, 80.1, 76.3, 72.2, 32.4, 32.3, 30.2, 29.9, 29.5, 29.4, 29.2, 29.1, 23.3, 23.2, 14.53, 14.49, 2.43, 2.35. HRMS Calcd for C$_{71}$H$_{99}$CoSi$_4$: 1122.6156. Found: 1122.6134.

Appendix: Crystallographic Data

Table 1 Crystal Data and Collection Parameters for **47**, **60**, and **62**.

	47	**60·½Toluene**	**62·½THF**
Empirical Formula	$C_{24}H_{12}$	$C_{37.5}H_{31}Co$	$CoC_{36}H_{31}O_{0.5}$
Formula Weight	300.34	540.59	530.37
Temperature (K)	220	149.2	138.2
Crystal System	Monoclinic	Triclinic	Monoclinic
Space Group	$P2_1/c$	P-1	C2/c
A	15.468(3)	7.0791(7)	14.4895(8)
B	3.8318(7)	13.176(1)	9.0045(5)
C	25.454(5)	15.734(9)	40.411(2)
α (°)	90	111.494(2)	90
β (°)	101.002(4)	95.570(2)	96.501(1)
γ (°)	90	100.867(2)	90
V	1480.9	1318.7(2)	5238.5(5)
Z	4	2	8
D_{calc} (g/cm^3)	1.347	1.360	1.345
Radiation	Synchrotron (0.6880 Å)	MoK_α (0.7107 Å)	MoK_α (0.7107 Å)
2Θ Range (°)	5.20 – 47.8	3.6– 45.0	3.0 – 45.0
μ (mm^{-1})	0.077	0.677	0.681
T_{min}, T_{max}	0.964, 0.999	0.880, 0.990	0.589, 0.934
Crystal Dimensions (mm)	0.01 x 0.01 x 0.48	0.12 x 0.17 x 0.23	0. 10 x 0.19 x 0.23
No. of Reflections Measured	5602	6660	11489
No. of Unique Reflections	2534	4179	4775
No. of Observations	1690 ($I > 2\sigma$)	2988 ($I > 3\sigma$)	2605 ($I > 3\sigma$)
No. of Variables	218	346	333
R_{int}	0.0355	0.047	0.059
GOF	0.972	1.593	1.32
R, R_w, R_{all}	0.0550, 0.1279, 0.0787	0.0532, 0.065, 0.083	0.039, 0.040, 0.080

Table 2 Crystal Data and Collection Parameters for **66** and **99**.

	66	99
Empirical Formula	$C_{30}H_{14}$	$C_{71}H_{99}CoSi_4$
Formula Weight	374.41	1123.79
Temperature (K)	180	150
Crystal System	Monoclinic	Monoclinic
Space Group	C2/c	C2/c
a	28.606(11)	49.205(18)
b	5.033(2)	19.155(6)
c	13.201(5)	14.824(5)
α ($^{\circ}$)	90	90
β ($^{\circ}$)	111.107(6)	107.336(6)
γ ($^{\circ}$)	90	90
V	1773.1(12)	13337(8)
Z	4	8
D_{calc} (g/cm^3)	1.403	1.119
Radiation	Synchrotron (0.6900 Å)	Synchrotron (0.6904 Å)
2Θ Range ($^{\circ}$)	5.92 – 47.8	5.76 – 37.2
μ (mm^{-1})	0.080	0.368
T_{min}, T_{max}	0.9765, 0.9996	0.9469, 0.9963
Crystal Dimensions (mm)	0.005 x 0.04 x 0.30	0.01 x 0.02 x 0.15
No. of Reflections Measured	3907	15125
No. of Unique Reflections	1491	5559
No. of Observations	1052 ($I > 2\sigma$)	3364 ($I > 2\sigma$)
No. of Variables	136	577
R_{int}	0.0386	0.1272
GOF	1.001	1.074
R, R_w, R_{all}	0.0567, 0.1319, 0.0835	0.1683, 0.4334, 0.2155
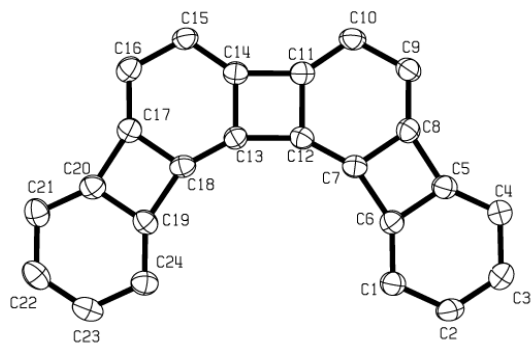
Table 3 Bond distances (Å) in **47**.

atom	atom	distance	atom	atom	distance
C1	C6	1.365(3)	C12	C13	1.488(3)
C1	C2	1.399(3)	C13	C18	1.343(3)
C2	C3	1.369(3)	C13	C14	1.440(3)
C3	C4	1.410(3)	C14	C15	1.361(3)
C4	C5	1.357(3)	C15	C16	1.429(3)
C5	C6	1.413(3)	C16	C17	1.351(3)
C5	C8	1.500(3)	C17	C18	1.437(3)
C6	C7	1.494(3)	C17	C20	1.508(3)
C7	C12	1.345(3)	C18	C19	1.500(3)
C7	C8	1.440(3)	C19	C24	1.358(3)
C8	C9	1.355(3)	C19	C20	1.412(3)
C9	C10	1.426(3)	C20	C21	1.366(3)
C10	C11	1.361(3)	C21	C22	1.393(4)
C11	C12	1.440(3)	C22	C23	1.374(4)
C11	C14	1.491(3)	C23	C24	1.398(3)

Table 4 Bond angles (in °) in **47**.

atom	atom	atom	angle	atom	atom	atom	angle
C6	C1	C2	115.3(2)	C11	C12	C13	90.10(18)
C3	C2	C1	122.4(2)	C18	C13	C14	118.4(2)
C2	C3	C4	122.0(2)	C18	C13	C12	151.6(2)
C5	C4	C3	115.8(2)	C14	C13	C12	90.01(18)
C4	C5	C6	121.7(2)	C15	C14	C13	124.0(2)
C4	C5	C8	147.5(2)	C15	C14	C11	146.0(2)
C6	C5	C8	90.81(19)	C13	C14	C11	89.98(18)
C1	C6	C5	122.8(2)	C14	C15	C16	117.4(2)
C1	C6	C7	146.9(2)	C17	C16	C15	118.2(2)
C5	C6	C7	90.24(19)	C16	C17	C18	124.4(2)
C12	C7	C8	118.0(2)	C16	C17	C20	146.7(2)
C12	C7	C6	152.0(2)	C18	C17	C20	88.96(18)
C8	C7	C6	90.01(18)	C13	C18	C17	117.6(2)
C9	C8	C7	124.1(2)	C13	C18	C19	152.3(2)
C9	C8	C5	147.0(2)	C17	C18	C19	90.09(18)
C7	C8	C5	88.95(19)	C24	C19	C20	122.8(2)
C8	C9	C10	118.2(2)	C24	C19	C18	147.0(2)
C11	C10	C9	117.6(2)	C20	C19	C18	90.22(19)
C10	C11	C12	124.1(2)	C21	C20	C19	121.6(2)
C10	C11	C14	145.9(2)	C21	C20	C17	147.7(2)
C12	C11	C14	89.90(18)	C19	C20	C17	90.74(18)
C7	C12	C11	118.0(2)	C20	C21	C22	115.6(2)
C7	C12	C13	151.9(2)	C23	C22	C21	122.7(2)
C22	C23	C24	121.8(2)	C19	C24	C23	115.5(2)
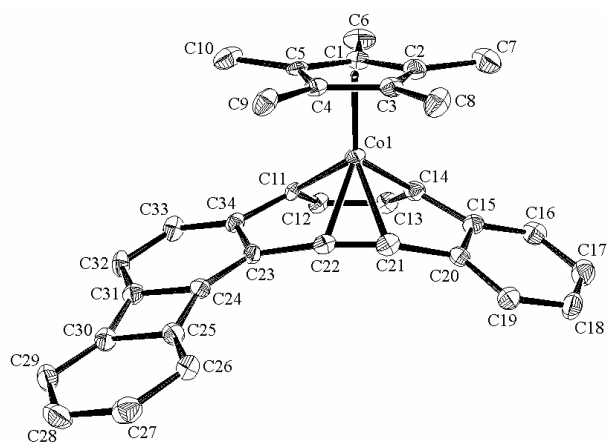
Table 5 Bond distances (Å) in **60**.

atom	atom	distance	atom	atom	distance
CO1	C1	2.033(5)	C11	C34	1.467(6)
CO1	C2	2.105(5)	C12	C13	1.455(7)
CO1	C3	2.150(4)	C13	C14	1.353(6)
CO1	C4	2.148(5)	C14	C15	1.483(6)
CO1	C5	2.105(5)	C15	C16	1.386(7)
CO1	C11	1.920(4)	C15	C20	1.417(6)
CO1	C14	1.923(5)	C16	C17	1.397(7)
CO1	C21	2.039(5)	C17	C18	1.386(7)
CO1	C22	2.042(5)	C18	C19	1.373(7)
CO1	C100	1.7208(7)	C19	C20	1.385(6)
C1	C2	1.431(6)	C20	C21	1.469(7)
C1	C5	1.450(7)	C21	C22	1.232(6)
C1	C6	1.497(6)	C22	C23	1.451(6)
C1	C100	1.243(4)	C23	C24	1.358(6)
C2	C3	1.396(6)	C23	C34	1.460(6)
C2	C7	1.500(7)	C24	C25	1.520(6)
C2	C100	1.236(5)	C24	C31	1.429(6)
C3	C4	1.434(6)	C25	C26	1.360(6)
C3	C8	1.506(6)	C25	C30	1.422(6)
C3	C100	1.188(4)	C26	C27	1.404(7)
C4	C5	1.410(6)	C27	C28	1.385(7)
C4	C9	1.495(6)	C28	C29	1.423(7)
C4	C100	1.180(5)	C29	C30	1.356(6)
C5	C10	1.496(6)	C30	C31	1.509(6)
C5	C100	1.211(5)	C31	C32	1.374(6)
C11	C12	1.358(6)	C32	C33	1.414(6)
C33	C34	1.379(6)			

Table 6 Bond angles (in °) in **60**.

atom	atom	atom	angle	atom	atom	atom	angle
C1	CO1	C2	40.4(2)	C4	CO1	C14	157.8(2)
C1	CO1	C3	66.3(2)	C4	CO1	C21	107.8(2)
C1	CO1	C4	67.0(2)	C4	CO1	C22	94.7(2)
C1	CO1	C5	41.0(2)	C4	CO1	C100	33.2(1)
C1	CO1	C11	101.4(2)	C5	CO1	C11	91.0(2)
C1	CO1	C14	98.7(2)	C5	CO1	C14	136.7(2)
C1	CO1	C21	156.9(2)	C5	CO1	C21	144.6(2)
C1	CO1	C22	159.6(2)	C5	CO1	C22	118.8(2)
C1	CO1	C100	37.5(1)	C5	CO1	C100	35.1(1)
C2	CO1	C3	38.3(2)	C11	CO1	C14	81.6(2)
C2	CO1	C4	65.6(2)	C11	CO1	C21	100.8(2)
C2	CO1	C5	66.9(2)	C11	CO1	C22	78.4(2)
C2	CO1	C11	140.3(2)	C11	CO1	C100	125.3(1)
C2	CO1	C14	92.4(2)	C14	CO1	C21	78.4(2)
C2	CO1	C21	116.5(2)	C14	CO1	C22	101.5(2)
C2	CO1	C22	140.9(2)	C14	CO1	C100	126.5(1)
C2	CO1	C100	36.0(1)	C21	CO1	C22	35.1(2)
C3	CO1	C4	39.0(2)	C21	CO1	C100	127.9(1)
C3	CO1	C5	65.4(2)	C22	CO1	C100	126.9(1)
C3	CO1	C11	120.6(2)	CO1	C1	C5	72.2(3)
C3	CO1	C21	95.1(2)	CO1	C1	C6	125.9(3)
C3	CO1	C22	105.5(2)	CO1	C1	C100	57.5(2)
C3	CO1	C100	33.5(1)	C2	C1	C5	107.2(4)
C4	CO1	C5	38.7(2)	C2	C1	C6	127.0(4)
C4	CO1	C11	116.9(2)	C2	C1	C100	54.5(3)
C5	C1	C6	125.4(4)	CO1	C4	C100	53.1(2)
C5	C1	C100	52.8(2)	C3	C4	C5	107.9(4)
C6	C1	C100	176.3(5)	C3	C4	C9	125.8(4)
CO1	C2	C1	67.1(3)	C3	C4	C100	53.0(3)
CO1	C2	C3	72.6(3)	C5	C4	C9	126.3(4)
CO1	C2	C7	126.9(4)	C5	C4	C100	54.9(3)
CO1	C2	C100	54.8(2)	C9	C4	C100	178.4(4)
C1	C2	C3	108.2(4)	CO1	C5	C1	66.9(3)
C1	C2	C7	125.3(4)	CO1	C5	C4	72.3(3)
C1	C2	C100	55.0(3)	CO1	C5	C10	127.4(3)
C3	C2	C7	126.5(4)	CO1	C5	C100	54.8(2)
C3	C2	C100	53.3(3)	C1	C5	C4	107.7(4)
C7	C2	C100	178.2(5)	C1	C5	C10	125.8(4)
CO1	C3	C2	69.1(3)	C1	C5	C100	54.8(3)
CO1	C3	C4	70.4(3)	C4	C5	C10	126.5(4)
CO1	C3	C8	128.4(3)	C4	C5	C100	52.9(3)
CO1	C3	C100	53.0(2)	C10	C5	C100	177.8(4)
C2	C3	C4	108.9(4)	CO1	C11	C12	114.4(3)

C2	C3	C8	127.1(4)	CO1	C11	C34	112.6(3)
C2	C3	C100	56.4(3)	C12	C11	C34	128.4(4)
C4	C3	C8	124.0(4)	C11	C12	C13	112.9(4)
C4	C3	C100	52.5(3)	C12	C13	C14	112.9(4)
C8	C3	C100	176.2(5)	CO1	C14	C13	114.5(4)
CO1	C4	C3	70.6(3)	CO1	C14	C15	112.1(3)
CO1	C4	C5	69.0(3)	C13	C14	C15	127.6(5)
CO1	C4	C9	128.1(3)	C14	C15	C16	130.0(4)
C14	C15	C20	111.5(4)	C27	C28	C29	121.4(4)
C16	C15	C20	118.4(4)	C28	C29	C30	115.6(4)
C15	C16	C17	119.6(5)	C25	C30	C29	122.5(4)
C16	C17	C18	121.0(5)	C25	C30	C31	90.4(4)
C17	C18	C19	120.3(5)	C29	C30	C31	147.1(4)
C18	C19	C20	119.2(5)	C24	C31	C30	90.1(4)
C15	C20	C19	121.4(4)	C24	C31	C32	121.9(4)
C15	C20	C21	111.8(4)	C30	C31	C32	148.0(4)
C19	C20	C21	126.7(4)	C31	C32	C33	116.9(4)
CO1	C21	C20	109.6(3)	C32	C33	C34	122.1(4)
CO1	C21	C22	72.6(3)	C11	C34	C23	110.0(4)
C20	C21	C22	164.7(5)	C11	C34	C33	129.4(4)
CO1	C22	C21	72.3(3)	C23	C34	C33	120.5(4)
CO1	C22	C23	108.6(3)	C21	C22	C23	165.7(5)
C22	C23	C24	131.3(4)	C22	C23	C34	112.0(4)
C24	C23	C34	116.7(4)	C23	C24	C25	148.5(4)
C23	C24	C31	121.8(4)	C25	C24	C31	89.6(3)
C24	C25	C26	147.6(4)	C24	C25	C30	89.9(4)
C26	C25	C30	122.5(4)	C25	C26	C27	115.6(4)
C26	C27	C28	122.4(4)	C1	C100	C5	72.4(3)
C2	C100	C3	70.3(3)	C2	C100	C4	144.8(3)
C2	C100	C5	142.9(3)	C3	C100	C4	74.5(3)
C3	C100	C5	146.7(3)	C4	C100	C5	72.2(3)
CO1	C100	C1	85.0(2)	CO1	C100	C2	89.2(2)
CO1	C100	C3	93.5(2)	CO1	C100	C4	93.7(2)
CO1	C100	C5	90.0(2)	C1	C100	C2	70.5(3)
C1	C100	C3	140.8(3)	C1	C100	C4	144.6(3)
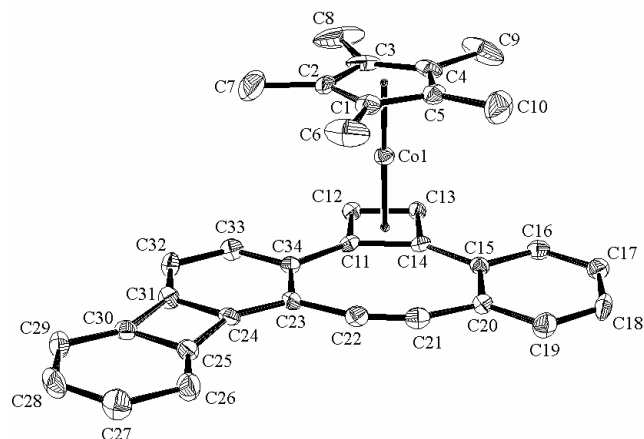
Table 7 Bond distances (Å) in **62**.

atom	atom	distance	atom	atom	distance
CO1	C1	2.047(4)	C5	C10	1.498(6)
CO1	C2	2.043(4)	C5	C100	1.205(4)
CO1	C3	2.035(4)	C11	C12	1.455(5)
CO1	C4	2.044(4)	C11	C14	1.500(5)
CO1	C5	2.060(4)	C11	C34	1.487(5)
CO1	C11	1.979(4)	C11	C101	1.043(4)
CO1	C12	1.965(4)	C12	C13	1.421(5)
CO1	C13	1.961(4)	C12	C101	1.018(4)
CO1	C14	1.997(4)	C13	C14	1.461(5)
CO1	C100	1.6499(5)	C13	C101	1.013(4)
CO1	C101	1.6834(5)	C14	C15	1.465(5)
O1	C35	1.403(6)	C14	C101	1.052(4)
O1	C35	1.403(6)	C15	C16	1.406(5)
C1	C2	1.402(5)	C15	C20	1.418(5)
C1	C5	1.420(5)	C16	C17	1.376(5)
C1	C6	1.505(6)	C17	C18	1.381(5)
C1	C100	1.205(4)	C18	C19	1.385(5)
C2	C3	1.440(6)	C19	C20	1.387(5)
C2	C7	1.506(6)	C20	C21	1.432(5)
C2	C100	1.209(4)	C21	C22	1.196(5)
C3	C4	1.409(6)	C22	C23	1.416(5)
C3	C8	1.499(6)	C23	C24	1.375(5)
C3	C100	1.209(4)	C23	C34	1.446(5)
C4	C5	1.418(5)	C24	C25	1.516(5)
C4	C9	1.509(6)	C24	C31	1.412(5)
C4	C100	1.202(4)	C25	C26	1.357(5)
C25	C30	1.417(5)	C31	C32	1.372(5)
C26	C27	1.416(5)	C32	C33	1.408(5)
C27	C28	1.379(5)	C33	C34	1.399(5)
C28	C29	1.405(5)	C35	C36	1.486(7)

C29 C30 1.368(5)   C36 C36 1.48(1)
C30 C31 1.514(5)

Table 8 Bond angles (in °) in **62**.

atom	atom	atom	angle	atom	atom	atom	angle
C1	CO1	C2	40.1(1)	C3	CO1	C101	142.4(1)
C1	CO1	C3	68.5(2)	C4	CO1	C5	40.4(1)
C1	CO1	C4	68.1(1)	C4	CO1	C11	174.2(2)
C1	CO1	C5	40.5(1)	C4	CO1	C12	134.9(2)
C1	CO1	C11	116.1(1)	C4	CO1	C13	111.9(2)
C1	CO1	C12	148.2(2)	C4	CO1	C14	130.3(2)
C1	CO1	C13	164.2(2)	C4	CO1	C100	36.0(1)
C1	CO1	C14	123.8(2)	C4	CO1	C101	142.9(1)
C1	CO1	C100	36.1(1)	C5	CO1	C11	140.2(1)
C1	CO1	C101	145.3(1)	C5	CO1	C12	171.3(2)
C2	CO1	C3	41.4(2)	C5	CO1	C13	129.2(2)
C2	CO1	C4	68.4(2)	C5	CO1	C14	113.4(1)
C2	CO1	C5	67.9(2)	C5	CO1	C100	35.8(1)
C2	CO1	C11	117.5(2)	C5	CO1	C101	144.7(1)
C2	CO1	C12	119.1(2)	C11	CO1	C12	43.3(1)
C2	CO1	C13	155.6(2)	C11	CO1	C13	62.9(1)
C2	CO1	C14	154.6(2)	C11	CO1	C14	44.3(1)
C2	CO1	C100	36.3(1)	C11	CO1	C100	149.4(1)
C2	CO1	C101	144.1(1)	C11	CO1	C101	31.8(1)
C3	CO1	C4	40.4(2)	C12	CO1	C13	42.4(1)
C3	CO1	C5	68.1(2)	C12	CO1	C14	63.0(1)
C3	CO1	C11	144.0(2)	C12	CO1	C100	148.0(1)
C3	CO1	C12	113.0(2)	C12	CO1	C101	31.2(1)
C3	CO1	C13	122.5(2)	C13	CO1	C14	43.3(1)
C3	CO1	C14	164.0(2)	C13	CO1	C100	147.7(1)
C3	CO1	C100	36.4(1)	C13	CO1	C101	31.1(1)
C14	CO1	C100	148.9(1)	CO1	C3	C8	128.3(3)
C14	CO1	C101	31.8(1)	CO1	C3	C100	54.2(1)
C100	CO1	C101	178.60(4)	C2	C3	C4	107.5(3)
C35	O1	C35	108.8(5)	C2	C3	C8	125.1(4)
CO1	C1	C2	69.8(2)	C2	C3	C100	53.4(2)
CO1	C1	C5	70.3(2)	C4	C3	C8	127.3(4)
CO1	C1	C6	127.3(3)	C4	C3	C100	54.0(2)
CO1	C1	C100	53.7(1)	C8	C3	C100	177.1(4)
C2	C1	C5	108.5(3)	CO1	C4	C3	69.5(2)
C2	C1	C6	125.7(4)	CO1	C4	C5	70.4(2)
C2	C1	C100	54.6(2)	CO1	C4	C9	126.8(3)

149

C5	C1	C6	125.8(4)	CO1	C4	C100	53.8(1)
C5	C1	C100	53.9(2)	C3	C4	C5	108.5(4)
C6	C1	C100	178.9(4)	C3	C4	C9	125.8(4)
CO1	C2	C1	70.1(2)	C3	C4	C100	54.5(2)
CO1	C2	C3	69.0(2)	C5	C4	C9	125.7(4)
CO1	C2	C7	127.1(3)	C5	C4	C100	54.0(2)
CO1	C2	C100	53.9(1)	C9	C4	C100	179.3(4)
C1	C2	C3	107.8(4)	CO1	C5	C1	69.3(2)
C1	C2	C7	125.7(4)	CO1	C5	C4	69.2(2)
C1	C2	C100	54.4(2)	CO1	C5	C10	127.8(3)
C3	C2	C7	126.5(4)	CO1	C5	C100	53.2(1)
C3	C2	C100	53.5(2)	C1	C5	C4	107.7(4)
C7	C2	C100	179.1(4)	C1	C5	C10	126.5(4)
CO1	C3	C2	69.6(2)	C1	C5	C100	53.9(2)
CO1	C3	C4	70.1(2)	C4	C5	C10	125.8(4)
C4	C5	C100	53.8(2)	CO1	C14	C15	124.0(3)
C10	C5	C100	178.9(4)	CO1	C14	C101	57.4(2)
CO1	C11	C12	67.8(2)	C11	C14	C13	88.0(3)
CO1	C11	C14	68.5(2)	C11	C14	C15	145.4(3)
CO1	C11	C34	122.2(2)	C11	C14	C101	44.0(2)
CO1	C11	C101	58.3(2)	C13	C14	C15	126.6(3)
C12	C11	C14	88.9(3)	C13	C14	C101	43.9(2)
C12	C11	C34	126.8(3)	C15	C14	C101	170.3(4)
C12	C11	C101	44.4(2)	C14	C15	C16	119.0(3)
C14	C11	C34	144.2(3)	C14	C15	C20	124.5(3)
C14	C11	C101	44.5(2)	C16	C15	C20	116.5(3)
C34	C11	C101	171.2(4)	C15	C16	C17	121.9(4)
CO1	C12	C11	68.9(2)	C16	C17	C18	120.5(4)
CO1	C12	C13	68.6(2)	C17	C18	C19	119.4(4)
CO1	C12	C101	58.9(2)	C18	C19	C20	120.5(4)
C11	C12	C13	91.3(3)	C15	C20	C19	121.1(3)
C11	C12	C101	45.8(2)	C15	C20	C21	113.7(3)
C13	C12	C101	45.5(2)	C19	C20	C21	125.2(4)
CO1	C13	C12	68.9(2)	C20	C21	C22	157.6(4)
CO1	C13	C14	69.7(2)	C21	C22	C23	156.3(4)
CO1	C13	C101	59.1(2)	C22	C23	C24	128.0(3)
C12	C13	C14	91.8(3)	C22	C23	C34	115.9(3)
C12	C13	C101	45.8(2)	C24	C23	C34	116.0(3)
C14	C13	C101	46.1(2)	C23	C24	C25	146.6(4)
CO1	C14	C11	67.2(2)	C23	C24	C31	123.1(3)
CO1	C14	C13	67.0(2)	C25	C24	C31	90.3(3)
C24	C25	C26	147.2(4)	C1	C100	C3	144.1(3)
C24	C25	C30	89.6(3)	C1	C100	C4	144.4(3)
C26	C25	C30	123.2(3)	C1	C100	C5	72.2(3)
C25	C26	C27	115.1(4)	C2	C100	C3	73.1(3)
C26	C27	C28	121.9(4)	C2	C100	C4	144.6(3)

C27	C28	C29	122.6(4)	C2	C100	C5	143.2(3)
C28	C29	C30	115.3(4)	C3	C100	C4	71.5(3)
C25	C30	C29	122.0(4)	C3	C100	C5	143.7(3)
C25	C30	C31	90.2(3)	C4	C100	C5	72.2(3)
C29	C30	C31	147.8(4)	CO1	C101	C11	89.9(2)
C24	C31	C30	89.9(3)	CO1	C101	C12	89.8(2)
C24	C31	C32	121.9(3)	CO1	C101	C13	89.8(2)
C30	C31	C32	148.2(4)	CO1	C101	C14	90.8(2)
C31	C32	C33	116.0(4)	C11	C101	C12	89.8(3)
C32	C33	C34	123.5(4)	C11	C101	C13	178.5(3)
C11	C34	C23	122.1(3)	C11	C101	C14	91.5(3)
C11	C34	C33	118.4(3)	C12	C101	C13	88.8(3)
C23	C34	C33	119.4(3)	C12	C101	C14	178.6(3)
O1	C35	C36	106.6(4)	C13	C101	C14	90.0(3)
C35	C36	C36	101.8(3)	CO1	C100	C3	89.4(2)
CO1	C100	C1	90.2(2)	CO1	C100	C4	90.2(2)
CO1	C100	C2	89.9(2)	CO1	C100	C5	91.0(2)
C1	C100	C2	71.0(3)				
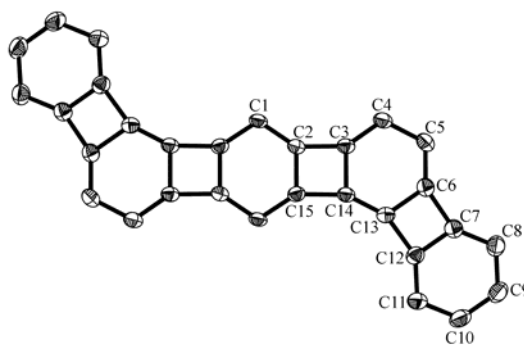
Table 9 Bond distances (Å) in **66**.

atom	atom	distance	atom	atom	distance
C1	C2	1.382(3)	C1	C15	1.391(3)
C2	C15	1.434(3)	C2	C3	1.502(3)
C3	C4	1.358(3)	C3	C14	1.470(3)
C4	C5	1.443(3)	C5	C6	1.360(3)
C6	C13	1.463(3)	C6	C7	1.505(3)
C7	C8	1.372(3)	C7	C12	1.412(3)
C8	C9	1.406(3)	C9	C10	1.382(4)
C10	C11	1.401(3)	C11	C12	1.384(3)
C12	C13	1.512(3)	C13	C14	1.343(3)
C14	C15	1.501(3)	C15	C1	1.391(3)

Table 10 Bond angles (in °) in **66**.

atom	atom	atom	angle	atom	atom	atom	angle
C2	C1	C15	112.61(19)	C1	C2	C15	124.2(2)
C1	C2	C3	145.3(2)	C15	C2	C3	90.46(17)
C4	C3	C14	124.7(2)	C4	C3	C2	145.8(2)
C14	C3	C2	89.51(17)	C3	C4	C5	117.8(2)
C6	C5	C4	117.5(2)	C5	C6	C13	124.7(2)
C5	C6	C7	145.9(2)	C13	C6	C7	89.33(17)
C8	C7	C12	122.6(2)	C8	C7	C6	146.5(2)
C12	C7	C6	90.91(18)	C7	C8	C9	115.4(2)
C10	C9	C8	122.0(2)	C9	C10	C11	122.9(2)
C12	C11	C10	114.9(2)	C11	C12	C7	122.2(2)
C11	C12	C13	146.8(2)	C7	C12	C13	91.00(18)
C14	C13	C6	118.1(2)	C14	C13	C12	153.2(2)
C6	C13	C12	88.74(18)	C13	C14	C3	117.2(2)
C13	C14	C15	153.7(2)	C3	C14	C15	89.08(17)
C1	C15	C2	123.2(2)	C1	C15	C14	145.9(2)
C2	C15	C14	90.95(17)				

References

1. Kekulé, A. *Bull. Soc. Chim.* **1865**, *3*, 98.

2. For discussions of aromaticity, see: (a) Garratt, P. J. *Aromaticity*; Wiley, Inc.: New York, 1986; (b) Cyrañski, M. K.; Krygowski, T. M.; Katritzky, A. R.; Schleyer, P. v. R. *J. Org. Chem.* **2002**, *67*, 1333; (c) Minkin, V. I.; Glukhovtsev, M. N.; Simkin, B. Ya. *Aromaticity and Antiaromaticity – Electronic and Structural Aspects*; Wiley: New York, 1994.

3. (a) Loudon, G. M. *Organic Chemistry*; Benjamin/Cummings Publishing: Menlo Park, California, 1988, pp 615-630; (b) Carroll, F. A. *Perspectives on Structure and Mechanism in Organic Chemistry*; Brooks/Cole Publishing Company: Pacific Grove, 1998, pp 178-213.

4. Lothrop, W. C. *J. Am. Chem. Soc.* **1941**, *63*, 1187.

5. Fawcett, J. K.; Trotter, J. *Acta Cryst.* **1966**, *20*, 87.

6. For a review of the synthesis and properties of biphenylene and related molecules containing bis(methylene)cyclobutene or tetrakis(methylene)cyclobutane moieties, see: Toda, F.; Garratt, P. *Chem. Rev.* **1992**, *92*, 1685.

7. Salfeld, J. C.; Baume, E. *Tetrahedron Lett.* **1966**, 3365.

8. Logullo, F. M.; Seitz, A. H.; Friedman, L. *Org. Syn.* **1973**, *Coll. Vol. 5*, 54.

9. Cava, M. P.; Mitchell, M. J.; DeJongh, D. C.; Van Fossen, R. Y. *Tetrahedron Lett.* **1966**, 2947.

10. Brown, R. F. C.; Gardner, D. V.; McOmie, J. F. W.; Solly, R. W. *Aust. J. Chem.* **1967**, *20*, 139.

11. MacBride, J. A. H. *J. Chem. Soc., Chem. Commun.* **1972**, 1219.

12. Kabir, S. M. H.; Hasegawa, M.; Kuwatani, Y.; Yoshida, M.; Matsuyama, H.; Iyoda, M. *J. Chem. Soc., Perkin Trans. 1* **2001**, 159.

13. Barton, J. W.; Rowe, D. J. *Tetrahedron Lett.* **1983**, *24*, 299.

14. Barton, J. W.; Rowe, D. J. *Tetrahedron Lett.* **1978**, 1005.

15. Barton, J. W.; Shepherd, M. K. *Tetrahedron Lett.*, **1984**, *25*, 4967.

16. Diercks, R.; Vollhardt, K. P. C. *J. Am. Chem. Soc.* **1986**, *108*, 3150.

17. Rausch, M. D.; Tokas, E. F.; Gardner, S. A.; Clearfield, A.; Chinn, J. W. Jr.; Bernal, I. *J. Organomet. Chem.* **1981**, *212*, 247.

18. Gesing, E. R. F. *J. Org. Chem.* **1982**, *47*, 3192.

19. Berris, B. C.; Lai, Y.-H.; Vollhardt, K. P. C. *J. Chem. Soc., Chem. Commun.* **1982**, 953.

20. Jonas, K.; Deffense, E.; Habermann, D. *Angew. Chem., Int. Ed. Engl.* **1983**, *22*, 716.

21. For a recent theoretical study of this mechanism, see: Hardesty, J. H.; Koerner, J. B.; Albright, T. A.; Lee, G.-Y. *J. Am. Chem. Soc.* **1999**, *121*, 6055.

22. (a) For **2-4**, see: Vollhardt, K. P. C.; Mohler, D. L. In *Advances in Strain in Organic Chemistry*; Halton, B., Ed.; JAI: London, 1996, pp 121-160. (b) For **17** see: Eickmeier, C.; Holmes, D.; Junga, H.; Matzger, A. J.; Scherhag, F.; Shim, M.; Vollhardt, K. P. C. *Angew. Chem., Int. Ed. Engl.* **1999**, *38*, 800. (c) For **18** see, Kumaraswamy, S. *Ph. D. Thesis*, UC Berkeley, 1999. (d) For **19** see Han, S.; Anderson, D. R.; Bond, A. D.; Chu, H.; Disch, R. L.; Holmes, D.; Schulman, J. M.; Teat, S. J.; Vollhardt, K. P. C.; Whitener, G. D. *Angew. Chem. Int. Ed.,* in press.

23. Berris, B. C.; Hovakeemian, G. H.; Lai, Y.-H.; Mestdagh, H.; Vollhardt, K. P. C. *J. Am. Chem. Soc.* **1985**, *107*, 5670.

24. Hirthammer, M.; Vollhardt, K. P. C. *J. Am. Chem. Soc.* **1986**, *108*, 2481.

25. Iwamoto, M. Undergraduate Research Report, 2001.

26. Boese, R.; Matzger, A. J.; Mohler, D. L.; Vollhardt, K. P. C. *Angew. Chem., Int. Ed. Engl.* **1995**, *34*, 1478.

27. Diercks, R.; Vollhardt, K. P. C. *Angew. Chem., Int. Ed. Engl.* **1986**, *25*, 266.

28. Boese, R.; Matzger, A. J.; Vollhardt, K. P. C. *J. Am. Chem. Soc.* **1997**, *119*, 2052.

29. Schmidt-Radde, R. H.; Vollhardt, K. P. C. *J. Am. Chem. Soc.* **1992**, *114*, 9713.

30. Aihara, J.-I. *Bull. Chem. Soc. Jpn.* **1990**, *63*, 1956.

31. See: Faust; R.; Glendening, E. D.; Streitwieser, A.; Vollhardt, K. P. C. *J. Am. Chem. Soc.* **1992**, *114*, 8263 and references cited therein.

32. Stanger, A. *J. Am. Chem. Soc.* **1998**, *120*, 12034.

33. Holmes, D.; Kumaraswamy, S.; Matzger, A. J.; Vollhardt, K. P. C. *Chem. Eur. J.* **1999**, *5*, 3399.

34. Schleifenbaum, A.; Feeder, N.; Vollhardt, K. P. C. *Tetrahedron Lett.* **2001**, *42*, 7329.

35. (a) Silverstein, R. M.; Bassler, G. C. Morrill, T. C. *Spectrometric Identification of Organic Compounds*; John Wiley & Sons: New York, 1991, pp 171-177. (b) Memory, J. D.; Wilson, N. K. *NMR of Aromatic Compounds*; John Wiley & Sons: New York, 1982, pp 18-39.

36. In cases such as [18]annulene, in which protons are located inside the aromatic circuit, strong shielding is observed. See: Jackman, L. M.; Sondheimer, F.; Amiel, Y.;

Ben-Efraim, D. A.; Gaoni, Y.; Wolovsky, R.; Bothner-By, A. A. *J. Am. Chem. Soc*. **1962**, *84*, 4307.

37. For a listing of the chemical shifts of common compounds in standard NMR solvents, see: Gottlieb, H. E.; Kotlyar, V.; Nudelman, A. *J. Org. Chem.* **1997**, *62*, 7512.

38. Schulman, J. M.; Disch, R. L.; Jiao, H.; Schleyer, P. v. R. *J. Phys. Chem. A* **1998**, *102*, 8051.

39. Radde, R. H. *Ph. D. Thesis*, UC Berkeley, 1989.

40. For a review of the reactivity of biphenylene, see: Shepherd, M. K. *Cyclobutarenes: The Chemistry of Benzocyclobutene, Biphenylene, and Related Compounds*; Elsevier: New York, 1991, pp 173-235.

41. Mohler, D. L.; Vollhardt, K. P. C.; Wolff, S. *Angew. Chem., Int. Ed. Engl.* **1990**, *29*, 1151.

42. Mohler, D. L.; Vollhardt, K. P. C.; Wolff, S. *Angew. Chem., Int. Ed. Engl.* **1995**, *34*, 563.

43. Mestdagh, H.; Vollhardt, K. P. C. *J. Chem. Soc., Chem. Commun.* **1986**, 281.

44. Grotjahn, D. B.; Vollhardt, K. P. C. *J. Am. Chem. Soc*. **1986**, *108*, 2091.

45. Sheppard, G. S.; Vollhardt, K. P. C. *J. Org. Chem.* **1996**, *51*, 5498.

46. See: Diercks, R.; Eaton, B. E.; Jalisatgi, S.; Matzger, A. J.; Radde, R. H.; Vollhardt, K. P. C. *J. Am. Chem. Soc.* **1998**, *120*, 8247 and references cited therein.

47. Perthuisot, C.; Edelbach, B. L.; Zubris, D. L.; Jones, W. D. *Organometallics* **1997**, *16*, 2016.

48. Jalisatgi, S. Postdoctoral Research Report, 1997.

49. (a) For biphenylene, see: ref. 5. (b) For angular [3]phenylene, see: ref. 27. (c) For linear [3]phenylene, see ref. 34. (d) For triangular [4]phenylene, see: ref. 33.

50. Han, S.; Bond, A. D.; Holmes, D.; Teat, S. J.; Vollhardt, K. P. C.; Whitener, G. D. *Angew. Chem. Int. Ed.*, in press.

51. See: Beckhaus, H-D.; Faust, R.; Matzger, A. J.; Mohler, D. L.; Rogers, D. W.; Rüchardt, C.; Sawhney, A. K.; Verevkin, S. P.; Vollhardt, K. P. C.; Wolff, S. *J. Am. Chem. Soc.* **2000**, *122*, 7819 and references therein.

52. Professor P. von Ragué Schleyer, private communication.

53. Beevor, R. G.; Frith, S. A.; Spencer, J. L. *J. Organomet. Chem.* **1981**, *221*, C25.

54. Schneider, J. J.; Krüger, C.; Nolte, M.; Abraham, I.; Ertel, T. S.; Bertagnolli, H. *Angew. Chem., Int. Ed. Engl.* **1994**, *33*, 2435.

55. Green, M. L. H.; Pardy, R. B. A. *J. Chem. Soc., Dalton Trans.* **1979**, 355.

56. Alkyl substitution has a negligible effect on the Co-C_{alkyne} bond distances in a series of R_xCpCo(CO)(alkyne) systems: Benisch, C.; Chávez, J; Gleiter, R.; Nuber, B.; Irngartinger, H.; Oeser, T.; Pritzkow, H.; Rominger, F. *Eur. J. Inorg Chem.* **1998**, 629.

57. For examples of Co(I) complexes with shorter Co-alkyne bonds, see: (a) ref 56. (b) Foerstner, J. Kettenbach, R.; Goddard, R.; Butenschön, H. *Chem. Ber.* **1996**, *129*, 319. (c) Okuda, J.; Zimmermann, K. H.; Herdtweck, E. *Angew. Chem., Int. Ed. Engl.* **1991**, *30,* 430. For a discussion of how bond distances may vary with oxidation state, see: (d) Frenking, G.; Fröhlich, N. *Chem. Rev.* **2000**, *100,* 717.

58. Gleiter, R.; Merger, R. In *Modern Acetylene Chemistry,* Stang, P. J., Diederich, F., Eds.; VCH: Weinheim, 1995, pp 285-319.

59. De Graaff, R. A. G.; Gorter, S.; Romers, C.; Wong, H. N. C.; Sondheimer, F. *J. Chem. Soc., Perkin Trans. 1* **1981**, 478.

60. For a tabulation, see: Benisch, C.; Gleiter, R.; Staeb, T. H.; Nuber, B.; Oeser, T.; Pritzkow, H.; Rominger, F. *J. Organomet. Chem.* **2002**, *641*, 102.

61. Diercks, R. Postdoctoral Research Report, 1985.

62. Haley, M. M. Postdoctoral Research Report, 1993.

63. Matzger, A. J. *Ph. D. Thesis*, UC Berkeley, 1997.

64. Bong, D. T.-Y., Gentric, L.; Holmes, D.; Matzger, A. J.; Scherhag, F.; Vollhardt, K. P. C. *Chem. Commun.* **2002**, 278.

65. This strong bond localization is also observed in the crystal structure of a bis(trimethylsilyl) derivative of **70**. See: ref. 64.

66. Eickmeier, C.; Junga, H.; Matzger, A. J.; Scherhag, F.; Shim, M.; Vollhardt, K. P. C. *Angew. Chem., Int. Ed. Engl.* **1997**, *36*, 2103.

67. Holmes, D. *Ph. D. Thesis*, UC Berkeley, 1999.

68. Matzger, A. J.; Vollhardt, K. P. C. *J. Chem. Soc., Chem. Commun*. **1997**, 1415.

69. (a) Wiersum, U. E.; Jenneskens, L. W. *Tetrahedron Lett.* **1993**, *34*, 6615. (b) Brown, R. F. C.; Choi, N.; Coulston, K. J.; Eastwood, F. W.; Wiersum, U. E.; Jenneskens, L. W. *Tetrahedron Lett.* **1994**, *35*, 4405.

70. Jacob, J. *Pure Appl. Chem*. **1996**, *68*, 301.

71. Preda, D. V.; Scott, L. T. *Org. Lett.* **2000**, *2*, 1489. (b) see also: Sarobe, M.; Kwint, H. C.; Fleer, T.; Havenith, R. W. A.; Jenneskens, L. W.; Vlietstra, E. J.; van Lenthe, J. H.; Wesseling, J. *Eur. J. Org. Chem.* **1999**, 1191.

72. Schulman, J. M.; Disch, R. L. *J. Phys. Chem. A* **1997**, *101*, 5596.

73. For mechanistic reviews of flash vacuum pyrolysis chemistry, see: (a) Necula, A.; Scott, L. T. *J. Anal. Appl. Pyrolysis* **2000**, *54*, 65. (b) Jenneskens, L. W.; Sarobe, M.; Zwikker, J. W. *Pure Appl. Chem.* **1996**, *68*, 219. (c) Brown, R. F. C. *Eur. J. Org. Chem.* **1999**, 3211.

74. See: Slanina, Z.; Zhao, X.; Uhlík, F.; Ozawa, M.; Ōsawa, E. *J. Organomet. Chem.* **2000**, *599*, 57, and references therein.

75. The synthesis of acepentalene and its tribenzo derivative have been reported: Haag, R.; Schröder, D.; Zywietz, T.; Jiao, H.; Schwarz, H.; Schleyer, P. v. R.; de Meijere, A.; *Angew. Chem., Int. Ed. Engl.* **1996**, *35*, 1317; Haag, R.; Ohlhorst, B.; Noltemeyer, M.; Fleischer, R.; Stalke, D.; Schuster, A.; Kuck, D.; de Meijere, A. *J. Am. Chem. Soc.* **1995**, *117*, 10474.

76. For spectra of **75** and **84**, see: Sarobe, M.; Jenneskens, L. W. *J. Org. Chem.* **1997**, *62*, 8247 and Karcher, W.; Fordham, R. J.; Dubois, J. J.; Glaude, P. G. J. M.; Ligthart, J. A. M. *Spectral Atlas of Polycyclic Aromatic Compounds*, Reidel, Dordrecht, 1985. For spectra of **82**, see: Sarobe, M.; Snoeijer, J. D.; Jenneskens, L. W.; Slagt, M. Q.; Zwikker, J. W. *Tetrahedron Lett*. **1995**, *36*, 8489. For spectra of **83**, see: Mulder, P. P. J.; Boere, B. B.; Cornelisse, J.; Lugtenburg, J. *Recl. Trav. Chim. Pay-Bas* **1993**, *112*, 255.

77. Schulman, J. M.; Disch, R. L. *J. Am. Chem. Soc.* **1996**, *118*, 8470.

78. Compounds **75** and **84** are known to interconvert at temperatures greater than those used in the present study, see: Plater, M. J. *Tetrahedron Lett.* **1994**, *35*, 6147 and Jenneskens, L. W.; Sarobe, M.; Zwikker, J. W. *Pure Appl. Chem.* **1996**, *68*, 219.

79. Negishi, E.; Kotora, M.; Xu, C. *J. Org. Chem.* **1997**, *62*, 8957.

80. There was spectral evidence for additional minor label scrambling in all products which was not amenable to analysis. However, the finality of the label distribution could be ascertained at least for **75**-$^{13}C_2$, for which sufficient quantities were available to allow for repyrolysis under the same conditions. This control experiment showed no discernible change in the ^{13}C NMR spectrum.

81. For a review, see: Wiersum, U. E., Jenneskens, L. W. In *Gas Phase Reactions in Organic Symthesis;* Vallée, Y., Ed.; Gordon and Breach: Amsterdam, 1997, pp 143-194.

82. Mulder, P. P. J.; Boere, B. B.; Cornelisse, J.; Lugtenburg, J. *Recl. Trav. Chim. Pays-Bas* **1993**, *112*, 255.

83. Jans, A. W. H.; Tintel, C.; Cornelisse, J.; Lugtenburg, J. *Magn. Reson. Chem.* **1986**, *24*, 101.

84. Brooks, M. A.; Scott, L. T. *J. Am. Chem. Soc.* **1999**, *121*, 5444.

85. Claridge, T. D. W. *High-Resolution NMR Techniques in Organic Chemistry*; Pergamon: New York, 1999; Chapter 6, pp. 221-257.

86. Banciu, M. D.; Brown, R. F. C.; Coulston, K. J.; Eastwood, F. W.; Jurss, C.; Mavropoulos, I.; Stanescu, M.; Wiersum, U. E. *Aust J. Chem.* **1996**, *49*, 965.

87. Sahali, Y.; Kwon, H.; Skipper, P.; Tannenbaum, S. R. *Chem. Res. Toxicol*. **1992**, *5*, 157.

88. Rajca, A.; Safronov, A.; Rajca, S.; Ross, C. R., II; Stezowski, J. J. *J. Am. Chem. Soc.* **1996**, *118*, 7272.

89. Blanco, L. Helson, H. E.; Hirthammer, M.; Mestdagh, H.; Spyroudis, S.; Vollhardt, K. P. C. *Angew. Chem., Int. Ed. Engl.* **1987**, *26*, 1246.

90. Blanco, L. Postdoctoral Research Report, 1986.

91. (a) Sekiguchi, A.; Matsuo, T.; Watanabe, H. *J. Am. Chem. Soc.* **2000**, *122*, 5652. (b) Sekiguchi, A.; Tanaka, M.; Matsuo, T.; Watanabe, H. *Angew. Chem. Int. Ed.* **2001**, *40*, 1675.

92. Hirthammer, M. Postdoctoral Research Report, 1985.

93. The formation of CpCo-linear phenylene complexes like **99** during cobalt-mediated cycloadditions may the result of a haptotropic shift of CpCo from its initial location on a terminal benzene ring (see Figure 1.5) to a central cyclobutadiene, though binding of CpCo to free phenylenes may also be a source of these molecules.

94. King, J. A., Jr.; Vollhardt, K. P. C. *J. Organomet. Chem.* **1989**, *369*, 245.

95. Albright, T. A.; Hofmann, P.; Hoffmann, R.; Lillya, C. P.; Dobosh, P. A. *J. Am. Chem. Soc.* **1983**, *105*, 3397.

96. See: ref. 3b, pp 332-349.

97. Lambet, J. B.; Shurvell, H. F.; Verbit, L.; Cooks, R. G.; Stout, G. H. *Organic Structure Analysis*; Macmillan: New York, 1976, p 116.

98. Braun, S.; Kalinowski, H.-O.; Berger, S. *100 and More Basic NMR experiments*, VCH: New York, 1996, pp 121-123.

99. Kehoe, J. M.; Kiley, J. H.; English, J. J.; Johnson, C. A.; Petersen, R. C.; Haley, M. M. *Org. Lett.* **2000**, *2*, 969.

100. Mattern, D. L., *J. Org. Chem.*, **1983**, *48*, 4772.